INTRACELLULAR TRAFFICKING OF NEURONAL NICOTINIC ACETYLCHOLINE RECEPTORS: ROLE OF THE TUMOR SUPPRESSOR PROTEIN, ADENOMATOUS POLYPOSIS COLI

TULAYA POTAROS

A THESIS SUBMITTED IN PARTIAL FULFILLMENT
OF THE REQUIREMENTS FOR
THE DEGREE OF DOCTOR OF PHILOSOPHY
(BIOPHARMACEUTICAL SCIENCES)
FACULTY OF GRADUATE STUDIES
MAHIDOL UNIVERSITY
2008

Thesis
Entitled

INTRACELLULAR TRAFFICKING OF NEURONAL NICOTINIC ACETYLCHOLINE RECEPTORS: ROLE OF THE TUMOR SUPPRESSOR PROTEIN, ADENOMATOUS POLYPOSIS COLI

…….
Miss Tulaya Potaros
Candidate

…….
Assoc. Prof. Srichan Phornchirasilp
Ph.D. (Pharmacology)
Major-Advisor

…….
Prof. Dennis B. McKay
Ph.D. (Pharmacology)
Co-Advisor

…….
Assoc. Prof. Suvara Wattanapitayakul
Ph.D. (Pharmacology)
Co-Advisor

…….
Prof. Banchong Mahaisavariya
M.D.
Dean
Faculty of Graduate Studies

…….
Assoc. Prof. Primchanien Moongkarndi
Dr. rer. nat. (Immunology)
Chair
Doctor of Philosophy in
Biopharmaceutical Sciences
Faculty of Pharmacy

Thesis
Entitled

INTRACELLULAR TRAFFICKING OF NEURONAL NICOTINIC ACETYLCHOLINE RECEPTORS: ROLE OF THE TUMOR SUPPRESSOR PROTEIN, ADENOMATOUS POLYPOSIS COLI

was submitted to the Faculty of Graduate Studies, Mahidol University
for the Degree of Doctor of Philosophy (Biopharmaceutical Sciences)
on
16 May, 2008.

…….
Miss Tulaya Potaros
Candidate

…….
Assoc. Prof. Supatra Srichairat
Dr. rer. nat. (Pharmacology)
Chair

…….
Assoc. Prof. Srichan Phornchirasilp
Ph.D. (Pharmacology)
Member

…….
Prof. Dennis B. McKay
Ph.D. (Pharmacology)
Member

…….
Assoc. Prof. Suvara Wattanapitayakul
Ph.D. (Pharmacology)
Member

…….
Assoc. Prof. Chongkol Tiangda
Dr. rer. nat. (Pharmacology)
Member

…….
Prof. Banchong Mahaisavariya
M.D.
Dean
Faculty of Graduate Studies
Mahidol University

…….
Prof. Ampol Mitrevej
Ph.D. (Pharmaceutics)
Dean
Faculty of Pharmacy
Mahidol University

ACKNOWLEDGEMENTS

I would like to express my deepest gratitude to my major advisor, Assoc. Prof. Dr. Srichan Phornchirasilp for her invaluable guidance, assistance and encouragement. Without her, my thesis would not have been completely successful.

I wish to greatly thank my co-advisor, Assoc. Prof. Dr. Suvara Wattanapitayakul, who has been my best teacher throughout my study. Her kindness, advice and tireless effort in reviewing this research are highly appreciated.

I am deeply and forever indebted to my co-advisor, Prof. Dr. Dennis B. McKay, who greatly enriched my knowledge with his professional insights into the scientific research, specifically the field of Neuropharmacology.

The sincere gratitude also goes to Mrs. Susan B. McKay for her abundant help, useful suggestions, research guidance as well as love and care.

I acknowledge the financial support by a scholarship from Ministry of Higher Education, Thailand and NIH grant (DA 10569), USA. I would like to convey thanks for Division of Pharmacology, College of Pharmacy, The Ohio State University for providing the laboratory facilities.

I would like to specially thank all of my best friends both in Thailand and USA for their endless friendship and support. A special thank also goes to Tatiana Gonzalez Cestari and Brandon Henderson for their invaluable help and being my great friends throughout my stay at OSU.

Very deep appreciation attends to Miss Saisamorn Yenphasuk for her sincerity and administrative organization.

Lastly, I wish to express my heartfelt gratitude to my beloved family for their endless love, inspiration, understanding, support and encouragement throughout my entire life.

Tulaya Potaros

INTRACELLULAR TRAFFICKING OF NEURONAL NICOTINIC ACETYLCHOLINE RECEPTORS: ROLE OF THE TUMOR SUPPRESSOR PROTEIN, ADENOMATOUS POLYPOSIS COLI

TULAYA POTAROS 4636670 PYBS/D

Ph.D. (BIOPHARMACEUTICAL SCIENCES)

THESIS ADVISORS: SRICHAN PHORNCHIRASILP, Ph.D.(PHARMACOLOGY), DENNIS B. MCKAY, Ph.D.(PHARMACOLOGY), SUVARA WATTANAPITAYAKUL, Ph.D.(PHARMACOLOGY)

ABSTRACT

Alterations of neuronal nicotinic acetylcholine receptors (nAChRs) expression have been correlated to several pathological conditions. Although APC, adenomatous polyposis coli, has been demonstrated to participate in neuronal nAChRs expression, the involvement of α3β4 subtype is completely unknown. Hence, the study investigated the effect of APC protein on trafficking of α3β4* subtype in adrenal chromaffin cells (BAC) and in HEK293 cells expressing recombinant bovine α3β4* nAChRs (BMα3β4). First, the presence of APC mRNA and protein in BAC and BMα3β4 was found. Using RT-PCR, cDNA sequences with high homologies (>90%) to human or bovine APC sequence were detected in both cell types. Using Western Blot technique, the presence of 270 KD and 283 KD APC protein in BAC and BMα3β4, respectively, were confirmed. In order to knockdown APC gene, BMα3β4 were then transfected with APC-siRNA overnight and receptor binding assay coupled with receptor alkylation were conducted in these cells at 0, 24 and 48 hours after complete transfection. With 72% transfection efficiency, APC siRNA caused the reduction of APC protein to 52% and 62% of control at 24 and 48 hours, respectively. The total population of nAChRs (Rt) in control and siRNA treated cells remained constant over 48 hours. The intracellular receptors (Ri) in siRNA treated cells were significantly reduced to 72±3% and 68±4% of control at 24 and 48 hours, respectively. Contrarily, a significant increment of surface receptors (Rs) level to 357±21% and 299±34% of control at 24 and 48 hours was observed. The effect of protein synthesis on BMα3β4 trafficking was also studied by treating cells with 10 μg/well puromycin, a protein synthesis inhibitor, overnight. Puromycin treatment caused the dramatic reduction of APC protein, Rt, Ri and Rs to 83±3%, 23±3%, 16±2% and 40±13%, respectively. In conclusion, APC siRNA transfection caused a reduction of APC production within BMα3β4 which led to movement of Ri to cell surface for maintenance of normal Rs expression.

KEY WORDS: α3β4 nAChRs/ RECEPTOR TRAFFICKING/ APC/ siRNA/ PUROMYCIN

169 pp.

บทบาทของโปรตีน APC ต่อการสัญจรภายในเซลของ neuronal nicotinic acetylcholine receptors (INTRACELLULAR TRAFFICKING OF NEURONAL NICOTINIC ACETYLCHOLINE RECEPTORS: ROLE OF THE TUMOR SUPPRESSOR PROTEIN, ADENOMATOUS POLYPOSIS COLI)

ตุลยา โพธารส 4636670 PYBS/D
ปร.ด. (เภสัชศาสตร์ชีวภาพ)
คณะกรรมการควบคุมวิทยานิพนธ์: ศรีจันทร์ พรจิราศิลป์, Ph.D.(Pharmacology), Dennis B. McKay, Ph.D.(Pharmacology), สุวรา วัฒนพิทยกุล, Ph.D.(Pharmacology)

บทคัดย่อ

การเปลี่ยนแปลงการแสดงออกของตัวรับนิโคตินิกชนิดระบบประสาท (neuronal nAChRs) มีความสัมพันธ์ต่อการเกิดพยาธิสภาพหลายชนิด มีรายงานการศึกษาแสดงถึงความเกี่ยวข้องของโปรตีน APC ต่อการแสดงออกของ neuronal nAChRs แต่ยังไม่มีข้อมูลชัดเจนที่อธิบายความเกี่ยวข้องของโปรตีนนี้กับการสัญจรของ $\alpha 3\beta 4$ nAChRs การวิจัยนี้มีวัตถุประสงค์เพื่อศึกษาผลของโปรตีน APC ต่อการสัญจรของ $\alpha 3\beta 4$ nAChRs ใน bovine adrenal chromaffin cells (BAC) และเซลล์ BM$\alpha 3\beta 4$ จากการศึกษาเบื้องต้น พบว่า มีโปรตีน APC อยู่ในเซลล์ทั้งสองชนิด จากการศึกษาโดยอาศัยเทคนิค RT-PCR พบว่าในเซลล์ BAC และ BM$\alpha 3\beta 4$ มี cDNA ที่มีลำดับเบสคล้ายคลึงมากกับลำดับเบสของ APC ในวัวและคน (มากกว่าร้อยละ 90) แสดงว่ามี mRNA ของ APCในเซลล์ทั้งสองชนิด ส่วนผลการทดลองโดยใช้ Western Blot พบว่า ในเซลล์ BAC และ BM$\alpha 3\beta 4$ มีโปรตีน APC ขนาด 270 กิโลดาลตันและ 283 กิโลดาลตันตามลำดับ เมื่อ transfect APC-siRNA ในเซลล์ BM$\alpha 3\beta 4$ นาน 24 ชั่วโมง เพื่อทำลาย APC gene แล้ววัดจำนวนตัวรับของเซลล์ด้วยวิธี receptor binding assay ร่วมกับ receptor alkylation ณ เวลาที่ 0, 24 และ 48 ชั่วโมงภายหลัง transfection อย่างสมบูรณ์ ผลการทดลองพบว่า APC-siRNA ที่มีประสิทธิภาพในการ transfection ร้อยละ 72 สามารถลดระดับของโปรตีน APC เหลือร้อยละ 52 และ 62 ของกลุ่มควบคุมที่เวลา 24 และ 48 ชั่วโมงตามลำดับ และในเซลล์ดังกล่าวมีจำนวนตัวรับทั้งหมด (total receptors) ค่อนข้างคงที่ตลอดเวลา 48 ชั่วโมง ในขณะที่มีจำนวนตัวรับภายในเซลล์ (intracellular receptors) ลดลงอย่างมีนัยสำคัญทางสถิติ เหลือร้อยละ 72±3 และ 68±4 ของกลุ่มควบคุมที่เวลา 24 และ 48 ชั่วโมงตามลำดับ แต่จะมีตัวรับที่ผิวเซลล์ (surface receptors) เพิ่มขึ้นอย่างมีนัยสำคัญทางสถิติ เป็นร้อยละ 357±21 และ 299±34 ของกลุ่มควบคุมที่เวลาดังกล่าว นอกจากนี้เมื่อศึกษาผลของกระบวนการสร้างโปรตีนต่อการสัญจรของตัวรับนิโคตินิกในเซลล์ BM$\alpha 3\beta 4$ โดยบ่มเซลล์ด้วยพูโรมัยซิน ซึ่งเป็นสารยับยั้งการสร้างโปรตีน ผลการทดลองพบว่า พูโรมัยซินทำให้ปริมาณโปรตีน APC ลดลงอย่างมีนัยสำคัญทางสถิติ จำนวนของตัวรับทั้งหมด, ตัวรับภายในเซลล์ และตัวรับที่ผิวเซลล์ ลดลงเหลือร้อยละ 23±3, 16±2 และ 40±13 ตามลำดับ จากผลการทดลองทั้งหมด สามารถสรุปได้ว่า APC-siRNA transfection ทำให้เกิดการลดลงของการสร้างโปรตีน APC ภายในเซลล์ BM$\alpha 3\beta 4$ ซึ่งนำไปสู่การเคลื่อนย้ายตัวรับภายในเซลล์ไปยังผิวเซลล์ เพื่อรักษาระดับปกติของตัวรับที่ผิวเซลล์

169 หน้า

CONTENTS

CONTENTS (cont.)

LIST OF TABLES

LIST OF TABLES (cont.)

LIST OF FIGURES

LIST OF FIGURES (cont.)

LIST OF ABBREVIATION

%	=	percentage
ºC	=	degree Celsius
μg	=	microgram
μl	=	microliter
μM	=	micromolar
APC	=	Adenomatous polyposis coli
BAC	=	Bovine adrenal chromaffin cells
dl	=	deciliter
g	=	gram
hr	=	hour
kg	=	kilogram
kD	=	kilodalton
l	=	liter
M	=	molarity
mg	=	milligram
min	=	minute
mM	=	millimolar
N	=	normality
nAChRs	=	nicotinic acetylcholine receptors
nm	=	nanomolar
PCR	=	polymerase chain reaction
q.s.	=	quantum sufficit (as much as sufficient)
Ri	=	intracellular receptor
Rs	=	surface receptor
Rt	=	total receptor
sec	=	second
SEM	=	standard error of mean
siRNA	=	short interference RNA

CHAPTER I
INTRODUCTION

Neuronal nicotinic acetylcholine receptors (nAChRs) has physiological roles on neuronal systems both the central nervous system (CNS) and the peripheral nervous system (PNS) as well as on the non-neuronal system (1, 2). In CNS, they act as auto- and heteroreceptors regulating the release of neurotransmitters such as acetylcholine, dopamine, norepinephrine, serotonin, etc. Consequently, they are involved in many processes connecting to cognitive function, learning and memory, arousal, sleep etc. (1). In PNS, they mediate autonomic neurotransmission, and subsequently lead to sympathetic and parasympathetic responses throughout the body (3). They also participate in other peripheral processes such as inflammation (4). Among a variety of nAChRs subtypes, $\alpha4\beta2$ and $\alpha7$ have been found to be predominantly expressed in CNS, whereas $\alpha3\beta4$ is a major subtype in PNS (5). Although, $\alpha3\beta4$ subtype has lower abundant in CNS, it also possesses a presynaptic modulatory function. All these functions of $\alpha3\beta4$ subtype indicated the importance of this nicotinic acetylcholine receptor subtype.

Alterations in neuronal nicotinic acetylcholine receptors (nAChRs) expression have been associated with many neurological and non-neurological diseases (4, 6). For example, mutation of $\alpha3$ subunit has been found to be responsible for megacystis-microcolon-intestinal hypoperistalsis syndrome (MMHIS) in both rats and human (7, 8). MMHIS has been characterized as an enlarge bladder with dribbling urination, urinary stones or infection, mydriasis without light response. All rats with MMHIS die before weaning. Moreover, lack of $\alpha3$ nAChR has been related to autoimmune autonomic neuropathy (ANN) in both human and animal model (9, 10). $\alpha4\beta2$ subtype in striatum is responsible for dopamine release. The reduction of $\alpha4\beta2$

level has been found in the cerebral cortex of patients with Parkinson's disease (1). Consistently, the pathology of Parkinson's disease showed the loss of dopaminergic neuron in the nigro-striatal pathway. Despite of the importance of neuronal nAChRs expression, very little information is available on the intracellular trafficking of these receptors. Moreover, most of the studies worked on $\alpha4\beta2$ or $\alpha7$ subtypes (11, 12). Recently, Free et al. investigated the cellular mechanism which involved in the expression of neuronal $\alpha3\beta4$* nAChRs in bovine adrenal chromaffin cells (13). Their results supported the surface expression of these receptors as constitutive turnover requiring de novo protein synthesis. Due to the limited information and the important functions of $\alpha3\beta4$ nAChRs, it is necessary to explore the detail of $\alpha3\beta4$ nAChRs and their roles in intracellular trafficking.

Adenomatous polyposis coli (APC) protein has been identified as a tumor suppressor protein. Mutation of APC typically occurred in colorectal cancer. Its tumor suppressive effect appeared to be resulted from a function of APC protein as a negative regulator of Wnt pathway (14). Moreover, APC protein also exhibited many other functions associated with cell migration, adhesion, chromosome segregation, spindle assembly, apoptosis and neuronal differentiation (15, 16). Regarding to its role in neuronal system, APC protein expressed at higher level in brain than in peripheral tissues and this level varied with the stage of brain development (17). The role of APC protein has been found to be involved in neuronal differentiation and development of synapses. Dobashi et al. (18) showed that there was APC protein up-regulation during NGF (neural growth factor) induced differentiation of rat pheochromocytoma (PC12) cells. In addition, Leroy et al. (19) found the up-regulation of APC expression in astrocytes in Alzheimer's Disease (AD) and in other pathological conditions. They suggested that there was the involvement of APC-positive astrocytes with Aβ (β-amyloid) deposits and inflammatory process in AD. Wang et al. also found the requirement of APC protein in nAChRs clustering to postsynaptic site of neuromuscular junction (20). Furthermore, Temburni et al. established the function of APC protein in localizing $\alpha3$-nAChRs to neuronal postsynaptic site in chick ciliary ganglion (CG) neurons (21). Interestingly, Farias et

al. (22) reported that Wnt-7a, an active ligand in the canonical Wnt signaling pathway, increased the number and size of coclusters of APC and α7-nAChRs in presynaptic terminals. These results indicated the involvement of the canonical Wnt pathway in regulating the presynaptic localization of APC and α7-nAChRs. Thus, the available data suggested the involvement of APC protein to neuronal nAChRs trafficking. However, more information is required to confirm this proposed evidence.

To study on neuronal nAChRs surface trafficking, both the native and recombinant cell lines such as bovine adrenal chromaffin cell (BAC cell) and stably transfected HEK293 cell expressing recombinant bovine adrenal α3β4 nAChRs (BMα3β4 cell) could be used. BAC cells, derived from neural crest tissue represent the autonomic ganglion (23). Activation of nAChRs on these cells triggers catecholamine secretion. At least 2 subtypes of nAChRs were expressed on these cells. α-bungarotoxin (Bgt) sensitive subtype composed of α_7 subunit (24) and α-Bgt insensitive subtype, mAb35-nAChR, which was supposed to be responsible for catecholamine secretion (25). Concerning to BMα3β4 cells, their pharmacological characteristics were found to be similar to the native bovine α3β4* nAChRs (26). Since BMα3β4 cells expressed only α3β4 subtype, it would be easier to investigate the α3β4 nAChR surface expression in BMα3β4 cells rather than in BAC cells which expressed more than 1 subtype of nAChRs. In addition, BMα3β4 cells possessed more than 100 fold of the number of nAChRs expression higher than in native bovine chromaffin cells (26, 27). These information suggested the potential of using BMα3β4 cells as neuronal model for studying α3β4 nAChRs expression.

Therefore, the hypothesis of this study was that APC protein, expressed in BM$\alpha_3\beta_4$ cells was involved in surface receptor trafficking of neuronal nAChRs

Objectives

The objective of this study was to investigate the involvement of APC protein in the trafficking of $\alpha3\beta4^*$ neuronal nAChRs in BMα3β4 cells by

1. Identify and confirm the presence of APC mRNA and protein in bovine adrenal chromaffin cells and BMα3β4 cells by using RT-PCR technique and Western Blot analysis.

2. Demonstrate that APC protein is involved in the regulation of neuronal nAChRs to the cell surface. APC-siRNA transfection would be done in BMα3β4 cells to decrease APC protein expression which should result in alteration of nAChRs both surface and intracellular receptors. These changes in nAChRs would be determined by a receptor binding assay, coupled with receptor alkylation.

3. Investigate the importance of de novo protein synthesis in maintaining both the surface and intracellular pools of nAChRs. A receptor binding assay, coupled with receptor alkylation would be performed in puromycin treated BMα3β4 cells.

CHAPTER II
REVIEW LITERATURE

Receptor Trafficking

Few studies have addressed the questions on the intracellular trafficking of receptors. This trafficking modulated receptors expression which directly influenced their functional activities. Ionotropic glutamate receptors have been identified into 3 classes as AMPA (the alpha-amino-3-hydroxy-5-methyl-4-isoxazolepropionic acid), kainate and NMDA (N-methyl-D-aspartic acid) receptors. AMPA receptors appeared to be dynamics for their cell surface expression. They could cycling between cell surface and intracellular compartments by the process depending on NSF (*N*-ethyl-maleimide-sensitive factor) for receptor membrane insertion and the dynamin-clathrin dependent endocytosis for receptor removal (28). Quick increasing the number of postsynaptic AMPA receptors generated long-term potentiation while decreasing in AMPA receptors resulted in long-term depression (28). Different sets of proteins have been implicated in the clustering of each receptors. Glutamate receptors appeared to be mainly associated with PDZ (Post synaptic density protein, Dorsophila disc large tumor suppressor and Zonula occluden-1 protein) domain containing proteins such as GRIP1 (Glucocorticoid receptor interacting protein 1), whereas GABA (Gamma-aminobutyric acid) receptors appeared to be associated with gephyrin and GABARAP (GABA receptor-associated protein) (28).

nAChRs, ligand-gated ion channels have essential roles in neuronal and non-neuronal systems. The changes in expression or distribution of nAChRs directly influenced their function activities which have been associated with a variety conditions and diseases. Desensitization appeared to be an intrinsic property of nAChRs which characterized as a decline in response to nicotine after acute or repetitive exposure to nicotine (29). There was also a negative association between

cigarette smoking and Parkinson disease, Alzheimer's disease which indicated that nicotine and desensitized nAChRs have a neuroprotective action. Normally, nAChRs existed in 3 states: resting (R), activated (O) and desensitized (D) states. The conformation of nAChR at the R state had a low affinity for agonist, thereby only the high concentration of agonist was able to activate them and opened the ion channel. Contrarily, the conformation of nAChRs at D state had a high affinity for agonist, hence it needed lower concentration of agonist to activate them. Desensitized state was divided into 2 types, the fast onset or intermediate desensitized state (I) and the slow onset or chronically desensitized state (D). Marszalec et al. (30) designated these two desensitized states as D1 and D2. D1 state had a rapid entry and recovery rate while D2 had a slow entry and recovery rate. They suggested that shorter application of agonist produced desensitization via D1, while longer application preferred D2 conformation.

In addition, acute or 14 days of repetitive nicotine administration induced rapid desensitization of nAChRs in male Lewis rats (31). Desensitization usually occurred within seconds or minutes after the initial exposure and remains after 14 days of administration. The researchers also suggested that desensitization was a mediating factor in the induction of dependence. Nicotine increased the sensitivity of brain reward system mediating via $\alpha4\beta2$ nAChRs, therefore no escalation in drug intake was found in case of nicotine addiction (32). On the contrary, other drug abuse usually reduced the sensitivity of brain reward system, hence it needed escalation in drugs intake. Moreover, chronic nicotine exposure enhanced DA release on mesolimbic pathway which mediated addictive effect of nicotine (29). In contrast, chronic nicotine exposure in mice triggered the opposing processes differentially mediated by $\alpha7^*$ and $\beta2^*$ nAChRs which led to nicotine addiction (33). Recently, Robinson et al.(34) proposed that the nicotine-induced acute tolerance effect in rats was related to its ability to elicit nAChR desensitization.

With longer exposure duration, receptor down-regulation or receptor up-regulation developed over several hours. Chronic nicotine exposure induced down-regulation of $\alpha6\beta2^*$ nAChR in rat dopaminergic mesostriatal pathway (35). In

contrast, it caused up-regulation of α4β2 nAChR in these rats. However, most of the evidence supported that chronic nicotine exposure usually produces up-regulation of nAChRs such as α3β4*, α7*, α4β2* containing nAChRs (36). And receptor up-regulation occurs with some neuronal nAChRs subtypes. Sokolova et al. (36) proposed the mechanism underlying nAChR up-regulation that chronic nicotine exposure induced rapid desensitization of nAChRs leading to a deficit cholinergic function. Consequently, a cellular adaptation caused an increment in receptor number. In addition, chronic nicotine exposure induced α4β2 nAChRs up-regulation by influencing the early maturational step of ER-located species as posttranscriptional effect (37).

A variety of mechanisms of nAChR expression alteration were proposed including alteration of receptor synthesis and subunit assembly, exocytic pathway to surface expression, receptor recycling, receptor internalization and receptor degradation (29). The onset of desensitization appeared to be time- and concentration-dependent (29). At low concentration of agonist, the onset of desensitization was slower than recovery. Many factors were identified to regulate the kinetic of receptor activation and desensitization including subunit composition, phosphorylation, ligand and cellular environment. The α7 subunit was the most rapid desensitized among nAChRs. β subunit had strongly influence on the onset of desensitization. Desensitization rate of β2* containing nAChR was faster than that of β4* containing nAChR (29). α5 subunit was also responsible for the desensitization rate such as α3α5β4 was desensitized 3 fold faster than α3β4 nAChR, and α4α5β2 was desensitized faster than α4β2 nAChR. Regarding to another factor, phosphorylation enhanced recovery rate of desensitization while dephosphorylation stabilized nAChR in "stable inactivated state" (29). This finding was supported by Marszalec et al. (30) in which they found that protein kinase C activation and phosphatase 2B inhibitor promoted faster rate of desensitization recovery.

Concerning to ligand, the duration of exposure and concentration of agonist directly affected the process of desensitization and recovery. The longer ligand

exposure led to the slower in recovery from desensitization (29). Acute nicotine exposure elicited α4β2-activation and desensitization of α7 nAChR while chronic exposure elicited both receptor subtypes desensitization. Regarding to receptor up-regulation, chronic exposure could stabilize high affinity state of α4β2 nAChR or enhance changing of the pre-existing pool of immature subunits to high affinity nAChR state. The α7 nAChR up-regulation was mediated by phosphorylation (36).

In the receptor expression/ turnover process, there are at least 3 steps which regulate the number of functional nAChRs expressed on the cell surface. These steps included alterations in nAChRs formation and assembly (38), cell surface transportation (39) and cellular membrane stabilization (40). The rate limiting processes of receptor turnover might vary in different disease conditions. Chronic exposure to nicotine which elicited nAChRs up-regulation caused stabilization of receptors within cellular membranes (37, 41). Therefore, the regulation of nAChRs expression should be further explored. Insight to the nAChRs receptor regulation might be valuable in therapeutic management of several pathological conditions such as nicotine addiction, Alzheimer's disease (5).

The trafficking of muscle nAChRs

The process of surface trafficking or turnover of muscle nAChRs has recently been introduced (42, 43). The biosynthesis of muscle-type nAChR subunits was initiated on unbound cytoplasmic ribosomes. Then, most polypeptides were integrated into the membrane of endoplasmic reticulum (ER) through translocon. At the same time, they were also translated by ER membrane-associated ribosomal complexes (44, 45). Translocon, comprised of a specific set of membrane proteins regulated the movement of polypeptides through the bilayer. Hence, it maintained the membrane permeability barrier. The nascent subunit subsequently underwent many post-translational modifications in ER to be matured subunit. These processes included cleavage of its signal sequence, oxidation of its disulfide bond, N-glycosylation of specific residues and the trimming of the oligosaccharides, fatty acylation and the attachment of other membrane anchors, proline isomerization and phosphorylation (46, 47).

The α-subunit maturation and assembly were expressed in a muscle cell line, BC3H-1 cells. Smith et al. (48) confirmed that subunit maturation and pentameric assembly occurred in the ER. They also found that receptor biosynthesis involved with the assembly of newly synthesized α-subunit into a form capable of binding α-bungarotoxin. Inhibition of glycosylation with tunicamycin decreased the number of functional AChRs which was resulted from the blockade of assembly of subunit precursors to mature complex. Therefore, both glycosylation and a time-dependent posttranslational modification were required for an efficient assembly and subsequent expression of AChRs (49, 50). Consistently, Mitra et al.(38) studied the rearrangement of α subunits muscle nAChR during formation of ligand binding sites. They proposed that during nAChR assembly, subunits were rapidly associated into αβγ trimers. Then, $\alpha_{187\text{-}189}$ glycosylation of these subunits occurred and provided a conformational change of the 187-199 region which increased Bgt binding site formation three folds. The association of δ subunit with αβγ trimers to αβγδ tetramer, triggered the appearance of Ach binding site on α and γ interface of tetramers. This explained a significant delay during AChR assembly, before δ subunit was associated with αβγ trimers, despite of an abundance of δ subunit. Mitra et al. (38) suggested that $\alpha_{187\text{-}189}$ glycosylation was a part of the rate-limiting step of nAChR assembly. An alternative model for muscle nAChR subunit assembly has been proposed (47, 51). After the α subunit maturation, it was oligomerized with either γ or δ subunits to form αδ and αγ heterodimers. Then, the two heterodimers associated with the β subunit and with each other to form $\alpha_2\beta\gamma\delta$ complex.

Regarding to the maturation and assembly of nAChRs, Blount et al. (52) investigated the structure required for these processes using fibroblasts transfected with mutated α-subunits. They indicated that a disulfide bridge between cysteines 128 and 142 was necessary for the attainment of a mature conformation of α-subunit. Moreover, mutated α-subunit retained the capacity to assemble with δ-subunit, but these complexes with nonglycosylated α-subunit were quickly degraded. Thus, rapid degradation of immature subunits may be a mechanism to preclude surface expression of nonfunctional AChRs.

In addition to α-subunit glycosylation, chaperone proteins also have an important role on recognition and stabilization of intermediates during polypeptide folding and subunits oligomerization (47). ER contained a group of chaperone proteins differing from those found in cytoplasm. There was evidence indicated the role of the immunoglobulin-binding protein (BiP) in the folding and assembly of AChR subunits in BC3H-1 cells (53) as well as COS cells and C2 muscle cells (54). It was believed that BiP, an ER protein, associated with the newly synthesized unassembled α as well as αγ and αδ assembly intermediates, but not with the more mature form of α-subunit containing an intramolecular disulfide bridge. This phenomenon implicated the function of BiP in the assembly process of nAChR subunits. On the other hand, the role of calnexin on maturation of AChR subunits was investigated by using muscle cells and COS cells transfected with mouse AChR-α-subunit. Gelman et al.(55) reported that calnexin, an ER chaperone formed complexes with nascent AChR α-subunit. This finding was in agreement with the result observed by Keller et al.(56, 57) in which they confirmed the association of calnexin with un-assembly α, β, δ-subunits in HEK293 cells transfected with nAChR subunits. Therefore, the association was thought to facilitate the maturation of pentameric receptor via reducing the degradation of unassembled subunits in the ubiquitin-proteasome pathway.

After assembly of nAChRs, the assembled pentamers were ready to be transported into the secretory pathway from ER to golgi and cell surface. Unassembled subunits were retained in ER, stabilized by chaperone or degraded by the ER-associated proteasome (58). Wang and colleagues (59) established that the M1-domain of all subunits of muscle-nAChRs contains the retention signal, such as PLYFxxNV amino acid sequence in α-subunit. This signal prevented surface expression of unassembled subunits. Correctly assembled subunits obscured this signal and led to the export of AChR pentamers from ER to cell surface. This phenomenon was supported by the finding reported by Keller et al.(39). They found that subunit assembly masked Arg^{313}-Lys^{314}sequence in the cytoplasmic loop of the α-subunit AChR, thereby enabled the transport of nAChR from ER to golgi.

Moreover, they indicated that ubiquitination was another modulatory step for the golgi to cell surface trafficking of α-subunit. Subunit assembly also occluded this ubiquitination (39). The interruption of both signals made the assembled subunits expressing on cell surface.

More detail in nAChR trafficking was studied in the chinese hamster ovary cells expressing mouse α2βδε muscle nAChR (CHO-K1/A5) grown in long-term cholesterol deprivative condition. Using this model, Pediconi et al.(60) found the reduction in cell-surface AChR in concomitant to an increment in intracellular AChR and accumulating particular in golgi apparatus. However, there was unchanged in pharmacological properties of nAChR. Thus, they suggested that cholesterol participated in the trafficking of nAChR to the plasmalemma. Consistently, Borroni et al. (61) confirmed that this cholesterol depletion elicited by acute CDx (methyl-beta-cyclodextrin) exposure activated rapid internalization of submicron-sized AChR domains located at the cell membrane. Furthermore, Kellner et al.(62) showed that cholesterol depletion by acute CDx exposure also altered the organization of AChR nanoclusters on the cell surface.

Regarding to nAChR expression in other cell type, Roccamo et al. (63) found that cell surface muscle nAChRs in CHO-K1 cells with αM4 mutants were diminished while unassembled. The nAChRs were retained in ER. They suggested the important of His(408) and Arg(429) of α subunit M4 transmembrane segment in the process of assembly and cell surface targeting of muscle nAChRs. Recently, Baier et al. (64) demonstrated that inhibition of sphingolipid (SL) biosynthesis in CHO-K1/A5 cells impaired the normal transport of nAChR to the plasma membrane and promoted its accumulation. It also affected the early stage of the exocytic pathway and caused the retention of unassembled receptor in ER. These results indicated that SLs possessed a chaperone-like activity in the assembly and trafficking of nAChRs.

At NMJ, nAChRs were found in postsynaptic membrane with 1000 fold higher in concentration than in muscle surface elsewhere. The high level of nAChR at NMJ

was influenced by the coordinative action of nerve- and muscle-derived factor and the signaling proteins as well as cytoskeletal proteins in muscle. Agrin, a principal nerve-derived factor stimulated AChRs clustering on the surface of cultured muscle cells. Both agrin- and nerve-independent AChR clustering required the activity of muscle specific tyrosine kinase (MuSK), which was modulated by tyrosine phosphatase (65).

Alternatively, Aridor et al. (66) focused on the intracellular trafficking of mature protein to the appropriated destinations. This process was found to be mediated by vestibular/tubular carriers. The carriers, which are cytosolic coat proteins formed complex with their target membranes and deformed these membranes into bud and vesicles. Then, this complex specifically bound to cargo protein and delivered to its destination. Assembled nAChR subunits were exported from ER to golgi in a coat protein complex II (COP II) vesicle (46, 66). While COP II was important for exporting from ER, COP I was important for retrieval transport back to ER. Furthermore, Christianson et al. (67) investigated the effect of proteasome inhibitors on increasing surface nAChRs in mouse myotubes. They indicated that nAChRs were regulated by the ubiquitin-proteasome system (UPS) in ER. UPS, a part of endoplasmic reticulumn-associated degradation (ERAD), mediated the degradation of both assembly-competent and unassembly subunits of receptors. Therefore, inhibition of proteasome led to the increase in surface receptors.

The trafficking of neuronal nAChRs

As described above, the trafficking of muscle-type nAChRs appeared to be widely elucidated. Nevertheless, a few studies have focused on the surface trafficking of neuronal nAChRs. Ren et al. (46) found that highly conserved hydrophobic residues, primarily leucine, in the cytoplasmic domain of the $\alpha_4\beta_2$ AChR subunits were required for cell surface expression of neuronal nAChRs in HEK 293 and SH-SH5Y cell lines. Recently, the biosynthesis and maturation of $\alpha_4\beta_2$ nAChRs expressed in HEK293 cells have been studied (37, 46). The scenario of neuronal nAChRs trafficking has been proposed as follow, α and β subunits were initially synthesized and matured within ER as core-glycosylated high-mannose glycoproteins. The misfolded subunits were degraded by ERAD. Each subunit assembled into

pentameric receptor with masking of specific ER retention signal and properly folding of export motifs. Then, they exit from this compartment and trafficked through golgi apparatus. In golgi apparatus, sugar were trimmed and processed into the complex carbohydrate. Finally, nAChRs were exported to the surface. About 15% of total receptors were located on the cell surface, the rest were presented in intracellular pools. Surface receptors were internalized to the SKD1 endosomal compartment and degraded in Lamp1 (Lysosomal-associated membrane protein-1) lysosomal compartment (11).

In addition to the proposed nAChRs trafficking in neural cells, the regulation of receptor expression has also been explored. Corringer et al. (68) demonstrated that nicotine elicited up-regulation of α4β2 nAChRs expressed in HEK293 cells by promoting early maturation of nAChR subunits in ER. Darsow et al. (11) investigated membrane trafficking and nicotine-induced up-regulation of surface-expressed α4β2 nAChRs in HEK293 cells. They documented that nicotine-induced up-regulation required exocytic trafficking or secretory pathway rather than endocytic trafficking including internalization, postendocytic trafficking and lysosomal degradation. Gaimarri et al. (69) reviewed the available data concerning the regulation of neuronal nAChR traffic and expression. The molecular mechanisms underlying the increment of cell surface nAChRs have been investigated both in vitro and in vivo. In vitro studies, cells transfected with α7, α3β2, α4β2, α6β2 and α3β4 nAChR subtypes expressed nicotine-induced up-regulation of these receptor subtypes. In neuroblastoma cell lines express both α7* and α3* nAChRs, chronic nicotine exposure induced both subtypes up-regulation with a different extent and at higher doses than that induces α4β2 up-regulation. These results suggested that sensitivity and extent of up-regulation were different in each receptor subtype. In addition to nAChR subtypes, host cell type also affected the degree of up-regulation. Peng et al. (41, 69) demonstrated that chronic nicotine reduced α4β2 and α7 functional response in transfected oocytes, while Buisson et al.(70) found that chronic nicotine exposure up-regulated the function of α4β2 expressing HEK293 cells by increasing up-regulated acetylcholine evoked current and reducing the sensitivity to desensitization.

In vivo studies, chronic nicotine exposure caused no changes of α2, α3, α4, α5 or β2 mRNA levels in mouse brain, suggesting that post-transcriptional mechanisms were responsible for this up-regulation (69). Nguyen et al. (71) demonstrated that chronic nicotine exposure increases number of α4β2 nAChRs correlated well with increased in functional activity. They suggested that receptor up-regulation by chronic nicotine exposure was active. Moreover, nicotine was incapable to up-regulate both number and function of α3β4* nAChR in IPN, medial habenula and other brain area. Nuutinen et al. (72) identified the time and brain region specific for up-regulation of low affinity neuronal nAChRs, mainly α7 nAChR during chronic nicotine administration in mice.

The mechanisms of nAChR up-regulation remained to be explored and most of nAChR up-regulation information was based on the α4β2 subtype studies (69). The mechanisms of α4β2 subtype up-regulation after chronic nicotine exposure have been proposed as follow:

a. an increase in receptor trafficking to cell surface via secretory pathway (73).

b. a reduction of surface receptor internalization. Nicotine induced conformational changes that prevented the removal of receptor from cell surface (41, 69).

c. an increase in subunit assembly and/or a decrease in receptor turnover(11, 73).

d. the isomerization of surface receptor into a high affinity conformation(70, 74).

The important steps in nicotine-induced up-regulation appeared to be the assembly, trafficking of receptors and their cell surface expression (69). Sallette et al.(37) studied about chronic nicotine exposure-induced α4β2 subtype up-regulation in HEK293 cells and SH-SY5Y neuroblastoma cells. They proposed that nicotine acted on the early maturation within ER on an oligomeric species. It bound to precursor subunit and promoted a critical subunit-subunit interaction step which facilitated the maturation process toward high affinity receptors. Ficklin et al.(75) described a role of ubiquilin-1 in regulating nicotine-induced neuronal nAChR up-regulation. Ubiquilin-1 was an ubiquitin-like protein which could interact with both the proteosome and ubiquitin ligase. It bound to α_3 or α_4 subunits and sequestered

them on proteosome, thus decreased the subunits bioavailability for assembly/trafficking of mature receptors. The expression of Ubiquilin-1 in cultured superior cervical ganglion neurons has been demonstrated to abolish nicotine-induced up-regulation of nAChR, but had no effect on the basal level of surface receptor.

In human kidney tsA201 cells, RIC-3 protein enhanced functional expression of nAChRs subtypes such as α3β4, α4β2, and α7 subtypes (76). Consistently, RIC-3 protein also enhanced α7 nAChR expression in COS cells (77). In contrast, this protein caused a marked functional inhibition of α3β4 and α4β2 expressed in xenopus laevis oocytes and COS cells (77). This discrepancy may be resulted from the difference in host cell factor. However, all results indicated the role of RIC-3 protein in modulating trafficking of neuronal nAChRs. Liu et al. (78) found that α_7 nAChRs on CG neuron were subjected to rapid SNARE dependent trafficking. This trafficking can be bidirectional, both recruitment of new receptor from intracellular pool to the cell surface and internalization of nicotine activated receptors to remove them from the cell surface. Nevertheless, the trafficking did not produce dramatic changes in receptor number and responsiveness. This process required extracellular calcium, calcium release from internal stores and CamkII.

Pon et al. (12) investigated the role of the extracellular C-terminus of α7-nAChR on exporting this receptor to the cell surface. They proposed that tyrosine residue of C-terminus interacted with the cys loop of the N-terminal domain, then it locked the receptor in a mature α-bungarotoxin binding conformation. Subsequently, this conformation masked a retention signal, allowing properly assembled and matured receptor to transport to the cell surface. Briggs et al. (79) found that untranslated regions (UTRs) of the nAChR transcripts can influence the expression of high- and low-sensitivity subform of α4β2 ans α3β2 nAChRs. To investigate the cellular distribution of α3β4 nAChRs, Grailhe et al. (80) tagged the N-terminus of α3β4 subunit with cyan and yellow fluorescent proteins (FP). They observed that most of the FP-α3β4 receptors located in the intracellular compartment of transfected HEK293 cells as well as in transfected hippocampal neuron. However, some

receptors reached the cell surface and responded to ACh, illustrating the high sensitivity of the electrophysiological assay.

Further investigation by Free et al. (13) on cellular mechanism involved in expression of neuronal $\alpha3\beta4^*$ nAChRs, using catecholamine secretion assays and receptor binding studies coupled with receptor alkylation in intact bovine adrenal chromaffin cells. They proposed a model for surface expression of adrenal $\alpha3\beta4^*$ nAChRs. At least 7 steps were involved with nAChRs expression, including transcription, translation, trafficking of newly synthesized receptors to cell surface, trafficking of receptors from intracellular pool to cell surface, endocytosis of surface receptors to intracellular pool and degradation of intracellular receptors (Figure 1). They also found that after alkylation, puromycin treatment prevented the functional recovery as well as caused a loss of both surface and intracellular [^{3}H] Epibatidine binding site which confirmed the requirement of de novo protein synthesis in trafficking. Therefore, they concluded that the predominant route of nAChRs surface expression was via trafficking of newly synthesized receptors to surface and was dependent on de novo protein synthesis (13).

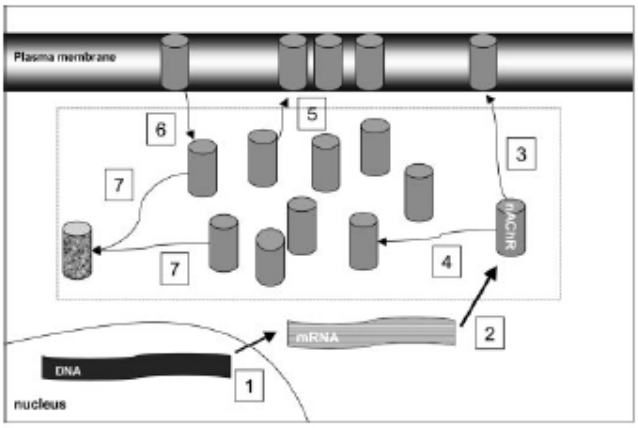

Figure 1 Proposed model for surface expression of adrenal $\alpha_3\beta_4$* nAChRs (13)

Several steps may be involved with the expression of pentameric nAChRs (solid cylinders): 1, transcription; 2, translation; 3, trafficking of newly synthesized nAChRs to surface; 4, trafficking of newly synthesized nAChRs to intracellular pool (dotted box); 5, trafficking of nAChRs from intracellular pool to surface; 6, endocytosis of nAChRs from surface to intracellular pool; and 7, degradation of intracellular nAChRs (mottled cylinder).

Molecular Pharmacology of Nicotinic Acetylcholine Receptors

Nicotinic acetylcholine receptors (nAChRs), belong to a superfamily of ligand-gated ion channel (LGIC), were pentameric assemblies of multiple subunits. As shown in Figure 2, each subunit was composed of 3 domains: an extracellular N terminal domain, a transmembrane domain and a short extracellular carboxy terminal domain (1-3, 5). Large hydrophilic N-terminal domains of the two α-subunits contained the binding sites for acetylcholine. A transmembrane domain had 4 hydrophobic membrane-spanning alpha-helical regions (M_1, M_2, M_3 and M_4). The M_2 regions of five subunits faced inside to form ion channel. Three negatively charged rings of 5 amino acids (one from each M_2 subunit) enhanced positively charged ion pass through the channel. At desensitized state of nAChR, the uncharged leucine ring at the center has responsibility to close the ion channel.

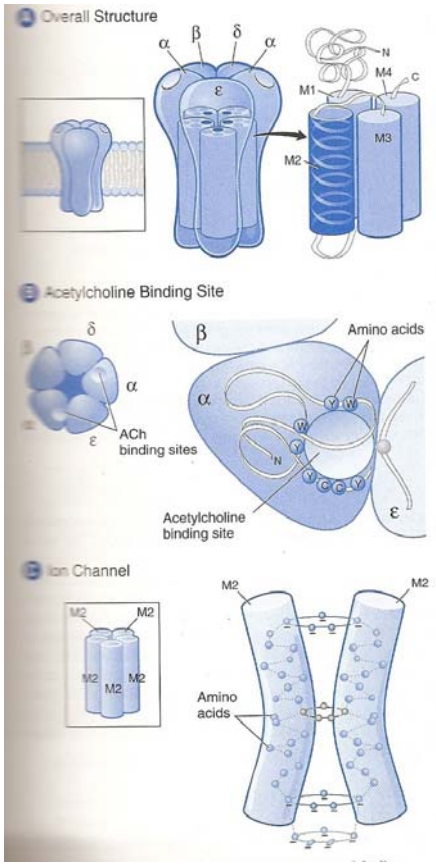

Figure 2 Structure of the nicotinic acetylcholine receptor (3)

As mentioned previously, nAChRs have been divided into muscle nAChRs and neuronal nAChRs (81). Currently, muscle nAChRs were found to compose of two α_1 subunits and each of β1, δ, and γ (in adult) or ε (in fetus). Differently, neuronal nAChRs were composed of 2 subunits; α (α2-α10) and β (β2-β4) subunits (82). There was strong evidence showed that neuronal nAChRs containing α7, α8, or α9 subunits were able to form functional homomers, while α2, α3, and α4 can form functional receptor only in combination with β2 or β4 subunits. α5 and β3 subunits required the presence of other α and β subunits to form functional receptors. The expression of β4 or possibly other α or β subunits was necessary for forming α6-functional receptors. α9 subunit associated with α10 to form heteromeric nAChR (83). Many subtypes, multiple heteromeric (α3β4*, α3α5β4, α4β2 etc.) and homomeric (α7, α8, α9) subtypes were expressed in neuronal nAChRs (1, 5, 84). The homomeric receptors had 5 identical Ach-binding sites per molecule located at the interface between two adjacent subunits. The heteromeric receptors were composed of at least two α-subunits. They had two ACh-binding sites per molecule located at the interface between α and β subunits (1).

Neuronal nAChRs

1. Distribution

Neuronal nAChRs were widely expressed in cholinergic neurons throughout both central nervous system (CNS) and peripheral nervous system (PNS) as in autonomic ganglia, adrenal medulla (1, 2, 5). Recently, they were also found in many different non-neuronal cell types throughout the body including T- and B-lymphocytes (85), macrophages, vascular endothelial cells, epithelial cells of intestine and lung, adipocytes, as well as skin keratinocytes (4, 86).

A variety of neuronal nAChR subtypes distributed in different tissues. In CNS, the majority nAChRs were α4β2* receptors (90%) and the others were α7* nAChRs. In peripheral, the predominant nAChRs appeared to be α3β4* nAChRs such as α3β4α5, α3β2β4, α3β2β4α5 receptors. α7* nAChRs constituted another major ganglionic nAChRs (5). In brain, the highest concentrations of α4β2 subtype were

located in the hippocampus, thalamus, striatum and cortex. α7 subunit was expressed particularly in the hippocampus, hypothalamus, cortex and motor nucleus of vagus nerve (1, 5). α6β3* subtypes were expressed in the optic pathway, the locus coeruleus and dopaminergic neurons of the mesostriatal pathways (1, 5). α9/α10 containing receptors were presented in the pituitary pars tuberalis, the olfactory epithelium and the cochlea. Although, α3β4 receptors were presented particularly in autonomic ganglia (87, 88), including sympathetic ganglia (89, 90), parasympathetic ganglia (91), myenteric neuron (92), sensory ganglia (90, 93) and adrenal gland (25, 94), they also existed in relatively high densities in the brain such as pineal gland (83, 95), cerebellum (96, 97), locus coeruleus (92, 96), the anteroventral nucleus of the thalamus (98), the subiculum of the hippocampus (99), the medial habenula and interpeduncular nucleus (83, 100-102), spinal cord and retina (87, 103).

Using in situ hybridization, Winzer-sershan et al.(104) examined α3 and β4 nAChR mRNAs expression during rat brain development and in adult. During embryonic development, α3 and β4 mRNAs strongly expressed in PNS especially retina, peripheral ganglia, the whisker barrels and taste bud of the tongue. In CNS, α3 and β4 mRNAs moderately expressed in embryonic day15 which decreased toward late gestation. However, both mRNAs expressed in a detectable level throughout the brain at all embryonic ages and in adult.

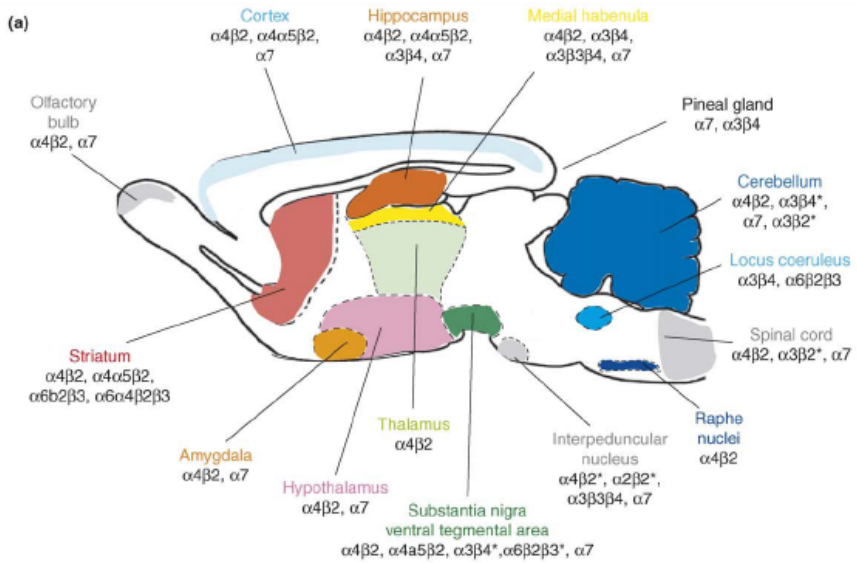

Figure 3 Localization of nAChR subtypes in rodent CNS.(69, 105)

2. Function

In CNS, nAChRs were involved in many processes connecting to cognitive functions, learning and memory, arousal, sleep, anxiety, food intake, reward, motor control and analgesia (1, 105). In brain, nAChRs were preferentially located at the presynaptic and preterminal sites which modulated the release of many neurotransmitters throughout the CNS. The neurotransmitters release was initiated by axonal firing or directly by inducing sufficient Na^+ and/or Ca^{2+} influx to cause local depolarization. Then, axonal firing activated the release machinery. nAChRs also acted as autoreceptors and heteroreceptors regulating the synaptic release of acetylcholine (ACh) and other important neurotransmitters such as dopamine, norepinephrine, serotonin. nAChR activation increased the release of Ach from cortex and hippocampus, DA from striatum and frontal cortex, NE from hippocampus, 5-HT, glutamate from cortex, medial habenula nucleus and hippocampus and GABA from interpeduncular nucleus (1, 106). This activation also enhanced the release of calcitonin gene-related peptide and substance P in the spinal cord (107). In addition, it mediated neurotrophic actions of nerve growth factor, brain-derived neurotrophic factor and α-fibroblast growth factor which provided neuroprotective effects (6), while nAChRs in pineal gland may influence melatonin secretion (86).

Due to the distinct nAChR subtypes localizing on these presynaptic sites, they provided the pleiotropic effects of nAChR agonists (105, 108). For example, α7* subtype regulated glutamate release whereas α4β2 subtype modulated DA release. Activation of these receptors induced calcium influx into the presynaptic site via voltage-dependent calcium channel or cation influx through receptors. Subsequently, the intracellular calcium led to neurotransmitter release (1, 5). Although most of nAChRs in CNS located in the presynaptic site, some, α7*, α3β4*, α4β2* subtypes have been identified at postsynaptic site (5).

In PNS, nAChRs played prominent roles in autonomic neurotransmission and adaptive responses to stress (3, 109). α7-nAChRs mediate Ca^{2+} signaling in T-

lymphocyte and were supposed to affect immune function (85). Therefore, the alterations in expression of neuronal nAChRs have been associated with a variety of neurological and non-neurological diseases (1, 2, 110, 111).

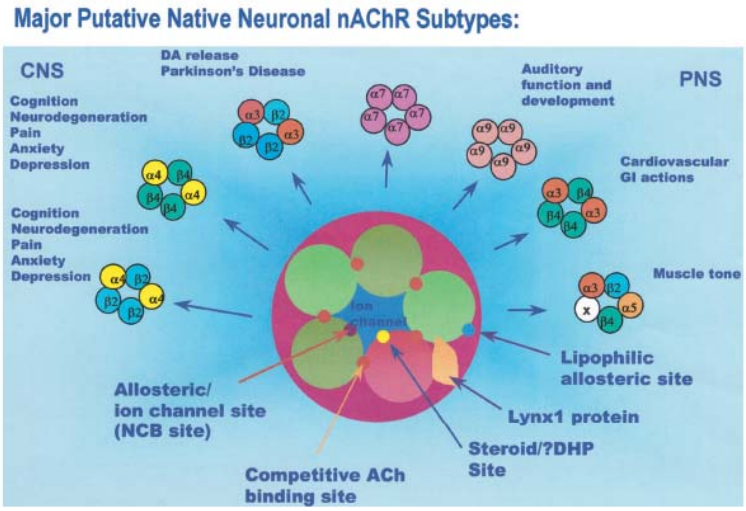

Figure 4 Schematic of the pentameric nAChR and possible function of known native constructs (6)

3. neuronal nAChRs and diseases

Both α6β3β2 and α4β2 subtypes in striatum were responsible for DA release from nerve endings. The loss of dopaminergic neuron in the nigro-striatal pathway was the pathology of Parkinson's disease. Also, the reduction of α4β2 level has been found in the cerebral cortex of Parkinson's disease patients (1). In Alzheimer's disease, the number of brain nAChRs especially α4β2 subtype was decreased in the neocortical area, hippocampus, and thalamic nuclei. In epilepsy, the mutation of α4 and β2 gene facilitated the synchronization in the thalamo-cortical circuits and generated seizure (1). The olfactory bulbectomy (OBX), a model of depression, led to up-regulation of cerebrocortical α4β2 subtype, but down-regulation of the striatal α7 subtype (110). On the other hand, schizophrenic patients had a reduction of α_7 receptor in the hippocampus, the reticular nucleus of thalamus and the cingulated and frontal cortex (112). Alternatively, the antinociceptive effects of nAChR agonists were mediated via the activation of α4β2 subtype (111).

In association with the effect of nicotine, the anxiolytic as well as antidepressant effect of nicotine were mediated via α4β2 nAChR (113). Decreased cholinergic function could contribute to both the cognitive deficits and the neuronal degeneration, associated with dementia. And, nicotine had neuroprotective effect via α4β2 and α7 nAChRs (114).

Regarding to the non-neurological diseases, small cell lung carcinomas (SCLC) has been related to smoking. The studies in SCLC cell lines suggested that an autocrine or paracrine cholinergic pathway was located in lung tumors. The activation of nicotine on nAChRs enhanced cell proliferation, probably through a Ca^{2+} influx, which stimulated MAP and Akt kinase. These MAP and Akt kinase activations occurred via an α7 and α4β2 subtypes, respectively (1). In addition, α9 nAChR-knockout mice showed a functional deafness (110). Arredondo (4, 147) also reported that nicotine and environmental tobacco smoke (ETS) enhanced expression of regulators of cell cycle and apoptosis, which was inhibited in human oral keratinocytes lacking of α_3 nAChR. NNK, 4-(methylnitrosamino)-1-(3-pyridyl)-1-butanone,a tobacco specific carcinogen stimulated cell proliferation in normal human bronchial epithelial cells (NHBE). It occured through activation of the NFκB, which up-regulate cyclin D1 expression. α3β4 nAChR was the major target mediating NNK-induced cyclin D1 expression in these cells (148). Consistently, Tsurutani et al.(149) reported that nicotine and NNK induce proliferation of NSCLC cells (non-small cell lung cancer) in an Akt-dependent manner. They also found that α3, α4 or α7 nAChRs agonist could activate Akt in NSCLC cells.

With regards to the inflammatory mediators, nicotine or ACh pretreatment of human peripheral blood mononuclear cells, reduced the amount of the tumor necrosis factor (TNFα) and other inflammatory cytokines such as IL-1β, IL-18, IL-6 (115, 116). α7-nAChR was therefore related to some anti-inflammatory effect. Smoking was a risk factor in development of premature facial wrinkling (4). Nicotine also inhibited keratinocyte migration (117), and slowed wound healing via α7 nAChR (118).

nAChRs has also been linked to some metabolic syndromes. However, it was a beginning period to study the role of nAChRs in adipose tissue (4). Insight to the effect of nicotine on glucose metabolism, smoking was a predisposing factor for insulin-resistance, which was associated with type 2 diabetes. Ilcol et al. (119) found that intraperitoneal injection of choline produced a dose-dependent increasing in serum glucose level in rat. This hyperglycemic effect was mediated solely by nAChRs. Cigarette smoking was implicated in the formation of occlusive vascular diseases. Pestana et al. (120) concluded that nicotine had a mitogenic effect on human aortic smooth muscle cells by increasing of platelet-derived growth factor (PDGF-BB) transcription and protein production as well as PDGFβ-receptor levels.

α3β4 nAChRs

In neuronal system, α3β4* nAChRs were expressed predominantly in postsynaptic neuron of all autonomic and sensory ganglia as well as in adrenal medulla cell. They mediated the fast excitatory signaling in all ganglia which influenced sympathetic and parasympathetic responses throughout the body. Although α3β4* receptors was found to be less abundance in the CNS, they had a presynaptic modulatory function in controlling the release of several neurotransmitters.

In CNS, Woo et al.(106) demonstrated that nicotine stimulated NE release through activation of α-bungarotoxin insensitive nAChRs in human cerebral cortex slices. The effect of nicotine was mediated by α/β heteromeric not α_7 homomeric receptor. Sershen and colleagues (121) suggested the possible involvement of α3 and β2 subunits in the control of NE released from rat hippocampal slices. In addition, Luo et al.(122) found that α3β4-containing nAChRs mediated NE released from rat hippocampal synaptosomes. In contrast, Azam et al. (123) reported that there were at least 2 populations, α6(α4)β2β3β4 and α6(α4)β2β3 subtypes, which contributed to NE release from mouse hippocampal synaptosomes. Species difference might partly be responsible for this discrepancy.

Modulation of dopamine-mediated neurotransmission had the crucial roles in the addictive properties, locomotor behaviour, cognitive function. Nicotine addictive properties were resulted from the activation of presynaptic nAChRs which enhanced DA release in cortical brain reward circuits. The nAChR regulating DA release from striatal terminal has been extensively studied in both rats and mice. Kulak et al.(124) reported that one-third of DA release in rat striatal synaptosomes was mediated by α3β2 subtype. This finding corresponded to that obtained from Luo et al.(122). Using rat hippocampal slices, Cao et al.(125) documented the role of $\alpha3\beta4^*$ and at least one other nAChR subtype in DA release. Knockout mice and immunoprecipitation studies have established α6β2* and α4β2* subtypes on the dopaminergic terminal (126). Consistently, Salminon et al. (127) also identified 2 classes of striatal presynaptic nAChRs mediating DA release in mice. They were the sensitive α-CtxMII, probably α6β3β2 and α4α6β3β2 subtypes, and the insensitive α-CtxMII, probably α4β2 and α4α5β2 subtypes. Based on these results obtained from Cao et al. and other researchers, α3-containing nAChRs was one of the variety subtypes which contribute to DA release.

Further studied in drug addiction, Taraschenko et al.(92) provided evidence that $\alpha_3\beta_4$ nAChRs were involved in 2 signs of morphine withdrawal, diarrhea and weight loss. The association of diarrhea to this receptor subtype was explained by the densely expressing of α3β4 nAChRs in the myenteric neurons of gut. It mediated excitatory cholinergic neurotransmission in the gut and regulated intestinal peristalsis. In addition, in the tail-flick assay which was used to test for a spinal reflex of pain, Marubio et al.(128) suggested that $\alpha_3\beta_4$ nAChRs modulated the peripheral antinociceptive effect of nicotine. Beside α7 homomeric subtype, Turner et al. (97) detected 6 heteromeric populations in rat cerebellum. Among these heteromeric, α3β4, α3β2β4, and α3α4β4 appeared in 22, 12 and 12 %, respectively. Dysregulation of the cerebellar nAChR activity could contribute to the developmental disorders of brain such as autism.

Moreover, α3β4 nAChRs were expressed at GABAergic presynaptic terminals in the area postrema of rats slice preparation and induced Ca^{2+} influx to trigger vesicular

release (129). The nicotine-activated α3β4 nAChRs regulated inhibitory postsynaptic currents (IPSCs). Zhu et al. (130), suggested that nicotinic activation increased the frequency of spontaneous inhibitory postsynaptic currents (sIPSCs) in rats basolateral amygdale (BLA) neuron. This activation mediated mainly on α3β4 nAChRs in GABAergic system and played an important role in the modulation of synaptic transmission in the amygdala. The amygdale circuit was involved in fear conditioned responses. Since GABA is an inhibitory neurotransmitter in CNS and α3β4 nAChRs were found to be existed in this inhibitory system, Salas et al.(131) examined the effect of nAChR subtypes on seizure in mutant mice. They found that $\alpha_3\beta_4$ nAChRs were responsible for nicotine-induced seizure and hypolocomotion.

Following the path from CNS, autonomic ganglia were the relay stations for transferring information from CNS to peripheral organs in order to control most of visceral organs (132). nAChRs were located on both pre and postsynaptic terminals. The presynaptic nAChRs facilitated neurotransmitter release while postsynaptic receptors mainly mediated fast synaptic transmission (fEPSP) to transfer neuronal information between pre and postganglionic cells. Although, autonomic ganglia expressed α3 and β4 subunits at high level, they also contained transcripts for α4, α5, α7 and β2 subunits (132, 133).

In the controlling cardiac functions, Bibevski et al. (134) confirmed the presence of α3, α7, β2 and β4 subunits in canine intracardiac ganglia. They also reported that functional ganglionic transmission in this ganglion was mediated mainly via α_3/β_2 containing nAChRs, with a smaller contribution via α7 nAChR. In addition, axotomy (transection of postganglionic nerves) of rat SCG resulted in the loss of α3 subunit mRNA (135) and protein (136) which contributed to a decrease in ganglionic synaptic transmission. Poth et al.(91) reported that α3 subunit was expressed at high level in all autonomic ganglia, including the sympathetic ganglia innervating heart and cardiac ganglionated plexus. The majority of superior cervical ganglia (SCG) neurons expressed $\alpha_3\beta_4^*$ subtype. A lack of α3 resulted in a severe cardiac phenotype which led to early mortality (25, 137). However, α7 nAChRs were expressed on both

sympathetic and parasympathetic neurons innervating heart and contributed to negative chronotropic effect. They summarize that there were at least 2 subtypes, α3β4* and α7* expressing in autonomic neuron for controlling cardiac function (132).

In the role of nAChRs on pelvic ganglion neuron (MPG) was reported by Park et al. (138). They found that the α3 and β4 subunits activation in rat MPG neurons stimulated fast inward current and intracellular calcium. Then, there was an increase in pelvic autonomic synaptic transmission.

Concerning to enteric nervous system (ENS), Zhou et al.(139) studied the electrophysiological and pharmacological properties of nAChRs in guinea pig small intestinal myenteric neurons. They indicated that myenteric neurons predominantly expressed nAChRs composed of α3, α5, β2 and β4 subunits. The pharmacological properties (IC_{50}) indicated that functional nAChRs contain α3 and β4 subunits.

α_3 subunit appeared to be important to normal autonomic functions in animal (132, 140-142) and in human. Autoimmune autonomic neuropathy (ANN) was a severe subacute autonomic failure which affected sympathetic, parasympathetic and enteric autonomic function(9). The symptoms were orthostatic hypotension, gastrointestinal dysmotility as gastroparesis and severe constipation, anhidrosis, lacking of pupillary light responses, dry eyes and dry mouth (sicca symptoms) and bladder dysfunction (143). Most of ANN patients had high serum autoantibodies specific to ganglionic neuronal nAChRs which predominantly correlated to severe dysautonomia (10). Immunization rabbit with a neuronal α3 nAChR subunit fusion protein produced ganglionic nAChR antibodies and lacking of surface nAChRs. These rabbits developed an autonomic failure (Experimental AAN, EAAN) which characterized as ANN in human (9). Consistently, Lennon et al. (144) reported gastrointestinal hypomotility, dilated pupils with impaired light response, distended bladder in rabbits immunized with a recombinant α3 subunit. They also confirmed that this disorder was a postsynaptic channelopathy. In addition, Vernino et al. (145)

found the autonomic dysfunction in mice passively injected with rabbit IgG containing ganglionic AChR antibodies. They suggested that EAAN is an α3 nAChR antibody-mediated disorder.

Likewise, knockout mice lacking of α_3-subunit survived to birth but had impaired growth and increased mortality before weaning (7). These mutant mice had an enlarge bladder, dribbling urination, urinary stones, bladder infections, mydriasis and lacking of pupil contraction in response to light. There was no bladder contraction in response to nicotine. These abnormalities resembled a megacystis-microcolon-intestinal hypoperistalsis syndrome (MMHIS) (7). In MMHIS patients, Richardson et al.(8) found that the α3 subunit mRNA was undetectable in the small bowel. They proposed that α3 subunit mutation was responsible for MMHIS. Other studies in knockout mice demonstrated the functional role of nAChR subunits in autonomic ganglia (141). The α3 subunit mediated fast postsynaptic current. The combinations of α3 with β2 or β4 subunits were the major nAChRs subtypes found in autonomic ganglia. The abundance and properties of β4 subunit led to a suggestion that this subunit seemed to be the predominant β component in autonomic ganglia. However, their absence could be compensated by up-regulation of β2subunit. These up-regulated β2 subunit formed postsynaptic α3β2 subtype to maintain normal ganglionic transmission (141, 146).

In addition, Terzano et al. (150) found the loss of α3-nAChRs in intact neurons of the entorhinal cortex in the late elderly. However, they observed no significant difference in α3-mRNA expression in hippocampus, entorhinal cortex and thalamus between Alzheimer's patients and controls.

All the above evidence confirmed the importance of α_3-containing receptor on neuronal (both CNS and PNS) and non-neuronal functions. However, the precise subunit composition as well as the physiological and pathophysiological roles of α_3-nAChRs remained unclear and needed to be elucidated.

Native and Recombinant Cell Line as Neuronal Model

In the studies of neuronal nAChRs surface trafficking, both native and recombinant cells line could be used such as bovine adrenal chromaffin cells, a stably transfected HEK293 (human embryonic kidney) cells expressing recombinant bovine adrenal α3β4 nAChRs (BMα3β4 cells), SH-EP1-pCEP4-hα7 cells (151). Adrenal chromaffin cells were derived from neural crest tissue and were regarded as autonomic ganglions. They were cholinergically innervated by the splanchnic nerve from the sympathetic nervous system. ACh activated nAChRs in chromaffin cells, and caused depolarization which triggered catecholamine secretion. The precise nAChR subtypes on these cells remained unclear. In earlier studies, the presence of mRNA for α3, α5, and β4 nAChR subunits has been demonstrated in PC12 cells (the rat pheochromocytoma cell line) (152, 153). Using (152) RT-PCR analysis and In situ hybridization, the α3, α5, α7 and β4 subunits were detected in bovine adrenal medulla (23, 24, 94, 154). For other species, Mousavi et al. (155) demonstrated the expression of mRNA for α3, α4, α5, α7, β2, β3 and β4 subunits in human adrenal medulla. All subunits in human adrenal medulla except β_3 subunit also existed in rat and mouse adrenal medulla. Therefore, the major populations of nAChR in adrenal medulla were probably composed of α3, α5, α7, and β4 subunits.

Bovine adrenal chromaffin cells expressed at least 2 subtypes nAChRs. The bound α-bungarotoxin (α-Bgt) subtype which was likely composed of α_7 subunit, and mAb35-nAChR which was insensitive to α-Bgt (26, 156). The catecholamine secretion was Bgt-insensitive. Therefore, the primary nAChR subtype responsible for catecholamine secretion in bovine adrenal chromaffin cells was proposed to be the mAb35-nAChR (23). The subunit composition of this subtype was unknown. Tachikawa et al. (25) supported that α3β4 or α3β4α5 were responsible for catecholamine secretion from bovine adrenal chromaffin cells. Meanwhile, mAb35-nAChRs on chick ciliary ganglion neuron have been reported to contain α3, α5 and β4 subunits (157, 158).

The available evidence suggested that adrenal chromaffin cells could provide an appropriate neuronal model. First, as a part of sympathetic nervous system, they

performed many typical functions such as neurosecretion (159). Activation of nAChRs led to the catecholamine release which modulated a variety of cellular responses including sympathetic effects on cardiovascular system in controlling blood pressure, heart rate and contractility. Second, they provided the results which alteration at molecular level should be corresponded to alterations at physiological and pharmacological levels. Finally, different experiments such as receptor binding assay, functional assay can be performed in parallel.

HEK293 cells were another appropriate model to study the expression of nAChR. These cells exhibited fast exponential growth with a doubling time of 24 hours (88). They were easy to culture, provided good adhesion to plastic or glass surfaces (86). They also had the relative high transfection efficiency. Since rat, bovine and human nAChR subtypes could stably express in this cell line, it enabled the possibility to compare rat, bovine and human receptors expressed in the same cell line. BMα3β4 cells were constructed as a heterologous HEK293 cell line expressing α3, and β4 subunits. The pharmacological characteristics of these recombinant receptors were similar to native bovine α3β4* nAChRs (26). Moreover, the number of nAChRs expressed in BMα3β4 cells was 100 fold higher than in the native chromaffin cells. These implicated the potential use of BMα3β4 cells to determine the regulation of α3β4 nAChR expression (26, 27).

APC Protein

1. APC: structure and physiological roles

Adenomatous polyposis coli (APC), a 300,000 mol.wt cytoplasmic protein with 2843 amino acids, contained an oligomerization domain and an armadillo region in the N-terminus, a number of 15- and 20- amino acid repeats in a central protein and a C-terminus which consisted of a basic domain, EB1 binding domain and PDZ binding motif (Figure 5) (14, 15). These multiple domains enabled the ability of APC protein to interact with a number of proteins such as Asef, β-catenin, axin, microtubule, an end binding protein (EB1) and the human disc large protein (hDLG). The interaction of APC with distinct proteins indicated its functions on the Wnt signaling pathway,

cell adhesion, migration, chromosome segregation, spindle assembly, apoptosis and neural differentiation (15).

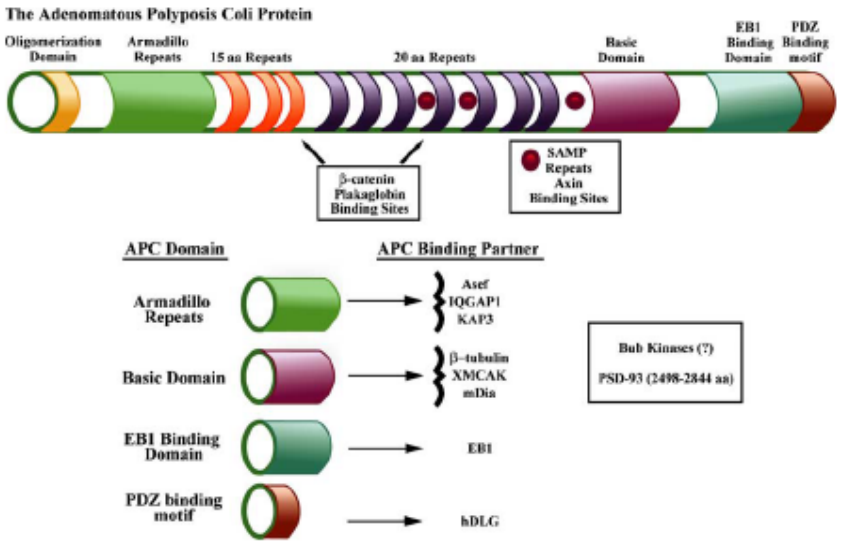

Figure 5 Functional domains of Adenomatous Polyposis Coli (APC) Protein (15)

The role of APC as a tumor suppressor protein has been extensively studied. Mutation of APC was typically identified in colorectal cancer. Its tumor suppressive effect can be explained by a classical function of APC protein as a negative regulator of Wnt pathway (16, 160). As shown in Figure 6 (16), in the absence of Wnt signaling, after binding to APC protein, the axin complex(APC/axin/GSK3-β) was active and phosphorylated β-catenin/Armadillo to earmark β-catenin for ubiquitin-mediated degradation by the proteasome. Subsequently, β-catenin was inactive and unable to act as a co-activator of transcription with the TCF/LEF family. Finally, TCF transcription was off. Contrarily, the binding of Wnt ligand to the Frizzled receptor led to the inactivation of axin complex by Dishevelled (Dsh). Unphosphorylated β-catenin accumulated, translocated to nucleus and bound to TCF/LEF. These processes stimulated the transcription of Wnt target genes and their proliferative activity(14, 16, 160). Therefore, a tumor suppressive activity of APC protein depended on its ability to down-regulate soluble β-catenin.

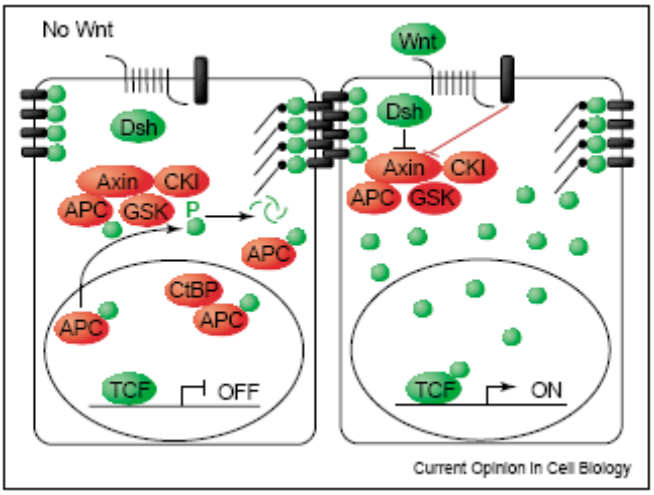

Figure 6 APC protein and the Wnt signaling pathway (16)

Horizontal black bars, E-cadherin; green dots, β-catenin/Armadillo; black dots, α-catenin; thin black lines, actin filament.

The localization of APC protein on sites of cell-cell adhesion indicated its role on cell-cell adhesion. APC protein caused to redistribution of β-catenin and E-cadherin, the adherens junction proteins, from cytoplasm to plasma membrane, which promoted the adhesive property of APC (16). The coordinated loss of Wnt signaling and gain in cell adhesion may explain the tumor suppressor property of APC protein. On the other hand, binding of APC protein and a different proteins located at the plus ends of microtubules may contribute to its role in cell migration (15, 161). It associated with EB1, mediated microtubule polymerization, stabilization and capture at the cell membrane to promote cell migration. It also interacted with Asef (guanine nucleotide exchange factor) and led to an increase in cell spreading and membrane ruffling. Langford et al. (162) studied about the trafficking of APC protein in mammalian cells (COS7 cells). They indicated that APC can be found in 2 populations at cell periphery. The first was highly dynamic and associated with microtubule. The second was static and associated with actin.

APC proteins mediated attachment of the kinetochore to microtubules of the mitotic spindle and promoted chromosome segregation (15). It also had a negative effect on cell growth by blocking G0/G1 to s-phase transition (15). This effect may

be resulted from inhibiting the transcriptional activation of proliferative Wnt target such as *c-myc* and *cyclin D1*. Moreover, this protein also induced apoptosis by unknown mechanism.

2. APC: distribution in brain

APC protein expressed higher level in brain than in peripheral tissues, including colon and postsynaptic side of the neuromuscular junction (17, 20, 163). In the brain of adult animals, APC protein was predominantly expressed in the olfactory bulb, hippocampus and cerebellum (164). However, a little differences in the pattern of APC protein distribution have been reported. In rats, immunohistochemical studied with a C-terminal APC antibody (163) indicated the distribution of APC protein particularly in large neurons, such as layer V cortical pyramidal neurons in hippocampus, cerebellar Purkinje cells, and olfactory bulb mitral cells. It could be found in the cytoplasm as well as dendritic and axonal process. The compiled data including in situ hybridization studies (17) confirmed the predominant expression of APC protein in neuron rather than in glial cells.

In contrast, the result obtained from immunohistochemical studies with an N-terminal APC antibody in rats (165) as well as immunohistochemical studies with a C-terminal APC antibody in mice (166). They demonstrated that APC protein expressed in glial cells rather than neuron. Senda et al. showed that APC protein was localized in the pericapillary astrocytic endfeet throughout the CNS, the astrocytic processes in the cerebellar granular layer, the terminal plexuses of the basket cell fibres around Purkinje cells (166). It was further expressed in neuronal cell bodies and nerve fibers in the olfactory bulb, hippocampus, brainstem, spinal cord and dorsal root ganglia. This discrepancy of result revealed the effect of species differences and insufficient sensitivity of antibodies used in each experiment (163).

With regards to the subcellular location, Brocardo et al.(167) illustrated that in human SW480 cells, full-length and mutant APC were primarily located in cytoplasm with CRM1(chromosome region maintenance1 protein)-dependent nuclear export.

Mutant APC shuttled in and out of nucleus more efficiently than the full-length APC in colon carcinoma cell line and MDCK cell line.

Moreover, the level of APC protein was changed in various developmental status of brain. During embryogenic and early postnatal development, high levels of APC protein were expressed throughout the rat brain. By 6 weeks after birth, it reduced to adult levels except in the olfactory bulb, which still be in a high level (17). In developing cultured rat hippocampal neuron, APC protein was expressed in high concentration at the growth cone and in the distal portion of the longest process which was growing very rapidly. It was also expressed but in a lower concentration in other processes with a slower growth rate (164). Thus, all evidence implicated the role of APC protein in the nervous system.

3. APC: neuronal functions

Evidence supported the role of APC protein in neuronal differentiation and development of synapses has been presented (15). Dobashi et al. reportd the APC protein-up-regulation during NGF (neural growth factor) induced differentiation of rat pheochromocytoma (PC12) cells (18). Matsumine et al. found APC protein colocalized and bound with hDLG at the synapse in cultured hippocampus neurons (168). hDLG, a member of SAP family appeared to mediate the clustering of NMDA receptor and K^+ channel at specific synaptic sites (169). Consistently, in muscle cells, neural agrin caused tyrosine phosphorylation of the nicotinic acetylcholine receptor (nAChRs) β-subunit and induced nAChRs clustering to postsynaptic cytoskeleton. It also recruited APC protein from cytoplasm and nucleus to the postsynaptic membrane. In addition, APC protein highly specifically bound to the C-terminus of β-subunit nAChRs. These showed the requirement of APC protein in nAChRs clustering to postsynaptic site of the neuromuscular junction (20).

With the neuronal functions of APC protein, it was proposed that many neural disease might be the result of abnormal APC expression. Leroy et al.(19) reported that APC expression was up-regulated in astrocytes of human brain in Alzheimer's disease, diffuse Lewy body disease, central infarcts, HIV encephalitis and prion

disease (Creutzfeldt-Jacob disease). APC-positive astrocytes seemed to be involving with Aβ deposits and inflammatory processes. Thus, the increment of APC immunoreactivity in astrocytes might be a useful marker in evaluation of Alzheimer's disease and other pathological conditions.

Recently, Temburni et al. established the function of APC protein in localizing α_3-nAChRs to neuronal postsynaptic sites in chick ciliary ganglion (CG) neurons. They also identified PSD-93, β-catenin and microtubule end binding protein (EB1) as APC protein binding partner. An in vivo overexpressed APC dominant-negative protein in CG neurons caused a dramatic reduction of α_3-nAChRs surface level. It also led to a reduction of surface membrane associated cluster of PSD-93 (postsynaptic density-93) and EB1 (21). PSD-93 colocalized with neuronal nAChRs at synapses of the sympathetic SCG (superior cervical ganglion) and parasympathetic SMG (submandibular ganglion). It also formed complex with neuronal nAChRs in vivo. Synaptic clusters of nAChRs disassembled faster in mice lacking PSD-93 compare to wild type mice. These results demonstrated that PSD-93 regulated synaptic stability particulary at neuronal cholinergic synapse (170).

Interestingly, Farias et al.(22) reported that Wnt-7a , an active ligand in the canonical Wnt signaling pathway, induced a dissociation of APC protein from β-catenin complex including an interaction of APC with α_7-nAChRs in hippocampal neurons. It also enhanced a relocalization of APC to membranes, a clustering of APC in neurites and a coclustering of APC with different presynaptic protein markers. In additions, it also increased the number and size of coclusters of APC and α_7-nAChRs in presynaptic terminals. These results established the involvement of the canonical Wnt pathway in regulating the presynaptic localization of APC and α_7-nAChRs.

This information indicated the importance of APC protein in neuronal signaling and the involvement of APC protein to neuronal nAChRs trafficking. However, in-dept information remained unclear and needed to be elucidated.

Antisense-Based RNA Technologies

RNA controlled gene expression through several mechanisms in both nucleus and cytoplasm. It affected transcriptional and post-translational processes. Over the past two decades, antisense-based mRNA knockdown technologies have been widely used for silencing gene expression. The major classes of antisense approaches included antisense oligonucleotides (AS-ODNs), ribozymes, DNAzymes and RNA interference (RNAi) (171). Both AS-ODNs and RNAi relied on the presence of a nuclease in the cells. With different mechanism, ribozymes had sequence-specific binding with RNA. They acted as an enzyme which directly cut the target mRNA (172).

Major classes of antisense approach

1. Antisense oligonucleotides (AS-ODNs)

AS-ODNs are the synthetic single-stranded short sequences of DNA, with typically 18-25 bases in length. They were designed to sequence-specifically hybridize with mRNA forming a duplex. This DNA-RNA duplex attracted RNase H, an endogenous nuclease which cleavaged the bound RNA. Then, the DNA antisense was free to rehybridize with another copy of mRNA (173, 174). The specificity of the antisense approach was based on Watson-Crick base-pairing interactions. In conclusion, the ODN-RNA duplex prevented protein translation by attracting RNase H to degrade RNA and steric hindrance of the ribosomal assembly.

The stability was one of the problems when using AS-ODNs. Unmodified AS-ODNs were very short lasting because they were rapidly breakdown by nucleases. A successful modification appeared as phosphorothioate in which a sulfur atom replaces one oxygen atom in the phosphorate group of the phosphodiester bond. This phosphorothioate modified AS-ODNs were nuclease resistant leading to increasing stability and affinity to target mRNA. AS-ODNs were primarily taken up by cells via endocytosis. Subsequently, they escaped from endosome/lysosome and entered the nucleus to bind with their RNA complement. It was difficult to directly permeate across cell membrane because of their hydrophobicity and macromolecule. In additions, cationic liposomes and electroporation were commonly used carriers.

2. Ribozymes

Discovered in the early 1980s, ribozymes were naturally RNA molecules containing enzymatic activity. Natural ribozymes were necessary for some normal cellular processes such as transcription in plant, animal cells and viruses. The synthetic ribozyme usage was aimed to reduce target RNA, thus lower levels of the protein encoded by the target RNA. Among several types of ribozymes, the hammerhead ribozyme and the hair-pin ribozyme were the most common used for research. Ribozymes recognized specific RNA sequences in the same manner as antisense pairing through strand complementarily. Then, they catalyzed a site-specific phosphodiester bond cleavage within target molecule, repeating the process (173, 174). Due to their ability to rapidly cleave multiple target molecules, ribozymes seemed to be more useful than other antisenses. It required a divalent metal ion, usually Mg^{2+} to promote proper folding of the catalytic core and to be a catalytic cofactor.

There were 2 methods for delivering ribozymes to cells as exogenous delivery and endogenous expression. Cationic liposome enhanced cellular uptake of ribozymes and protected them from serum RNase. The benefit of exogenous delivery was that foreign RNA molecules were fairly tolerant to the immune system. For endogenous expression, viral vectors and plasmid vectors may be used.

3. DNAzymes

DNAzymes or small catalytic DNAs were capable to site-specifically cleave RNA targets. They bound to their RNA substrates via Watson-Crick base pairing. Subsequently, they specifically cleaved the target mRNA resulting in 2′,3′ cyclic phosphate and 5′-OH termini. The cleavage of target mRNAs promoted their destruction and the DNAzymes recycle (171).

4. RNA interference (RNAi)

RNA silencing referred to a genetic regulatory mechanism which limited the transcription either by suppressing transcription (transcriptional gene silencing, TGS) or by activating a sequence-specific RNA degradation process (post transcriptional

gene silencing, PTGS/RNAi) (175). Naturally, RNAi represented a conserved cellular defense mechanism. This mechanism was for controlling the expression of foreign genes in almost all eukaryotic organisms including human.

RNAi

In 1998, Fire et al. discovered RNAi as the inhibition of gene expression by double-stranded RNA (dsRNA) (176). It was triggered by dsRNA precursor varying in length and origin(177). These dsRNA precursors were quickly changed into short RNA duplexes of 21-28 nucleotides in length. The duplex promoted recognition and cleavage or translational suppression of complementary single-stranded RNA such as mRNA.

According to their origin and function, RNAi were divided into 3 types of naturally small RNA as short interfering RNAs (siRNAs), repeated-associated short interfering RNAs (rasiRNAs) and microRNAs (miRNAs). dsRNA can be generated by RNA-templated RNA polymerization or by hybridization of overlapping transcripts. These dsRNA were processed to siRNA or rasiRNA which generally led to mRNA degradation and/or chromatin modification. In addition, endogenous transcripts contained complementary 20 to 50 basepair inverted repeats to form dsRNA hairpins. Short hairpin RNAs (shRNAs) referred as single-stranded RNA molecule processing intramolecular dsRNA domains. shRNAs were processed into miRNAs which mediated translational repression (177).

dsRNAs induced specific inhibition of vertebrate gene expression such as in mouse oocytes, in hamster ovary cells. However, in most mammalian cells, long dsRNAs (>30 nucleotides) induced nonspecific inhibitory response resulting from activation of type I interferon pathway. They also activated a mammalian cytoplasmic key enzymes, the protein kinase R (PKR) and 2′,3′-oligoadenylate synthetases whose products activated the latent ribonuclease RNaseL (176). PKR strongly inhibited cells growth by phosphorylation of the essential protein-synthesis-initiation factor eIF-2. PKR activation occurred non-specifically in all cells, leading to nonspecific degradation of RNA. Hence, PKR activation and interferon induction

had prevented the wide application of RNAi in mammalian cells. Recently, synthetic siRNA duplexes, with the same length and structure were produced from long dsRNA. They did not exhibit nonspecific side effects via activation of interferon and PKR (175, 176, 178). siRNA required cleavage of the passenger strand and usage of the guide (antisense) strand for effective RISC assembly, while miRNA did not require passenger strand cleavage (179).

Mechanism of RNAi

For entry into the cellular RNAi pathway, long dsRNAs were specifically recognized by RNase III type endonucleases, termed Drosha and Dicer (176, 177, 180). Drosha was specifically required for the processing of miRNA precursor in nucleus. The precursors were subsequently transported to cytoplasm via exportin-5, a nuclear export receptor. In cytoplasm, miRNA precursor and long dsRNAs were further processed by dicer yielding RNA duplexes of about 21-23 nucleotides in length with 5′-phosphates and 2 nucleotides 3'-overhangs (Figure 7)(176). Subsequently, miRNA or siRNA duplexes intermediate were incorporated by different mechanisms into a multi subunit protein complex, called miRNP (ribonucleoprotein particles) or RNA-induced silencing complex (RISC), respectively. RISC contained a helicase activity. This helicase unwound the two strands of RNA molecules. Then, an endonuclease (RNase III) hydrolyzed the target RNA at the site where the antisense strand was bound. This RISC/miRNP assembly required ATP.

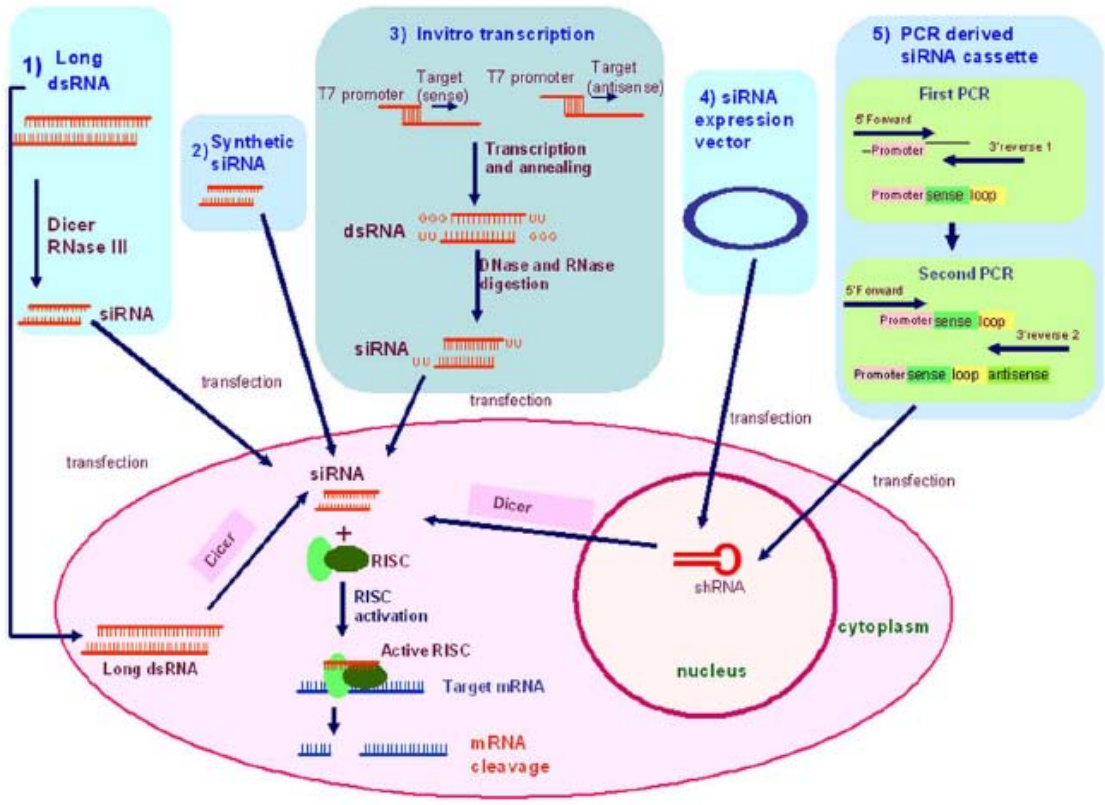

Figure 7 Mechanisms of RNAi (176)

Next, the single stranded siRNA in RISC guided sequence-specific degradation of complementary target mRNA, and therefore resulted in knockdown of the expression of the corresponding gene. RISC cleaved the target mRNA in the middle of the complementary region, 10 nucleotides upstream of the nucleotide paired with the 5′ end of the guide siRNA. RISC/miRNP complexes catalyzed hydrolysis of the target-RNA phosphodiester linkage, yielding 5′phosphate and 3′hydroxyl termini (177). The cleavage reaction by RISC/miRNP did not require ATP. In addition, miRNP mediated translational repression (181). Finally, the RISC/miRNP complexes can recycle and silence more copies of mRNA.

In comparison, gene knockouts in mice required up to nine months to complete the experiment, while RNAi in animals could generate result within days or weeks. Thus, RNAi has greatly advantage in the study of new drug targets with time-limitation. RNAi usually achieved incomplete 90% knockdown effect which might

reflect more accurately the situation in human disease,whose causing-genes involved at suboptimal levels. It also mimicked more closely the effect of drug which usually achieved an incomplete inhibition of its target(182).

Comparison of siRNA with other antisense approach

The advantages and disadvantages of antisense technologies have been summarized as shown in Table 1 (171).

Table 1 Relative advantages and disadvantages of antisense technologies (171)

Approach	Advantage	Disadvantage
Antisense ODNs	Can be modified to improve selectivity and efficacy Can be targeted to introns Easy to make	Can induce interferon (if long and has CpG) Can bind proteins (aptamer activity) Only exogenous delivery possible (synthetic) Off-target effects
Ribozymes	Can discriminate single base polymorphisms Can be used to correct defects Sequences can be appended to change target specificity Simple catalytic domain Can target introns/subcellular compartments	Requires GUCtriplet-limits choice of target Bind proteins (aptamer activity)
DNAzymes	Inexpensive to make Good catalytic properties Can be modified for systemic delivery	Only exogenous activity Off-target effects?
RNAi	Effective at low concentrations Bypasses interferon pathway Can be delivered by multiple pathways Tissue-specific expression possible Nontoxic? Last longer?	Can not target nuclear RNAs or introns No option for improving if target refractory Some reports of off-target effects

Recent studies directly compared AS-ODNs and RNAi techniques. Far Kazemi et al.(183) reported that the IC_{50} value for the siRNA was about 100 fold lower than that of AS-ODNs. Therefore, the activity of siRNA was much higher than that of AS-ODNs in mammalian cells, EC204 expressing ICAM-1 gene. Consistently, Bertrand et al.(184) supported that in cell culture, siRNA appeared to be more efficient thanh AS-ODNs (80% VS 75% inhibition, respectively). The effect of siRNA lasted longer than that of AS-ODNs because siRNA were more resistant to nuclease degradation.

Regardless to the stability, Vickers et al.(185) found that both siRNA and AS-ODNs were similar in term of potency, efficacy, specificity and duration of action. Senn et al.(186) observed that siRNA, encompassing the same gene sequence as AS-ODNs, induced a stronger inhibition of melanocortin MC_4 receptor expression in HEK293 cells than AS-ODNs. However, when fluorescence-labeled siRNA were applied intracerebroventricularly (i.c.v.) into rats, no labeled was detected in brain tissue. In contrast, the i.c.v. administered fluorescence-labeled AS-ODNs were taken up into brain cells. Thus, it seemed as naked AS-ODNs had more advantage than naked siRNA for in vivo experiment. However, in mouse, a rapid systemic injection of siRNA into tail vein promoted the effective inhibition of target gene expression in liver, kidney, spleen, lung and pancreas (173, 174).

Vicker et al.(185) also reported that the maximal inhibitory effect of siRNA was found at 24 hr post transfection and return to normal level by day 5. These results were similar to AS-ODNs except the maximal activity was achieved at 8 hr after transfection. Achenbach et al.(172) showed that siRNA could achieve complete knockdown for 96 hr in luciferase assay, while AS-ODNs were reported to down-regulate protein levels 48 hr after transfection. In addition, other studies indicated that inhibitory effect of siRNA was for up to 72 hr, while AS-ODNs were just 24 hr. In summary, the effects of RNAi and AS-ODNs were transient and only active for 24-72 hr, depending on the secondary readout (172). Moreover, both methods were differently distributed in cells. AS-ODNs acted in the nucleus, while siRNAs most likely acted in the cytoplasm (172).

Guideline for siRNA selection

Several parameters should be considered to optimize siRNA-induced gene silencing (175, 179).

a. Sequence asymmetry of siRNA duplexes

The primary sequence asymmetry of siRNA guide strand with the less stable 5′ end was favorably loaded into RISC, leading to improvement of efficiency and specificity.

b. siRNA duplex stability

The GC content of siRNAs should be ranging between 30-52%. Too low GC content may destabilize siRNA duplexes leading to reduction of the affinity for target mRNA binding. Too high GC content may impede RISC loading and cleavage-product release. Additionally, siRNA duplexes, lacking of internal repeats or palindromes were better silencers. Internal repeats or palindromes could form intrastrand secondary structures and interfered with targeting mRNA.

The center of siRNA duplex preferentially had low internal stability which influenced the effectiveness and ratio of loaded RISC complexes. Alteration of the structure and stability of siRNA duplexes could be controlled by incorporation of chemically modified nucleotide analogs.

c. Target accessibility

Local secondary structure in target mRNAs might limit the RISC accessibility and attenuate or abolish siRNA efficacy.

d. siRNA length and asymmetric 3'overhang

The 21 nucleotides siRNA with symmetric 2 nucleotides 3′overhangs represented the predominant processing intermediate in the RNAi pathway. The siRNA should have 5′phosphate and 3′hydroxyl group for efficiency. Likewise, 20-25 nucleotides siRNA duplex carrying 2 nucleotides 3′overhangs also had similar gene silencing efficiency in mammalian cell culture. The longer dsRNAs could be effectively transfected at lower concentrations than conventional siRNA, but it induced nonspecific response.

e. Sequence characteristics

Several sequence characteristics were preference for examples U or A at position 1, C or G at position 19, A+U richness between positions 1 and 7, A or U at position10. Extended runs of altering GC pairs (>7) or runs of more than three guanines were sometimes avoided.

f. Specificity

To enhance specificity, the guide strand of siRNA entering RISC had some mismatch to all undesired target mRNA especially their 3′UTRs. At least 3 mismatches were recommended between position 2 and 19. The mismatches near the 5′end and in the center of the examined strand should be assigned.

To evaluate siRNA, Chalk et al.(187) recommended the siRNA database providing information about siRNA thermodynamic properties, and the potential for sequence-specific off target effects.

siRNA delivery

The expensiveness of synthesizing siRNAs and their lack of amplification in mammalian cells have compelled the continuous supply of siRNA in cells. Two approaches have been developed for siRNAs expression as plasmid-based vectors and virus-based vectors (175). Plasmid-based vectors provided advantages over chemically synthesized siRNAs, but still had limitations including transient nature of siRNA expression, low and variable transfection efficiency. To circumvent these problems, virus-based vectors have been developed for high-efficiency siRNA delivery system such as the U6 promoter. Most of the siRNA expression vectors used RNA polymerase III regulatory units, which did not allow tissue-specific siRNA expression. However, there are also evidence supported the usage of tissue-specific siRNA expression with a polymerase II promoter-based plasmid (175). Now, a number of transfection reagents were available commercially for transfecting siRNA into different cell lines. Alternatively, electroporation has been used to transfect siRNA in some cell lines. In addition, hydrodynamic transfection methods have been used to deliver naked siRNA into adult mice to against hepatitis C virus infection in intact liver (175).

The method to detect specific gene knockdown by RNAi was to determine the target protein depletion by immunofluorescence and Western Blot technique. In addition, the knockdown phenotype and Northern Blot analysis could also be performed in order to detect the siRNA effects (175).

Therapeutic application of siRNA

siRNAs had greater propensity to be the useful technique to study many neurological disease including neurodegenerative disorder, CNS tumor, infectious disease, chronic pain and retinal disorder(176).

CHAPTER III
MATERIALS AND METHODS

MATERIALS

Chemicals

The compounds used in this study and their sources were as follows:

1. Dulbecco's modified eagle medium (DMEM) (Invitrogen)
2. Minimum essential medium (MEM), with Earle's salts (Invitrogen)
3. Fetal calf serum (Sigma-Aldrich)
4. Amphotericin B (Sigma-Aldrich)
5. Pen/Strep : Penicillin G sodium (10,000 unit/ml) and Streptomycin (10,000 μg/ml) in 0.85% saline (Sigma-Aldrich)
6. L-glutamine (200mM) (Invitrogen)
7. 5-fluoro-2′-deoxyuridine (FDU) (Sigma-Aldrich)
8. Geneticin (50 mg/ml) (Invitrogen)
9. Zeocin (100mg/ml) (Invitrogen)
10. MEM essential amino acid (10mM) (Invitrogen)
11. Sodium pyruvate (100mM) (Invitrogen)
12. Sodium bicarbonate (Fisher Scientific)
13. Trypsin (Tryple^{TM} express) (Invitrogen)
14. Insulin (Sigma-Aldrich)
15. Putrescine (Sigma-Aldrich)
16. Progesterone (Sigma-Aldrich)
17. Sodium selenite (Sigma-Aldrich)
18. Potassium chloride (Sigma-Aldrich)

19. Dextrose (Sigma-Aldrich)
20. HEPES (Sigma-Aldrich)
21. Collagenase (Sigma-Aldrich)
22. Dnase (Sigma-Aldrich)
23. Percoll^{TM} (GE Healthcare Bio-Sciences Ltd.)
24. Erythrosine B
25. M-PER^{TM} Mammalian protein extraction reagent (Pierce)
26. Bovine serum albumin, BSA (Sigma-Aldrich)
27. The DC protein detection kit (Bio-Rad)
28. β-mercaptoethanol (Bio-Rad)
29. Laemmli sample buffer (Bio-Rad)
30. 5% Tris-HCl ready gel (Bio-Rad)
31. Himark^{TM} Prestained HMW protein standard (Invitrogen)
32. Hybond ECL nitrocellulose membrane (Amersham Pharmacia Biotech.)
33. Tris base (Sigma-Aldrich)
34. Glycine (Sigma-Aldrich)
35. Sodium dodecyl sulfate (Sigma-Aldrich)
36. Methanol (Sigma-Aldrich)
37. Sodium phosphate dibasic, anhydrous (Na_2HPO_4) (Sigma-Aldrich)
38. Sodium phosphate monobasic ($NaH_2PO_4.2H_2O$) (Sigma-Aldrich)
39. Sodium chloride (Sigma-Aldrich)
40. Polyoxyethylene sorbitan monolaurate (Tween-20) (Sigma-Aldrich)
41. Sodium hydroxide (Fisher Scientific)
42. Hydrochloric acid (Fisher Scientific)
43. Potassium phosphate monobasic (KH_2PO_4) (Fisher Scientific)
44. Magnesium sulfate (Fisher Scientific)
45. Calcium chloride (Fisher Scientific)
46. Non fat dry milk
47. APC C20 rabbit polyclonal IgG (Santa Cruz Biotechnology)
48. Anti rabbit Ig horseradish peroxidase from donkey linked whole antibody (Amersham Pharmacia Biotech.)

49. Enhanced chemilumniscence (ECL) western blotting detection reagents (BioRad)
50. Trizol® reagent (Invitrogen)
51. DEPC-treated water (Diethylpyrocarbonate-treated water) (Invitrogen)
52. Double distilled water (ddH_2O) (OSU)
53. 3-(N-Morpholino) propane sulfonic acid (MOPS) (BioRad)
54. Sodium acetate (NaOAc) (Invitrogen)
55. EDTA (Invitrogen)
56. Ultrapure™ Agarose (Invitrogen)
57. Deionized formamide (Invitrogen)
58. Formaldehyde (Invitrogen)
59. Ethidium bromide (Fisher Scientific)
60. Ready load™ 100 bp DNA ladder (Invitrogen)
61. 10X Blue Juice™ Gel loading buffer (Invitrogen)
62. Nucleic acid sample loading buffer (Bio-Rad)
63. Boric acid (Invitrogen)
64. Superscript III RNase-H-RT (Invitrogen)
65. Taq PCR kit (Qiagen)
66. Primer (Operon Biotechnology)
67. (±)-[5,6-bicycloheptyl-^{3}H] Epibatidine (Perkin Elmer life and Analytical Sciences)
68. Ethanol (Fisher Scientific)
69. Bromoacetylcholine bromide (brACh) (Sigma/RBI)
70. Neostigmine bromide (Sigma-Aldrich)
71. Dithiothrietol (DTT) (Amersham Biosciences Inc.)
72. 5,5′-dithio-bis(2-nitrobenzoic acid) (DTNB) (Sigma-Aldrich)
73. Nicotine hydrogen tartrate (Sigma-Aldrich)
74. Carbamylcholine chloride (Carbachol) (Sigma-Aldrich)
75. Scintiverse E Scintillation Cocktail (Fisher Scientific)
76. Ultrafree-MC (Millipore Corp.)
77. Microcon®-YM30 PCR tube (Amicon)
78. TOPO TA cloning kit (Invitrogen)

79. Transforming one shot kit (Invitrogen)
80. Lubria-Bertani broth (LB-broth) (Lennox L Broth) (Invitrogen)
81. X-gal (5-bromo-4-chloro-3-indolyl-β-D-galactoside) (Invitrogen)
82. SOC medium (Sigma-Aldrich)
83. Fast plasmid mini kit (Invitrogen)
84. Kit for restriction enzyme digestion (Invitrogen)
85. Puromycin (Sigma-Aldrich)
86. APC stealth siRNA (Invitrogen)
87. Block-iT™ Florescent Oligo and Lipofectamine™ 2000 (Invitrogen)
88. Opti-MEM® I reduced serum medium (Invitrogen)

Equipments

1. pH meter (SevenEasy, Mettler Toledo, USA)
2. Balance (AE100 for μg and PL202-S for g, Mettler Toledo, USA)
3. Freezer (Fisher Scientific Isotemp -20°C freezer and REVCO -80°C Freezer)
4. Spectrophotometer microplate reader (μQuant, Bio-Tek Instruments, Inc.)
5. Spectrofluorometer (FlexStation, Molecular Devices)
6. Light microscope (Nikon Diaphot inverted microscope and Nikon Labophot Microscope)
7. Humidified carbon dioxide incubator (Automatic CO2 incubator, Precision and IG050, Jouan)
8. Hemacytometer (Bright-line hemocytometer, Reichert)
9. Cell counter
10. Water bath (Isotemp 202S, Fisher Scientific)
11. Autoclave
12. Millipore cartridge filter & 0.22 μM membrane filter (Sterivex 0.22 μm filter unit, Millipore for big volume and 0.22μm syringe filter, Fisherbrand for small volume)
13. Shaker (Gyrotory shaker model G2, New Brunswick Scientific Co.)
14. Centrifuge (IEC HN-SII Centrifuge, Danon/IEC Division and Microfuge 18 Centrifuge, Beckman Coulter)

15. Ultracentrifuge (J2-21 Centrifuge, Beckman for 20,000 rpm and L7 Ultracentrifuge, Beckman for 60,000 rpm)
16. Buchler multistatic pump with tubing
17. Sterile laminar flow cabinet/hood (SterilGUARD III Advance, The Baker Company)
18. Radioactive cabinet/hood
19. Liquid scintillation spectroscopy (Liquid Scintillation analyzer Tri-Carb 2100TR, Packard)
20. Scintillation vials with caps (7ml scintillation vials with cap, VWR International)
21. Gel electrophoresis chamber/tank (Horizon 11-14, Life Technologies for RNA gel and Mini-Protean II cell, BioRad for protein gel)
22. Rotator
23. X-ray film cassette & Classical blue sensitive autoradiograph film (Blue lite Autorad Film 8"x10", ISC BioExpress)
24. Film developer : KODAK X-OMAT 1000A Processor
25. Biochemi TM Imaging system (Epi Chemi II Darkroom, UVP Inc.)
26. PCR machine (: iCycler, BioRad)
27. PCR vials/tubes (PCR reaction tubes 0.2ml, Fisher Brand)
28. PCR tips (Choice barrier pipet tips, Genemate)

METHODS

1. Cells Culture

Isolation and Primary Culture of Bovine Adrenal Chromaffin Cells.

Adrenal chromaffin cells were dissociated from intact glands and plated in supplemented DMEM, as previously described by Free et al. (109, 188)**.** Cells were plated in Dulbecco's modified eagle medium (DMEM) media supplemented with 10% fetal calf serum, 250 ng/ml amphotericin B, 100 U/ml penicillin, 100 μg/ml

streptomycin, 2 mM L-glutamine, and 10 μM 5-fluoro-2'-deoxyuridine (FDU). Cells were plated on 24 well plates at a density of $5X10^5$ cells per well for intact cell binding assay . Two days after plating, media were replaced with serum-free, N2+ medium. One day prior to experimentation, culture media were removed and replaced with N2+ media free of amphotericin B and FDU. Cells should be used 4-7 days after isolation.

Procedure for Isolating Adrenal Chromaffin Cells

A. Procedure

The day prior to the isolation,

a. Autoclave appropriate equipment/supplies

b. Prepare solutions: 1 time-concentration and 10 time-concentration Locke's solution, Locke's with 0.05% BSA solution and sterile Percoll solution

c. Order adrenal glands from Meat Packing Company

The day of the isolation

a. Prepare all solutions

b. Set up the multistatic 4 channel pump and turn on the water bath for 37°C

c. Pick up the glands as soon as they are isolated. Glands are kept in plastic bag and packed in an ice-box during transportation.

1. Select glands that have no cuts penetrating into the medullae.

2. With the large scissors, remove each gland from the surrounding fatty tissue. Store the glands in ice-cold Locke's solution without BSA.

3. With the medium scissors and small forceps, remove as much fat as possible from the gland.

4. With the #3 scalpel (blade #10), make cuts about 1mm deep and 2 mm apart over the entire surface of the glands.

5. Use a 20 ml sterile syringe, inject each gland with 20 ml of Locke's solution without BSA. Then, insert the tygon tube into the portal vein of the gland and immerse the other end of the tube in the sterile perfusion solution (Locke's solution without BSA). Suspend the gland using the ringstand and wire mesh over the 2,000 ml beaker. Place 2 pieces of gauze over the wire mesh and another piece over the glands.

6. Perfuse (pump setting at 10) glands with about 150-300 ml of Locke's solution without BSA at room temperature for 15-30 minutes. Glands should be swelled up. This perfusion should remove most of the residual red blood cells which observe from the colourless (no red) waste solution. Repeat step 3-6 until all four glands are perfused.

7. At the end of the initial perfusion (step 6), pour 80 ml of the collagenase solution into a 150 ml beaker and draw 20 ml into a sterile syringe. The collagenase solution should be at least at room temperature. Remove the cannula from the gland and inject 5 ml of warm collagenase into each gland. Replace the cannula and place the glands into the 150 ml beaker with enough collagenase to entirely cover the glands. Perfuse the glands while recirculating the collagenase for 2 hours at room temperature. The actual time for this perfusion would depend upon the size of the gland. Small glands would digest faster than large glands.

8. Remove the glands from the perfusion apparatus and place them on ice. Make an incision around the perimeter of the glands with a #4 scalpel (with #22 blade). Peel the cortex (outer layer) back with a pair of forceps and carefully remove the medulla (yellow inner layer) from the cortex by pushing with the scalpel. If the collagenase perfusion goes properly, the medulla should very soft and should not require cutting or scrapping to separate it from the cortex. Place the medulla into a mincing bowl with a small amount of the collagenase solution (10 ml) on ice.

9. When all four medulla have been removed, mince the tissue thoroughly. When the tissue have been reduced to pieces of about 1x3 mm, placed the contents into a sterile

corning tube. Wash the bowl with about 15 ml collagenase and add the contents to the corning tube. Add collagenase into the 50 ml tube to bring the final volume to 30 ml. Seal the tubes with parafilm and incubate at 37°C for 30 minutes in a water bath shaking vigorously.

10. Remove the tubes from the water bath and pour the contents through the 210 μm nylon mesh filter. Wash out reaction tube with 10 ml of ice cold Locke's solution without BSA and pass wash through filter. Wash the tissue in the filter with 10 ml of ice cold Locke's solution without BSA applied with pipette-aid. Use "lift and reseat" method to facilitate drainage through the filter (stir with a spatula, only if necessary). Evaluate the amount of tissue leave over and the effectiveness of the DNAse. Centrifuge filtrate at 100xg (800 rpm), at room temperature for 10 minutes. Aspirate off the supernatant and carefully resuspend the pellet using Pipette-aid and a 10 ml sterile pipette. Add Locke's solution with BSA to a final volume of 50 ml and centrifuge at 100xg (800 rpm), at room temperature for 10 minutes.

11. Aspirate off the supernatant and resuspend the pellet as above. Bring the volume up to about 20 ml and pass the suspension through the 105 μm nylon mesh filter. Collect the filtrate in a sterile corning tube. Wash out the centrifuged corning tube and the filter with ice cold Locke's solution with BSA applied with a pipette-aid. Bring the filtered suspension up to 39 ml with Locke's solution with BSA.

12. Add the 39 ml of cell suspension to the 33 ml of Percoll/Locke's solution and swirl to mix. Divide the percoll/cell suspension equally between 2 sterile centrifuge tubes. These tubes must be balanced prior to high speed centrifugation. Centrifuge at 35,000xg (17,000 rpm), 4°C for 20 minutes or at 20,000xg (15,000 rpm) for 20 minutes. (189)

13. Remove the top layer of dead cells and save the middle layer above the blood cells layer in 3 sterile corning tubes. Discard the blood cell layer. Top the tubes up to 50 ml with Locke's solution with BSA and centrifuged at 100xg (800 rpm), at room temperature for 10 minutes

14. Aspirate off the supernatant. Resuspend the pellet and bring the volume up to 40 ml with Locke's solution with BSA. Count the cells by

- place 5 standard drops of cell suspension into microcentrifuge tube and add 1 drop of 0.4% erythrosine B in Phosphate Buffer Saline (PBS). Mix well.
- transfer 1 drop of cell-dye mixture to a hemocytometer. Using a hemocytometer under microscope, count both the live and dead cells in the grid
- calculate the percentage of viability using the following formula:

% viability = [number of live cells / (number of live + dead cells)] x 100

- calculate the number of cells present in cells suspension using the following formula:

Total number of cells = (number of live cells)(40 ml)($1x10^4$ cells)(6/5)(F)

Note: If count cells in total squares of the grid, "F" is equal to 1.
If count cells in some squares of the grid (5 from 25 squares), "F" is equal to 5.

15. Top the cells up to 50 ml with media and centrifuge at 100xg (800 rpm), at room temperature for 10 minutes.

16. Aspirate off the supernatant. Resuspend the pellet with media and bring volume up to achieve desired cell density (typically $1x10^6$ cells/ml). In 24 wells plate, add 1 ml/well of growth media, then add cells stock ($1x10^6$ cells/ml) in a volume to achieve desired cell density

17. Plate the cells. In 24 well plate, cells are plated at densities of $5x10^5$ to $2x10^5$ cells/well for receptor binding coupled receptor alkylation and catecholamine secretion assay, respectively. In 60 mm plate, cells are plated at a density of $5x10^6$ cells/well for RNA isolation and protein assay. Incubate the cells in 37°C, 5%CO_2 humidify incubator.

18. Plating is initially done in DMEM containing Pen/strep, glutamine, fungizone, fetal calf serum (FCS) and FDU. But on day 2 after the isolation, the media is changed to serum free $N2^+$ supplemented with Pen/strep, glutamine, fungizone, and

FDU. One day prior to using the cells, a fungizone and FDU free $N2^{+}$ is placed on the cells.

B. Isolation Solution

I. Locke's solution (1,500 ml)

1. Fill large graduated cylinder to 1,000 ml with double distilled water (ddH_2O and add the indicated amount of the following ingredients while stirring

Composition of Locke's solution

Stock solution concentration	MW (g/mol)	Stock	Volume	Final concentration
1.45 M NaCl (10times)	58.44	84.74g/1,000 ml H_2O	150 ml	145 mM
0.54 M KCl (100times)	74.55	4.03g/100 ml H_2O	15 ml	5.4 mM
0.10 M NaH_2PO_4 (100times)	155.99	1.56g/100 ml H_2O	15 ml	1.0 mM
Dextrose (MW=180)	180	-	3.03 g	11 mM
HEPES (MW=238)	238	-	5.36 g	15 mM

2. Adjust volume to 1,500 ml

3. Adjust pH to 7.3 with 1M NaOH (use about 50 drops of 1M NaOH to adjust pH from 5.3 to 7.3)

4. Divide this solution into 3 parts: 400 ml for preparing the Locke's with 0.5% BSA solution, 150 ml for preparing collagenase solution and 950 ml for filter sterilization.

II. Locke's solution with 0.5% BSA (400 ml)

To 400 ml of Locke's solution, add 2.0 g of BSA and stirred

III. 10 times-concentration Locke's solution (10 ml)

- Add 5 ml of ddH_2O to a corning tube (10 ml) and then add the indicated amounts of the following

Composition of 10 times-concentration Locke's solution

Stock solution concentration	MW (g/mol)	Stock	Volume	Final concentration
4.85 M NaCl (10times)	58.44	28.34g /100 ml H_2O	3 ml	1.45 M
0.54 M KCl (100times)	74.55	4.03g/100 ml H_2O	1 ml	0.054 M
0.10 M NaH_2PO_4 (100times)	155.99	1.56g/100 ml H_2O	1 ml	0.01 M
Dextrose (MW=180)	180	-	0.202 g	0.11 M
HEPES (MW=238)	238	-	0.357 g	0.15 M

IV. Filter sterilization

On experimental day, sterilized the isolation solutions by filtration (described above) as follows:

1. Using a Millipore cartridge filter (sterivex filter 0.22 μM), filter sterilize 950 ml of Locke's solution, then 400 ml of Locke's with 0.05% BSA solution.

2. To each sterile solution (400 ml of Locke's with 0.05% BSA solution and 950 ml of Locke's solution), add penicillin-streptomycin solution (1 ml Pen-Strep/100 ml buffer) and fungizone (0.1 ml fungizone/100 ml buffer) using sterile technique.

V. Collagenase Solution (150 ml)

Freshly prepare this solution (15 minutes before using).

1. Filter sterile 150 ml of Locke's solution

2. Weigh 150 mg of collagenase (final concentration 0.1%) and 6 mg of DNAse I (final concentration 40 μg/ml) in flask and add 150 ml of sterile Locke's solution.

3. Shake well until obtained a brown solution. Do not stir by magnetic bar, because it may cause collagenase degradation.

4. Filter sterile this solution and keep filtrate in sterile bottle.

5. Add penicillin-streptomycin solution (1 ml Pen-Strep/100 ml buffer) and fungizone (0.1 ml fungizone/100 ml buffer) using sterile technique.

VI. Percoll Solution

1. One day before the experimental day, sterile Percoll solution by autoclaving and keep sterile Percoll solution in the refrigerator.

2. Use a 0.22 μM syringe filter to sterile 10 ml of 10 times-concentration Locke's solution.

3. Add 29.7 ml of sterile Percoll solution to 3.3 ml of sterile 10 times-concentration Locke's solution in sterile 100 ml bottle. This Locke's solution is 10 fold concentrated but is diluted 10 fold here so that the percoll solution would be iso-osmotic.

VII. Growth media

$N2^+$ media

1. Empty contents of Dulbecco's modified eagle medium/F12 (DMEM/F12) package to about 600 ml of ddH_2O in a 1,000 ml graduated cylinder and rinse package twice with ddH2O. This solution is yellow.

2. Add 1.2 g of sodium bicarbonate ($NaHCO_3$) which changes the color of solution to red.

3. Add the following:

5 mg of insulin for final concentration at 5 μg/ml

16.4 mg of putrescine for final concentration at 100 μM

10 μl of 2 mM progesterone stock for final concentration at 20 nM

100 μl of 300 μM Na-selenite stock for final concentration at 30 nM

Note:

- 2mM progesterone stock is kept in freezer. Before using, thaw it by hand. Do not thaw by putting tube in 37°C water bath.

- 300 μM Na-selenite stock should be freshly prepared by dissolving 25.9 mg in 500 ml ddH_2O. (Na-selenite; MW=172.9 g/mol)

4. Add 5 g of BSA for final concentration of 0.5%

5. Adjust volume to 1,000 ml

6. Adjust pH to 7.3 with 20% NaOH (use about 3 drops of 1M NaOH to adjust pH from 7.16 to 7.31)

7. Filter sterilize and divide $N2^+$media into 2 equal parts: $N2^+$#1 and $N2^+$#2

8. Prepare 5 mM FDU solution by dissolving 4.7 mg of FDU in 3.8 ml of ddH_2O and filter sterilize this solution.

	500 ml of DMEM	500 ml of $N2^+$#1	500 ml of $N2^+$#2
FBS	50 ml	-	-
200 mM L-glutamine	5 ml	5 ml	5 ml
Penicillin/ Streptomycin	5 ml	5 ml	5 ml
Fungizone	0.5 ml	0.5 ml	-
5 mM FDU	1 ml	1 ml	-

Culture of HEK293 Expressing Recombinant Bovine Adrenal α3β4* nAChRs (BM α3β4 Cells).

BM α3β4 cells were cultured in a condition as described previously by Free et al. (26). These cells, at a density of $6x10^4$ cells per well for siRNA transfection and puromycin treatment, respectively, were plated in Minimum essential medium (MEM) containing 10% heat-inactivated fetal bovine serum, 2mM L-glutamine, 500μg/ml Geneticin and 400μg/ml Zeocin in 24 well Biocoat Poly-D-Lysine coated plate. For following procedures, all processes should be done with aseptic techniques.

A. Media for BMα3β4 cells

Growth Media

1. Thaw frozen ingredients such as fetal bovine serum (FBS), 200 mM L-glutamine, and Zeocin in 37°C water bath

2. To a 500 ml bottle of MEM, add 50 ml of FBS and 5 ml of 200 mM L-glutamine and label bottle "Completed media" with date. Keep complete media in refrigerator.

3. On the experiment day, add the amount of antibiotics which depends on the amount of needed media. A volume of 10 μl of Geneticin (G418, 50 mg/ml) is used for each ml of media. A volume of 4 μl of Zeocin (100 mg/ml) is used for each ml of media. Both Geneticin and Zeocin should be protected from light by wrapping container with foil. Geneticin is kept in refrigerator (2-8°C) ,while Zeocin was kept in freezer.

Composition of Growth media

Ingredients	Volume	Final concentration
MEM	500 ml	-
FBS	50 ml	10%
200 mM L-glutamine	5 ml	2 mM
Geneticin (G418, 50 mg/ml)	5 ml	500 μg/ml
Zeocin (100 mg/ml)	2 ml	400 μg/ml

Antibiotic	Complete Media					
	10 ml	20 ml	25 ml	30 ml	40 ml	50 ml
G418	100 μl	200 μl	250 μl	300 μl	400 μl	500 μl
Zeocin	40 μl	80 μl	100 μl	120μl	160 μl	200 μl

B. Trypsinization Procedure

BMα3β4 cells grew up as monolayer on 24 well plate in 37°C, 5%CO_2 humidify incubator .

1. Thaw the frozen ingredients such as Zeocin and warm up refrigerated ingredients such as Complete media, Trypsin (Tryple^{TM} express) to 37°C in 37°C water bath.

2. Remove culture dish or plate from 37°C, 5% CO_2 humidify incubator and scan the cells using microscope.

3. Place a 24 well plate in Sterile Laminar flow Hood. Aspirate off culture media in each well

4. Add 1ml/well of trypsin and incubate at room temperature for 1 minute.

5. Aspirate off excess volume of trypsin in each well.

6. Incubate cells in 37°C, 5%CO_2 humidify incubator for 10 minutes.

7. To stop trysinization, add 1 ml/well of growth media in each well. Pipette media up-down to deattach and resuspend cells.

8. Transfer all of cell suspension into sterile tube which is ready for further steps such as cell counting, cell splitting or plating, cell freezing.

C. Cell counting Procedure

1. Trypsinize cells and resuspend cells with growth media as cells suspension.

2. In eppendorf microtube, dilute 5 drops of cells suspension in 1 drop of 0.1% Erythrosine B in PBS. Mix well.

3. Transfer 1 drop of cells-erythrosine mixture on Hemacytometer and count number of living cells appeared on grid. Living cells appear to be colorless, whereas death cells are stained by erythrosine dye and appear to be red.

4. Calculate the number of cells present in cells suspension as the following formula:

Total number of cells = No. of live cells x Final vol. of cell suspension (ml) x Constant from Hemacytometer x Vol. of cells-erythrosine mixture (drops) / Vol. of diluted cells suspension (drops) x F

Note:

- Constant from Hemacytometer is equal to "$1x10^4$ cells"

- Vol. of cells-erythrosine mixture (drops) / Vol. of diluted cells suspension (drops) is equal to "6/5"

- In case of BMα3β4 cells, which usually counts cells in total squares of the grid, "F" is equal to "1".

In case of bovine adrenal chromaffin cells, which usually counts cells in some squares of the grid (5 from 25 squares), "F" is equal to "5".

D. Cell freezing Procedure

1. Trysinize cells and resuspend cells with growth media as cell suspension. Keep cell suspension in tight centrifuge tube.

2. Centrifuge cell suspension at speed of 100xg (800 rpm), at room temperature for 2 minutes. Then, cell suspension is separated into 2 layers: top layer of clear solution, media and bottom layer of cell pellet.

3. Discard supernatant and keep cell pellet in centrifuge tube.

4. Resuspend pellet with 100% FBS containing 10% DMSO in calculate volume to make cell suspension in final concentration of $1x10^6$ to $1x10^7$ cells/ml. Other media used for freezing cells is growth media containing 20% FBS.

5. Pipette 1.1 ml of cell suspension into cryopreserve tube/vial. Prior to this step, cryopreserve tube should be put in ice.

6. DMSO is a cytotoxic agent at room temperature. Thus, after adding DMSO to cells, immediately freeze cells suspension in -80°C freezer.

2. Protein Assay

A. Procedure for protein extraction from cells

Bovine adrenal chromaffin cells and BMα3β4 cells were plated until 90% confluence of cells. Then, total proteins were extracted from both cells by using M-PER™ mammalian protein extraction reagent following the company's instruction.

1. Remove culture dish or plate from 37°C, 5% CO_2 humidify incubator and scan the cells using microscope.

2. Carefully remove culture media from adherent cells by aspiration off or turn over culture dish or plate.

3. The culture media may contain ingredient that could interfere with subsequent protein analysis, so wash cells once with 1 ml/well of PBS pH 7.3 [Because, BSA may interfere the protein assay and PSS contains BSA, while PBS contains no BSA. This is the reason why PBS was used for washing cells.] PBS which was kept in refrigerator should be warmed up in 37°C water bath before using.

4. Add 200 µl/well of M-PER™ reagent and shake gently at room temperature for 5 minutes. The appropriate volume of M-PER™ reagent depends on size of culture plates as shown in Table 1. These recommended volumes are optimal for maximal cell lysis without scraping cells. If more concentrated extracts are preferred, a smaller volume could be used, however, scraping of the cells is necessary for maximal recovery. After shaking, if need, scrape cells to dissociate and break cells.

5. Collect the lysate and transfer to microcentrifuge tube.

6. To discard the cell debris, centrifuge sample (lysate) at 27,000xg at room temperature for 5-10 minutes (or 18,000xg =14,000 rpm for 15 minutes). The lysate is separated into 2 layers: top layer with clear solution and bottom layer with cell debris pellet. Transfer supernatant to a new tube for subsequent experiments such as protein content analysis, western blot analysis.

Table 2 Suggested volume of M-PER™ reagent used for different sizes of standard culture plates (Instruction from Pierce company)

Plate size	Volume of M-PER™ reagent
100 mm	500 µl – 1,000 µl
60 mm	250 µl – 500 µl
6-well plate	200 µl/well – 400 µl/well
24-well plate	100 µl/well – 200 µl/well
96-well plate	50 µl/well – 100 µl/well

PBS buffer pH 7.3

1. Prepare stock solutions and keep in refrigerator.
2. To 350 ml of ddH_2O in beaker, add each stock solutions as following and stir well with magnetic bar.
3. Adjust volume up to 500 ml in graduated cylinder.
4. Adjust pH to 7.3 with 4N HCl (used about 2 drops of 4N HCl to adjust pH from 7.66 to 7.33)

Composition of PBS, pH 7.3

Stock solution Concentration	MW (g/mol)	Stock	Volume	Final concentration
1.36 M NaCl (10times)	58.44	40 g/ ddH_2O 500 ml	50 ml	0.136 M
0.27 M KCl (100times)	74.55	1 g/ ddH_2O 50 ml	5 ml	2.7 mM
0.081 M Na_2HPO_4(10times)	155.99	5.75 g/ ddH_2O 500 ml	50 ml	8.1 mM
0.15 M KH_2PO_4 (100times)	136.09	1 g/ ddH_2O 50 ml	5 ml	1.5 mM

B. Protein content analysis

The amount of protein could be determined by using "The Bio-Rad® DC protein assay" According to the company instruction, this method was modified from Lowry assay.

1. To prepare BSA solutions as protein standard, dilute stock BSA protein standard (2mg/ml) with diluent (ddH_2O or buffer of unknown protein) as following

Stock BSA solution (2mg/ml) (μl)	**Diluent** (μl)	**Final concentration** (mg/ml)
10	90	0.2
20	80	0.4
30	70	0.6
40	60	0.8
50	50	1.0
60	40	1.2
70	30	1.4
80	20	1.6
90	10	1.8
100	0	2.0

2. To prepare working reagent, add 20 μl of reagent S to 1 ml of reagent A (an alkaline copper tartrate solution)

3. Pipette 5μL of BSA standard or unknown sample into microtiter plate.

4. Add 25 μL of reagent A and 200 μL of reagent B (a dilute Folin reagent) into each well.

5. Gently agitated plate on shaker at room temperature for 15 minutes to mix reagents.

6. Read the absorbance at wavelength of 750 nm in spectrophotometer plate reader.

The amount of protein was calculated from the standard curve which was prepared by using standard bovine serum albumin at concentrations 0, 0.2, 0.4, 0.6, 0.8, 1.0, 1.2, 1.4, 1.6, 1.8 and 2.0 mg/ml protein.

3. Western Blot Technique

The basic blotting procedure could be divided into the following steps

1. Sample preparation: Total proteins are isolated from either adrenal chromaffin cells or BM α3β4 cells by using M-PER^{TM} Mammalian protein extraction reagent as described above.

2. Gel electrophoresis: Equivalent amounts of protein (10-30 μg/lane) are separated in 5% SDS-polyacrylamide gels

3. Membrane transfer: Electroblotting is used to transfer protein from 5% SDS-polyacrylamide gel onto Hybond ECL nitrocellulose membranes.

4. Blocking non-specific binding

5. Addition of the primary and secondary antibodies. The blots are probed 1 hour at room temperature with 1:100 dilution of primary antibody (APC C20 rabbit polyclonal IgG). Bound antibodies are detected using 1:2,000 dilution of secondary antibody (Anti-rabbit Ig, horseradish peroxidase from donkey linked whole antibody). Western blots are probed according to the manufacturer's instructions,

6. Detection: Western blots are detected according to the manufacturer's instructions, using enhanced chemilumniscence (ECL). Blots are visualized using a Biochemi™ Imaging system. Molecular weight is determined using Labworks™ imaging software.

A. Gel electrophoresis

1. Add 25 μl of β-mercaptoethanol per 475 μl of Laemmli sample buffer for a final concentration of 5% β-mercaptoethanol, 710 mM.

2. Determine the amount of proteins in sample by protein assay as described above. Calculate and dilute samples to achieve the appropriate amount of protein for loading gel. For 5% Tris-HCl ready gel, the amount and volume of loaded sample should not exceed 30 μg protein/well and 30 μl/well.

Dilute 1 part of sample with 2 parts of Laemmli sample buffer in eppendorf tube with locked cap.

3. To reduce and denature proteins, heat diluted sample at 95°C for 5 minutes in brass mold filled with distilled water.

4. Cool down the temperature by putting sample tube in ice. Then, centrifuge sample at 18,000 x g (14,000 rpm), 4°C for 45 seconds to settle down all volume.

5. Prepare 5 times-concentration Running buffer. Then, dilute 100 of 5 times-concentration running buffer with 400 ml of ddH2O for a final concentration of 1 time-concentration Running buffer. (Normally, about 300 ml of 1 time-concentration

Running buffer was used per run.)

6. 5% Tris-HCl ready gels are used in this experiment.

- Remove gel from plastic bag
- Remove comb at the top of gel. Cut the black line and peel plastic tape from gel.
- Bring gel together with cassette and immerse thoroughly in 1 time-concentration running buffer.
- To clean and get rid of contamination or air bubbles, rinse each well thoroughly by a long tip micropipette.
- Apply the appropriate amount of samples to each well. Run the HiMark™ Pre-Stained HMW Protein standard (12 μl/well) in order to monitor the transfer of protein from gel to solid support (nitrocellulose membrane) during the membrane transfer step.
- Place this gel-cassette into running apparatus filled with 1 time-concentration running buffer up to lower level of gel (white line)
- Run gel electrophoresis at 200 V for 30-45 minutes. During running electric, make sure that 1 time-concentration running buffer covers upper level of each well in gel-cassette. This influences the electrophoresis efficiency which needs enough volume of running buffer without air bubbles.
- Stop electrophoresis when bromophenol blue dye front reach the bottom of gel or phenol red tracking dye reach two-third level from the top of gel.

B. Electrotransblotting

This step aimed to transfer the protein fractionated by SDS-PAGE to nitrocellulose membrane (western blotting) by electroblotting. In this procedure, a sandwich of gel and nitrocellulose membrane (solid support membrane) was compressed in a cassette and immersed in transfer buffer between two parallel electrodes. A current was passed from cathode (-) to anode (+) at right angles to the gel. This caused the separated proteins to electrophorese out of the gel and onto nitrocellulose membrane. The nitrocellulose membrane then was referred to as a "blot".

Following gel electrophoresis,

1. Prepare (1 time-concentration) Transfer buffer

- add 200 ml of methanol to 600 ml of ddH_2O and mix in beaker.

- add Tris base and stirred well by magnetic bar for 15-20 minutes.

- add glycine

- Bring final volume up to 1 liter in graduated cylinder and store transfer buffer at 2-8°C

Composition of Transfer buffer

Tris-base	3.03	g
Glycine	14.40	g
Methanol	200	ml
ddH_2O qs	1	liter

2. Separate gel from gel elctrophoresis-cassette. Cut stacking gel on the top of gel, to solve the problem about gel tightly attached to membrane. Then, immerse gel in transfer buffer for 5-15 minutes depends on gel thickness. This helps to reduce SDS concentration and enhances binding of protein to membrane.

3.Cut the Hybond ECL nitrocellulose membrane (1 sheet) and filter paper (4 sheets) to fit the gel exactly. It is important to wear gloves all the times while handling the membrane to prevent cross contamination.

4. Pre-wet nitrocellulose membrane first in distilled water then transfer to the appropriate transfer buffer and equilibrate for at least 10 minutes before using.
Place 2 of sponge filter pads and 4 of filter papers in transfer buffer for 15 minutes.

5. Use 2 of soaked filter papers to carefully remove the gel from the glass plate.

6. Assemble a transfer sandwich with the following layers in order from cathode (-) to anode (+)

1. Sponge filter pad (1 sheet)
2. Filter papers (2 sheets)
3. gel
4. nitrocellulose membrane (Membrane must be on the anode side of gel. To solve the problem about gel tightly attaches to membrane, membrane should be faced on gel at glass attached side.

5. Filter papers (2 sheets)

6. Sponge filter pad (1 sheet)

7. Remove all air bubbles between gel and membrane by rolling a pasture pipette across the surface of the gel/membrane sandwich.

8. Place the transfer sandwich in the transfer apparatus, which membrane is on the anode side. Put the ice pack in transfer apparatus to maintain temperature at 4°C for prevention of overheating and buffer decomposition. Stir magnetic bar all the times to circulate buffer solution.

9. Transfer the separated protein using current at 40 V overnight or 30 V for 2 days, at 4°C. If the transfer apparatus run properly, there are air bubbles floating up.

10. Remove the membrane from transfer apparatus.

C. Blocking non-specific binding

Prior to addition of primary antibody, the membrane must be incubated with a suitable blocking protein solution to block remaining hydrophobic binding site on the membrane. This would reduce background and prevent binding of the primary antibody to the membrane itself.

1. Prepare PBS-T solution (Phosphate Buffer Saline-Tween) pH 7.5

- To 2 liters of ddH_2O, add Na_2HPO_4 and stir with magnetic bar for 30 minutes.

- dissolve NaH_2PO_4 and NaCl

- add high viscous Tween-20 solution

- adjust pH to 7.5 with conc. NaOH

- add 3 liters of ddH_2O to final volume of 5 liters.

Composition of PBS-T solution

Ingredients	**Amount**	**Final concentration**
Na_2HPO_4	57.5 g	80 mM
NaH_2PO_4	14.8 g	20 mM
NaCl	29.2 g	100 mM
Tween-20	5 ml	0.1%
ddH_2O qs.	5 liters	

2. In plastic dish, immerse membrane in 10% non-fat dried milk in PBS-T solution (6g of non-fat dried milk in 60 ml of PBS-T) for 1 hr at room temperature on an orbital shaker.

3. Discard blocking solution from container and briefly rinse membrane with two changes of PBS-T.

4. Immerse membrane in PBS-T solution and wash for 1 time for 15 minutes and 1 time for 5 minutes with fresh changes of PBS-T solution at room temperature on an orbital shaker.

D. Addition of the antibodies

1. Dilute primary antibodies in PBS-T solution at dilutions of 1:100, 1:200, 1:500 and 1:1,000

2. On transparency film, use laser blade to cut membrane into small piece. Each piece contained 2 lanes of standard protein ladder and sample. Place a piece of membrane into tube containing each dilution of primary antibody, 500 μl/tube and capped tube tightly. Incubate membrane with diluted primary antibodies for 1 hour at room temperature on rotator.

3. Pull a piece of membrane out of tube. Briefly rinse membrane with two changes of PBS-T and washed the membrane for 1 time for 15 minutes and 2 times for 5 minutes with fresh changes of PBS-T solution at room temperature on an orbital shaker. Keep diluted primary antibodies at 2-8°C in refrigerator. These antibodies can be reused for 3-4 times.

4. Dilute secondary antibody in PBS-T solution at dilution of 1:2,000

5. In dish, incubated membrane in diluted secondary antibodies for 1 hour at room temperature on an orbital shaker.

6. Briefly rinse membrane with two changes of PBS-T solution and wash the membrane for 1 time for 15 minutes and 4 times for 5 minutes with fresh changes of PBS-T solution at room temperature on an orbital shaker.

E. Detection

Enhanced chemilumniscence (ECL) western blotting detection reagents were used to detect western blot according to the manufacturer's instruction. The principal

of ECL detection was that in alkaline condition, the HRP/Hydrogen peroxide catalyzed oxidation of luminol to an excited state. Immediately following oxidation, luminol in excited state decayed to ground state via a light emitting pathway. The light produced by this oxidation peaked after 5-20 minutes and decayed slowly with an approximately half life of 60 minutes. The maximum light emission was at a wavelength of 428 nm which can be detected by a short exposure to blue-light sensitive autoradiography film.

1. Mix an equal volume of detection solution A and B allowing sufficient total volume to cover the membrane (0.125 ml/cm^2 membrane, or about 0.5 ml/piece of membrane)

2. Drain the excess PBS-T solution from the washed membrane and place them, protein side up, on a transparency film. Pipette the mixed detection reagent on to the membrane.

3. Incubate for 1 minute at room temperature.

4. Drain the excess detection reagent by holding the membrane gently with forcep (with round, non-serrated tips) and touching the edge against a tissue. Place the blot on a new transparency film. Wrap up the blots and gently smooth out air bubbles.

5. Place the wrapped blots, protein side up, in an X-ray film cassette.

6. Place a sheet of autoradiography film (such as Hyperfilm ECL) on top of the membrane. Close the cassette and expose for 15 seconds.

7. Remove the film and develop immediately in Film developer. If film is too dark, it indicates too long exposure time, and it is better to decrease the exposure time.

8. Determine molecular weight and amount of band on film by using Labworks™ imaging software in Biochemi™ Imaging system.

4. RNA isolation

BAC and BMα3β4 cells were plated at densities of $5x10^6$ cells/plate in 60 mm plate for 4 and 2 days, respectively. Total RNA were isolated from both cells by using Trizol® reagent as recommended by the company. Trizol® reagent, a mono-phasic solution of phenol and guanidine isothiocyanate was used for the single-step RNA isolation method developed by Chomczynski and Sacchi (190). The procedures

were composed of 4 steps.

A. Homogenization

1. Twice wash cells in culture dish with 5 ml of PBS pH7.3

2. Lyse cells directly by adding 1 ml of Trizol® reagent to a 3.5 cm diameter (60 mm) dish and passing the cell lysate several times through a pipette. The amount of the added Trizol reagent is depend on the area of culture dish (1ml per 10 cm^2) and not on the number of cells present. An insufficient amount of reagent may result in contamination of the isolated RNA with DNA.

3. Transfer all solution into new microtube.

B. Phase separation

1. Incubate sample in microtube at room temperature for 5 minutes in order to complete dissociation of nucleoprotein complexes.

2. Add 0.2 ml of chloroform per 1 ml of Trizol® reagent. Cap microtube and seal with parafilm.

3. Shake microtube vigorously by hand for 15 seconds and incubate them at room temperature (15-30°C) for 2-3 minutes.

4. Centrifuge the samples at 12,000xg at 2-8°C for 15 minutes.

5. Following centrifugation, the mixture is separated into 3 phases: lower red (phenol-chloroform) organic phase, an interphase and a colorless upper aqueous phase. RNA remains exclusively in the aqueous phase. The volume of aqueous phase is approximate 60% of the volume of Trizol® reagent.

6. Collect the aqueous phase by pipetting into new microtube.

C. RNA precipitation

1. Mix the aqueous phase with 0.5 ml of isopropyl alcohol per 1 ml of Trizol® reagent used for the initial homogenization.

2. Incubate sample at 15-30°C for 10 minutes.

3. Centrifuge sample at 12,000xg at 2-8°C for 10 minutes. The RNA precipitate forms a gel-like yellow pellet on the side and bottom of the tube.

D. RNA wash

1. Discard supernatant using micropipette.

2. Wash the RNA pellet once with ethanol. At least 1 ml of 75% EtOH per 1 ml of Trizol® reagent is used for the initial homogenization.

3. Mix sample with vortex. Pellet should not dissolve.

4. Centrifuge sample at 7,500xg at 2-8°C for 5 minutes.

5. Discard supernatant using micropipette. Keep pellet in 0.5 ml of 75% EtOH at -20°C for 1 year or at 2-8°C for 1 week

5. RT-PCR (Reverse transcriptase- Polymerase Chain Reaction)

Total RNA were isolated from either bovine adrenal chromaffin cells or BM α3β4 cells by using Trizol® according to the manufacturer's instruction. To confirm that total RNA was complete without degradation, gel electrophoresis on 1% agarose gel prior to other steps was run. Next, random primed cDNA was generated using SuperScript III RNase-H-RT (Some components were from ProSTAR™ kit). Primers were designed from aligned sequences of the APC human, bovine and rat cDNA sequences from Genbank. Since the APC sequence was highly conserved, the same primers were used for PCR for both bovine adrenal chromaffin and BM α3β4 cells cDNA: GGAATATGAGGCAAGGCAAA (sense) and TTCGAGGAGCAGAATGTGTG (anti-sense). To amplify cDNA template, PCR was performed using Taq PCR kit (Qiagen). After an initial denaturation at 94◦C for 3 min, PCR for 35 and 45 cycles for bovine adrenal chromaffin and BM α3β4 cells, respectively consisted of (a) 94◦C for 1 min, (b) 55◦C for 1 min, and (c) 72◦C for 1 min. A final extension at 72◦C for 10min completed the cycling. Subsequently, in order to analyze PCR products, these products were separated on a 2% agarose gels, bands of the correct size were cut out, concentrated, purified, and cloned into pCRII-TOPO using the TA Cloning kit . Sequencing would be performed by the OSU Plant Genomics Facility.

A. RNA gel electrophoresis

1. Re-dissolved RNA

- After RNA isolation using Trizol reagent, RNA pellet is kept in 0.5 ml of 75% EtOH at -20°C.

- Centrifuge at high speed (or 7,500xg according to Trizol protocol), 4°C for 5 minutes. Discard the supernatant by turn over the tube.

- Air dry the pellet for 10 minutes or vacuum dry but not by centrifugation under vacuum. The reason is that the latter would greatly decrease RNA pellet's solubility.

- Dissolve pellet in 10 μl of Diethylpyrocarbonate-treated water (DEPC-treated water) by adding DEPC-treated water, and waiting for 5 minutes, then pipette solution up-down through end-cut tip. If pipette immediately, the pellet may occlude the tip.

2. Prepare 10 times-concentration 3-(N-Morpholino) propane sulfonic acid (MOPS) buffer 500 ml

- To 400 ml ddH_2O, dissolve each gradient

- Bring final volume up to 500 ml with ddH_2O

- Adjust pH to 7.0 with 6N NaOH

Composition of 10 times-concentration MOPS buffer

Ingredients	MW	Amount	Final concentration
MOPS	209.27	20.95 g	-
NaOAc	82	2.05 g	0.05 M
EDTA	380	1.9 g	0.01 M
ddH_2O qs.		500 ml	

note : All ingredients are electrophoresis grade.

3. Prepare 1% Agarose gel in 10 times-concentration MOPS buffer

- Dissolve agarose in 10 times-concentration MOPS and ddH_2O and swirl in Erlenmeyer flask.

- Melt agarose solution by heating in microwave for 1 minute then swirl flask. Heat for 30 seconds and swirl. Repeat this step for 3 times or until obtain a clear agar solution.

- Cool down the temperature and add formaldehyde in laminar hood.
- Pour gel and let it harden (about 30 minutes). During this time, do step3-4.
- Cover with plastic wrap (not running buffer) until use

Composition of 1% Agarose gel

Ultrapure™ Agarose	0.5 g
10 times-concentration MOPS	5 ml
ddH_2O	35 ml
Formaldehyde	10 ml

4. Prepare Running buffer 500 ml by diluting 100 ml of 10 times-concentration MOPS with 400 ml of ddH_2O

5. Prepare 100 µl of loading buffer (using PCR tip/tube)

Composition of loading buffer

Deionized formamide	70 µl
37% Formaldehyde	20 µl
10 times-concentration MOPS buffer	10 µl
Ethidium bromide (10mg/ml)	1 µl

- Mix 1 part of RNA with 3 parts of loading buffer (1 µl + 3 µl) in PCR tube
- Heat sample at 60°C for 10 minutes on heater (Fisher Scientific), then cool on ice. Centrifuge at high speed (18,000xg) for 15 seconds in order to pull volume down.

6. Before loading gel, add running buffer to cover gel surface and pull off a comb from gel. Load gel with 4 µl/well of sample as well as nucleic acid sample loading buffer. This nucleic acid sample loading buffer, containing bromophenol is used to check that electric current run from negative to positive.

6. Run gel electrophoresis at 100 V for 1 hour

7. See the separated band under UV-light (UV reader or Biochemi™ Imaging system, UVP Inc.)

B. First-Strand cDNA synthesis

1. Thaw each component by hand (did not thaw in water bath). Before using, gently mix and centrifuge at high speed (18,000xg) for 15 seconds to pull volume down. Keep the solution on ice after complete thawing.

2. To a nuclease-free, thin-walled PCR microtube, add the following components in order of mixing. Gently mix and make sure that all the components are at the bottom of tube by centrifuge at high speed (18,000xg) for 15 seconds.

Components	**Stock concentration**	**Experimental tube**	**Control tube**
50-250 ng of random primer[1]	(100 ng/μl)	1 μl	1 μl
10 pg – 5 μg of total RNA	(5 μg/μl)	1 μl	1 μl[1]
10 mM each of dNTP mix[1]	(40mM total)	1 μl	1 μl
DEPC-H_2O or sterile distilled water	qs 13 μl	10 μl	10 μl

Note : [1] : used ProSTAR^{TM} Kit

3. Heat mixture to 65°C for 5 minutes. Cool each reaction tube on ice for 5 minutes in order to allow the primers to anneal to the RNA.

4. Collect the contents of the tube by brief centrifugation and added

5 times-concentration First-strand buffer	4 μl
0.1 M Dithiothrietol (DTT)	1 μl
RNaseOUT^{TM}	1 μl
200 units/μl of Superscript RT III	1 μl

Note : RNaseOUT^{TM},Recombinant RNase inhibitor is necessary addition when using less than 50 ng of starting RNA. In this experiment, 5 μg RNA was used, so no need for RNaseOUT^{TM}. To adjust final volume to 20 μl, 1 μl of DEPC-H_2O was added.

5. Mix by pipetting gently up and down. Because of random primer, incubate tube at 25°C for 5 minutes.

6. Incubate tube at 50°C for 60 minutes. The reaction temperature could be increase to 55°C for gene-specific primer or difficult template.

7. Inactivate the reaction by heating at 70°C for 15 minutes.

The cDNA could be used as a template for amplification in PCR. If didn't use immediately, stored cDNA product in -20°C freezer.

C. Amplifying the cDNA template

1. Thaw each component by hand. Gently mix before use and centrifuge at high speed (18,000xg) for 15 seconds to pull volume down. Keep the solution on ice after complete thawing.

2. Prepare a master mix as following.

Master Mix	**(+)ve**	**(-)ve**	**Final concentration**
10 times-concentration Qiagen PCR buffer (contained 15 mM $MgCl_2$)	10 µl	10 µl	1 time
5 times-concentration Q-solution	20 µl	20 µl	1 time
dNTP mix (10 mM of each dNTP)	2 µl	2 µl	200 µM each
Primer A (sense 100 ng/µl)	2 µl	2 µl	0.2 µM
Primer B (anti-sense 100 ng/µl)	2 µl	2 µl	0.2 µM
Taq DNA Polymerase	0.5 µl	0.5 µl	2.5 units/reaction
DEPC H_2O or distill water	61.5 µl	63.5 µl	qs. 100 µl
Template DNA			
Template cDNA	2 µl	-	≤ 1 µg/reaction

3. Mix the master mix thoroughly by pipette up and down a few times or spin by hand. It is recommended that PCR tubes are kept on ice before placing on the thermal cycler.

4. Add template cDNA to individual tubes containing the master mix.

5. Place the amplification reaction tubes in a thermal cycler and perform the following thermal cycling condition. Then, PCR product is ready for analyzing step.

Thermal cycling condition	**Cycle**	**Temperature**	**Time**
Initial denaturation	1 time	94°C	3 min
3-step cycling	35 and 45 times for BAC and BMα3β4, respectively		
Denaturation		94°C	1 min
Annealing		55°C	1 min (Tm-5°C)
Extension		72°C	1min (1min/kb DNA)
Final extension	1 time	72°C	10 min
		4°C	∞

Oligonucleotide data sheet

Sequence 5′ to 3′	OD	length	MW	μg	Tm	E260
GGAATATGAGGCAAGGCAAA (sense) (50 nmole, salt free)	10.2	20	6248.14	281.9	58.35	226077.8
TTCGAGGAGCAGAATGTGTG (anti-sense) (50 nmole, salt free)	15.07	20	6237.14	458.36	60.4	205064.9

Primer dilution

GGAATATGAGGCAAGGCAAA (sense)

1. Primer powder 281.9 μg + DEPC H_2O 281.9 μl = stock 1 μg/μl
   Diethylpyrocarbonate-treated water
2. Stock (1 μg/μl) 1 μl + DEPC H_2O 9 μl = stock 100 ng/μl
   Diethylpyrocarbonate-treated water

TTCGAGGAGCAGAATGTGTG (anti-sense)

1. Primer powder 458.36 μg + DEPC H_2O 458.36 μl = stock 1 μg/μl
   Diethylpyrocarbonate-treated water
2. Stock (1 μg/μl) 1μl + DEPC H_2O 9 μl = stock 100 ng/μl
   Diethylpyrocarbonate-treated water

6. Analyze PCR Product

A. DNA separation from PCR product by DNA gel electrophoresis.

B. DNA purification from agarose gels

1. The Ultrafree® -DA was a centrifugal filter device designed to extract 100-10,000 bp DNA from agarose gel slice.

2. Micron-PCR was a centrifugal filter device designed for purification of PCR product. It concentrated amplified DNA and removed primers as well as unincorporated dNTPs.

C. DNA cloning and transforming

TOPO TA cloning® kit was composed of TOPO TA cloning reagent and Regular One shot® Chemical competent kit for DNA cloning and transforming, respectively.

1. Set up TOPO cloning reaction and incubated for 5 minutes at room temperature (22-23°C)

2. Transform TOPO® cloning reaction into Regular One shot® Chemically competent cells

3. Select and analyze 10 white or light blue colonies for insert.

D. Plasmid purification and DNA sequencing

FastPlasmid® Mini procedure was used to purify plasmid containing an interested DNA. Subsequently, purify plasmid was done by 2 processes.

1. To confirm the presence and correct orientation of the plasmid insertion, restriction enzyme digestion was performed to cut DNA fragments off the plasmid. Then, DNA gel electrophoresis was used to separate copies DNA fragments.

2. For DNA sequencing, purify plasmid was sent to the OSU Plant Genomics Facility.

A. DNA gel electrophoresis

1. Prepared 5 times-concentration TBE buffer

- To 800 ml of ddH_2O, add Tris base and boric acid. Stir by magnetic bar.

- Prepare stock 0.5 M EDTA (MW 416.20) solution by dissolving 20.81 g in 100 ml of ddH_2O. Due to its low solubility, gradually add EDTA and stir well. Keep EDTA solution at 2-8°C.

- Pipette 0.5 M EDTA to this solution.

- Bring final volume up to 1,000 ml with ddH_2O

Composition of 5 times concentration TBE buffer

Tris base	54 g
Boric acid	27.5 g
0.5 M EDTA solution	20 ml
ddH_2O qs.	1 liter

2. Prepare 2% Agarose gel in 5 times-concentration TBE buffer

- Dissolve agarose in 5 times-concentration TBE buffer and ddH_2O and swirl in Erlenmeyer flask.

- Melt agarose solution by heating in microwave for 1 minute then swirl flask. Heat for 30 seconds and swirl. Repeat this step for 3 times or until obtain a clear agar solution.

- Cool down the temperature and add 5 µl of EtBr per 100 ml of gel solution.

- Pour gel and let it harden (about 15-20 minutes, 2% agarose gel is harden faster than 1% gel).

- Cover with plastic wrap (not running buffer) until use

Composition of 2% Agarose gel in 5 times-concentration TBE buffer

Ultrapure™ Agarose	2 g
5 times-concentration TBE buffer	20 ml
ddH_2O	80 ml
Ethidium bromide (EtBr)	5 µl

3. Prepare 1,000 ml Running buffer by diluting 200 ml of 5 times-concentration TBE with 800 ml of ddH_2O. Before using, add 50 µl of EtBr to 1,000 ml of Running buffer.

Composition of Running buffer

5 times-concentration TBE buffer	200 ml
ddH_2O	800 ml
Ethidium bromide (EtBr)	50 µl

4. In PCR tube, mix 9 parts of PCR product with 1 parts of Sample loading buffer, 10 times-concentration BlueJuice™ gel loading buffer (27 µl + 3 µl/well).

5. Before loading gel, add running buffer to cover gel surface and pull off a comb from gel. Load gel with 30 µl/well of sample as well as 5 µl/well of DNA ladder, Ready-Load™ 100 bp DNA Ladder.

6. Run gel electrophoresis at 100 V for 1.5-2 hours. (2% agarose gel separate bands slower than 1% gel)

7. Locate the interest band under UV-light (UV reader or Biochemi™ Imaging system, UVP Inc.). With a razor blade, cut out the slice of agarose containing the interested band

8. Keep this gel slice in -20°C freezer for further DNA sequencing.

Note The commercial protocol recommended using 2% agarose gel for Ready-Load™ 100 bp DNA Ladder. 2% agarose gel can separate low molecular weight band better than 1% agarose gel.

B. DNA purification from agarose gel

1. **Procedure to use Ultrafree®-DA** as recommend by the company (Millipore)

1. Pre-assemble the Ultrafree®-DA from top to bottom as followed gel nebulizer, ultrafree-MC and vial

2. From DNA electrophoresis, place gel slice containing the interested band into gel nebulizer and seal device with a cap attached to vial.

3. Spin at 5,000xg for 10 minutes. Centrifuge force the agarose gel through the gel nebulizer and convert it to fine slurry which is captured by Ultrafree-MC. Extruded DNA in electrophoresis buffer passes through the micropore membrane in Ultrafree-MC and collect into the filtrate vial.

4. Discard the Ultrafree-MC and gel nebulizer. Keep extruded DNA in filtrate.

2. **Procedure for Microcon-PCR** as recommend by the company (Amicon)

1. Insert Microcon-YM30 PCR sample reservoir into vial.

2. Fill the reservoir with all volume of extrude DNA in filtrate and adjust to final volume of 500 µl with DEPC-H_2O.

3. Spin the Microcon-PCR device at 1,000xg for 15 minutes.

4. To recover DNA, remove sample reservoir from the filtrate collection vial and place in a clean vial. Add 20 μl of DEPC-H_2O to sample reservoir. Then, invert the reservoir and spin at 1,000xg for 2 minutes to retrieve the purified DNA.

C. DNA cloning and transforming

Long DNA molecules could be cleaved into shorter fragments using restriction nucleases and these fragments could be joined back together using DNA ligase. DNA cloning referred to the act of making many identical copies of DNA molecules. One way for DNA cloning was to introduce the DNA to be copied into a rapidly dividing bacterium such as *E.Coli*. The mechanism of introduction DNA into bacteria was called transformation. An advantage of this technique was that naked DNA from any source, not just from same bacterial species could be taken up. Some bacteria naturally took up DNA molecules presented in surrounding by pulling the DNA through their cell membrane to the inside of cells. Then, this introduced DNA was incorporated into the bacterial genome. Each time the bacterium replicated its own DNA, it also copied the introduced DNA. In addition, a small circular DNA plasmid was used as a vector or carrier to transport outside DNA into bacterial cells.

The principle of TOPO cloning was that

1. In PCR process, Taq polymerase had transferase activity which added a single deoxyadenosine (A) to the 3′ ends of PCR product, the DNA that was needed in this experiment.

2. The TOPO plasmid vectors had single overhanging 3′ deoxythymidine (T) residues. This allowed the specific binding between 3′-T residues on TOPO vector and 3′-A ends of needed DNA.

3. Enzyme DNA topoisomerase I had a dual functions both as a restriction enzyme and a ligase. Its biological roles were to cleave and rejoin DNA during replication. This enzyme recognized the sequence 5′-(C/T)CCTT-3′ and specifically formed a covalent bond with the phosphate group of the 3′-thymidine of TOPO plasmid vector. After enzyme-TOPO vector (activated vector) bound with DNA, topoisomerase I cleaved one DNA strand, enable the DNA to unwind. Then, it religated the ends of cleaved strand and released itself from DNA.

1. **Procedure for TOPO® cloning reaction** as recommend by the company (Invitrogen)

In our experiment, TOPO® cloning reaction was set up for eventual transformation into chemically competent *E.Coli* .

Reagent	Chemically competent *E.Coli*
Fresh PCR product	4 μl
Salt solution	1 μl
Diluted salt solution	-
Sterile water (qs to 5 μl)	-
TOPO® vector (PCR®4-TOPO®)	1 μl
Final volume	6 μl

1. After thawing TOPO® cloning reagent, Mix reaction gently and incubate at room temperature (22-23°C).

3. Place the reaction tube on ice and proceed to Transforming One Shot® Competent cells.

4. When finish, keep all reagents in -20°C freezer.

2. **Protocol for transformation using Regular One Shot® Chemically competent kit**

This process is the transforming PCR®4-TOPO construct into the competent *E.Coli* as recommend by the company (Invitrogen). Kanamycin was used as a selective agent for the regular chemical transformation procedure.

Preparation

1. Set up a water bath to 42°C

2. Thaw the vial of SOC medium which is kept in -80°C freezer and warm up the vial in a water bath to room temperature. SOC medium may also be stored at -20°C or at room temperature.

3. Prepare Lubria-Bertani (LB) agar plate

- To 500 ml of ddH2O, dissolve 10 g of LB-broth and 7.5 Bactro-agar and adjust pH to 7.2

- Autoclave agar solution at 100°C for 25 minutes.

- Cool the temperature down then add kanamycin to 50 μg/ml.

- Pour LB agar solution to culture plates and let it harden. If LB agar plates are not used, keep them in refrigerator.

- Before use, warm up a selective LB agar plate at 37°C for 30 minutes in incubator.

4. Prepare 5 bromo-4-chloro-3-indolyl-β-D-galactoside (X-gal) stock solution

- Dissolve 100 mg of X-gal in 2.5 ml of dimethylformamide to make 40mg/ml stock solution. Keep this solution at -20°C and protect from light.

- Pipette 40 μl of the 40 mg/ml X-gal stock solution onto the selective plate. Spread evenly and let it dry for 15minutes. Protect plate from light and incubate at 37°C in incubator until ready for use. (Heat the tip of Pasteur pipette until become two red spots and bend it as a 90° angle for spreading X-gal

- Thaw on ice one vial of One shot® cells (keep in -80°C) for each transformation.

Note: X-gal, M.W.408.64 was a substrate for enzyme β-galactosidase. It will be hydrolyzed to a blue precipitate. For this reason, bacteria with active β-galactosidase activity could produce the blue colonies, which grew on the X-gal spreading selective plate.

Regular One Shot® Chemically Transformation

1. Add 2 μl of solution obtained from TOPO® cloning reaction into a vial of One shot® Chemically Competent *E.Coli* and gently mix by hand. Do not use pipette up-down for mixing because this technique make cells lyses.

2. Incubate a vial on ice for 30 minutes.

3. Heat shock the cells at 42°C for 30 seconds by putting a vial in a water bath without shaking.

4. Immediately transfer a vial to ice.

5. Add 250 μl of SOC medium at room temperature.

6. Cap a vial tightly and seal with parafilm. Shake a vial horizontally (200 rpm) at 37°C for 1 hour.

7. Spread a variable 10-50 μl from each transformation on a pre warmed selective plate. Plates were spread with two different volumes in order to make sure that at least one plate will have the well-spaced colonies. In this experiment, the volumes of 20 and 200 μl/ plate are used. To ensure even spreading of small volume, add 20 μl of SOC medium onto plate. Turn down selective plates and incubate in 37°C incubator overnight.

8. An efficient TOPO® cloning reaction should produce several hundreds colonies. Pick up about 10 white colonies for proceeding analysis.

3. **Procedure for pick up white colonies**

1. Prepare LB-broth medium

- To 1 liter of ddH_2O, dissolve 20 g of LB broth and adjust pH to 7.2
- Heat and stir for completely dissolve.
- Autoclave at 121°C for 15 minutes.
- Cool down to room temperature.
- Use sterile technique to add kanamycin (50 μg/ml) and pipette 5 ml of LB broth into each sterile tube.

2. To take the 10 white colonies, put the end of sterile pipette tip attached to desired colony, and pull out. Then, place the end of tip into LB broth tube and pipette up-down. When finish, the selective plate is sealed with parafilm and stored in refrigerator (4-8°C).

3. Lay the tubes in 45° angel in 37°C, 200 rpm shaker. Culture them overnight in LB medium. One LB medium tube is used as a blank.

4. After incubation, the solution in a blank tube should be clear which indicates no contamination. In the opposite, the solution in a sample tube should be turbid which indicates the growth of bacteria. The white colonies grow up and are ready for further step, plasmid isolation. If the further step should not be immediately performed, keep these tubes in refrigerator (18-24°C).

D. Plasmid purification and DNA sequencing

1. **FastPlasmid™ Mini Procedure** as recommended by the company. FastPlasmid Mini kit was kept in refrigerator.

1. Mix each LB broth tube thoroughly by vortex. Pipette 1.5 ml of bacterial culture into FastPlasmid culture tube.

2. Spin at least 12,000xg for 1 minute for pellet precipitation. Decant supernatant and keep the pellet.

3. Add 400 µl of ice-cold Complete Lysis Solution (FastPlasmid Mini Lysis solution). This solution must be ice-cold (0-4°C) to obtain maximum yield.

4. To completely dissolve pellet, vortex thoroughly for a full 30 seconds. This step is critical for maximum yield.

5. Incubate the lysate at room temperature for 3 minutes.

6. Transfer the lysate to a Spin Column Assembly by pipetting.

7. Spin a Spin Column Assembly at 12,000xg for 1 minute.

8. To wash DNA, add 400 µl of Diluted Wash Buffer (FastPlasmid Mini Wash Buffer) to a Spin Column Assembly.

9. Spin a Spin Column Assembly at 12,000xg for 1 minute.

10. Remove the Spin Column from the centrifuge and decant the filtrate from the Spin Column Assembly waste tube. Place the Spin Column back into the waste tube and return it to the centrifuge.

11. To dry the Spin Column, spin at 12,000xg for 1 minute.

12. Transfer the Spin Column into a Collection tube.

13. Add 50 µl of Elution Buffer (FastPlasmid Mini Elution Buffer) directly to the center of the Spin Column membrane. Do not attach the membrane. Cap the tube.

14. Spin at 12,000xg for 1 minute. Discard the Spin Column. The eluted DNA or purify plasmid is in the filtrate in the collection tube. This filtrate can be used immediately or stored at -20°C. When finish, keep FastPlasmid Mini kit in refrigerator

15. The purify plasmid is divided into 2 parts. First part is used for DNA sequencing. The other is ready for restriction enzyme digestion to confirm the presence and correct orientation of the plasmid insertion.

2. **Restriction enzyme digestion**

The restriction enzyme kit was kept in -20°C freezer.

1. Thaw reagent at 37°C before use.
2. In sterile tube, add each ingredient in order of mixing.
3. Incubate tube at 37°C for 1 hour in hot dryer.

	Control tube	Sample tube
Purify plasmid DNA	10 μl	26 μl
10 times-concentration react buffer no.3	3 μl	3 μl
ECO R1 enzyme	-	1 μl
ddH_2O	17 μl	-

4. Add 3 μl of Blue Juice Gel Loading Buffer to each tube and mixed well.
5. As described in topic of Analyze PCR product, run DNA electrophoresis on 2% agarose gel at 100 V for 1.5 hours.

7. siRNA Transfection into BMα3β4 Cells.

To block APC protein expression, APC stealth siRNA were transfected into BMα3β4 cells according to the modified method from Invitrogen protocol. Stealth siRNA, a chemically modified dsRNA, was used to knockdown target gene. BLOCK-iT^{TM} Fluorescent Oligo was a fluorescence-labeled, double-strand RNA duplex with the same length, charge, and configuration as standard siRNA. It allowed easy fluorescence-based assessment of dsRNA oligomer uptake into mammalian cells. Lipofectamine^{TM} 2000 reagent was a cationic lipid-based formulation suitable for delivery of the BLOCK-iT^{TM} Fluorescent Oligo and Stealth siRNA oligomers to mammalian cells.

Plan

Day 0 : Cultured BMα3β4 cells at a density of $6x10^4$ cells/ml/well in 24 well culture plate.

Day 1 : Changed culture media to media without antibiotic, 400 μl/well

Day 2 : Transfected cells with stealth siRNA and incubated for 24 hours in 37°C, 5%CO_2 humidify incubator.

Day 3-7 : Stopped transfection. Did the assays at 24, 48 and 72 hours post-siRNA transfection

a. Fluorescent reader : cell counting under fluorescent microscope and fluorescent plate reader.

b. Protein assays : protein extraction and protein content assay.

c. Western blot analysis.

d. [^{3}H] Epibatidine binding assay coupled with receptor alkylation.

Preparation

1. 20 μM siRNA stock solution

- Resuspend the 80 nmole siRNA powder in 800 μl DEPC-treated water to make a 100 μM stock solution. Dilute 100 μl of 100 μM stock solution with 400 μl DEPC-treated water to make a 20 μM working stock solution.

2. Media for BMα3β4 cells

Ingredients	**Volume**	**Final concentration**
MEM	500 ml	
FBS	50 ml	10 %
200 mM L-glutamine	5 ml	2 mM
10 mM MEM non-essential amino acid	5 ml	0.1 mM
100 mM Sodium pyruvate	5 ml	1 mM
(1.5 g/30 ml) $NaHCO_3$	15 ml	1.5 g/L
Penicillin/Streptomycin (antibiotics)	5 ml	100 U/ml Penicillin & 100 μg/ml Streptomycin

Note BMα3β4 cells grew in this growth media as well as in normal culture media.

Procedure

1. BMα3β4 cells, at a density of $6x10^4$ cells/well are cultured in growth media in 24 well culture plated in 37°C, 5%CO_2 humidify incubator.

2. One day before transfection, the media are removed and replaced with 400 µl/well growth media without antibiotics. Cells are 90% confluence at the time of transfection.

3. Prepare the transfected complexes as follows:

3.1 Stealth™ siRNA-Lipofectamine™2000-BLOCK-iT Fluorescent Oligo complexes

a. Before use, thaw siRNA, 20 µM BLOCK-iT and Lipofectamine™2000 at room temperature. Place them on ice.

b. Mix Lipofectamine™ 2000 gently before use, then dilute 1.5 µl/well of Lipofectamine™ 2000 in 50 µl/well of Opti-MEM®I. Mix gently by hand (Do not pipette up-down for mixing). Incubate this solution for 5 minutes at room temperature.

c. Dilute 5 µl/well of 20 µM (= 20 pmol/µl) BLOCK-iT in 45 µl/well of Opti-MEM®I to a final amount of 100 pmol/well. Mix gently by hand. After 5 minutes incubation of diluted Lipofectamine™ solution, add this diluted BLOCK-iT Oligo into diluted Lipofectamine™ solution and mix gently. Incubate for 10 minutes at room temperature to allow Lipofectamine-Oligomer complex formation. The solution may appear cloudy which will not interfere transfection.

d. Dilute 7.5 µl/well of 20 µM Stealth™ siRNA in 50 µl/well of Opti-MEM®I to a final amount of 150 pmol/well. Mix gently by hand. After 10 minutes incubation of Lipofectamine-Oligomer solution, add this diluted siRNA solution into Lipofectamine-Oligomer solution and mix gently by hand. Incubate for 15 minutes at room temperature.

3.2 Stealth™ siRNA-Lipofectamine™2000 complexes

a. Before use, thaw siRNA and Lipofectamine™2000 at room temperature. Place them on ice.

b. Mix Lipofectamine™ 2000 gently before use, then dilute 1.5 µl/well of Lipofectamine™ 2000 in 50 µl/well of Opti-MEM®I. Mix gently by hand (Do not

pipette up-down for mixing). Incubate this solution for 15 minutes at room temperature.

c. Dilute 7.5 µl/well of 20 µM Stealth™ siRNA in 50 µl/well of Opti-MEM®I to a final amount of 150 pmol/well. Mix gently by hand. After 15 minutes incubation of diluted Lipofectamine solution, add this diluted siRNA solution into Lipofectamine solution and mix gently by hand. Incubate for 15 minutes at room temperature.

4. As design, Add 159 µl/well of Stealth™ siRNA-Lipofectamine™2000-BLOCK-iT Fluorescent Oligo complexes or 109 µl/well of Stealth™ siRNA-Lipofectamine™2000 complexes to each well containing BMα3β4 cells and media without antibiotics. Mix gently on shaker for 5 minutes.

5. Incubate the cells in a 37°C, 5%CO_2 humidify incubator for 24 hours. It is not necessary to remove the complexes or change the media, however growth media may be replaced after 4-6 hours without loss of the transfection activity.

6. After 24 hours incubation, stop siRNA transfection by aspirating off old media and washing cells with 1 ml/well of sterile PBS. Then aspirate off PBS and replace with 1 ml/well of growth media with antibiotics.

Note - Using PCR-tubes and microtips for step 3-4.

- This protocol was modified from Invitrogen protocol as shown in the following diagrams

Lipofectamine + (Opti-MEM)
↓ 5 min, RT
+ [(BLOCK-iT) + (Opti-MEM)]
↓ 10 min, RT
+ [siRNA + (Opti-MEM)]
↓ 15 min, RT
Add 159 µl/well to cells in media without antibiotics
↓ shake for 5 min
Incubate cells in a 37°C, 5%CO_2 humidify incubator for 24 hrs.

(3.1)

Lipofectamine + (Opti-MEM)
↓ 15 min, RT
+ [siRNA + (Opti-MEM)]
↓15 min, RT
Add 109 µl/well to cells in media without antibiotics
↓ shake for 5 min
Incubate cells in a 37°C, 5%CO_2 humidify incubator for 24 hrs.

(3.2)

Lipofectamine + BLOCK-iT	**Lipofectamine + siRNA**
Lipofectamine + (Opti-MEM) ↓ 5 min, RT + [(BLOCK-iT) + (Opti-MEM)] ↓ 20 min, RT Add to cells in media without antibiotics ↓ shake for 5 min Incubate cells in a 37°C, 5%CO_2 humidify incubator until ready to assay	Lipofectamine + (Opti-MEM) ↓ 15 min, RT + [siRNA + (Opti-MEM)] ↓15 min, RT Add to cells in media without antibiotics ↓ shake for 5 min Incubate cells in a 37°C, 5%CO_2 humidify incubator for 6-24 hrs.

(Invitrogen Protocol)

8. Fluorescent Reader

To assess Oligo uptake, it is necessary to detect the fluorescence signal by 2 methods

a. Cell counting under fluorescent microscope

b. Fluorescent plate reader

a. **Cell counting under fluorescent microscope**

1. Remove plate from incubator and scan cells under microscope. Aspirate off media from each well by aspirator.

2. Add 1 ml/well of PBS pH 7.3 for washing, then aspirate off PBS.

3. Trypsinization

- Add 1 ml/well of trypsin (warm in 37°C water bath).
- Incubate at room temperature for 1 minute, then aspirate off excess trypsin.
- Incubate cells in 37°C, 5%CO_2 humidify incubator for 10 minutes.
- To stop trypsinizing process, add 1 ml/well of media.
- Pipette up-down 10 times to dissociate cells.

4. Take all solution from each well to microcentrifuge tube. To pellet the cells, centrifuge at 250xg for 10 minutes.

5. Discard supernatant and keep cell-pellet.

6. Resuspend cell-pellet by adding 100 µl/tube of media or PBS.

7. Using hemacytometer, Count the number of cells in cell-suspension under fluorescence microscope (x10 magnifier len).

8. Calculate the percentage of transfection efficiency.

[no. of cells with fluorescent-label] / [no. of total cells] x 100

b. **Fluorescent plate reader**

1. Remove plate from incubator and scan cells under microscope.

2. Aspirate off media from each well by aspirator. Add 1 ml/well of PBS pH 7.3 for washing, then aspirated off PBS.

3. Add 1 ml/well of PBS.

4. Using SPECTRAFluor Plus machine to read fluorescent signal from plate under the following conditions:

Excitation wavelength : 485 nm

Emission wavelength : 535 nm

Gain : 112

Read from bottom, plate with lid-cover.

9. Puromycin Treatment in BMα3β4 Cells.

Prepartion

1. Sterile 1 mg/ml of puromycin stock solution

- Dissolve 10 mg of puromycin in 10 ml of ddH_2O
- Filter sterilize this solution and keep in freezer.

Procedure

1. Culture BMα3β4 cells at density of $6x10^4$ cells/ml/well in 24 well culture plate for 2 days in 37°C, 5%CO_2 humidify incubator.

2. On the experiment day, remove plate from incubator and scan cells under microscope.

3. Into each well, add 10 μl of 1 mg/ml sterile puromycin stock solution to final concentration of 10 μg/well. In control well, add 10 μl of ddH_2O

4. Incubate cells in 37°C, 5%CO_2 incubator for overnight.

5. Aspirate off old media. Wash cells with 1 ml/well sterile PBS pH 7.3 and culture in normal growth media.

6. Puromycin-treated cells are ready for further analysis: protein extraction and analysis, [^{3}H] Epibatidine binding assay coupled with receptor alkylation, and western blot analysis at 24 hours post-puromycin treatment.

10. [^{3}H] Epibatidine Binding Assay Coupled with Receptor Alkylation to Intact BMα3β4 Cells.

[^{3}H] Epibatidine binding assay was performed to determine nonspecific and specific binding. To measure specific binding to both surface and intracellular

nAChRs, the permeant cholinergic agonist, 300 μM nicotine (> 1,000 times nicotine's Kd for BMα3β4 nAChRs) (26) was used to defined nonspecific binding. To measure specific binding to intracellular nAChRs, receptor alkylation technique was performed prior to binding assay in order to eliminate surface binding of cells . Specific binding to surface nAChRs was indirectly calculated by subtraction of intracellular binding values from total specific binding values.

In this experiment, BMα3β4 cells were used in [^{3}H] Epibatidine binding assay coupled with receptor alkylation at 24, 48 and 72 hours post-siRNA transfection as well as at 24 hours post-puromycin treatment.

A. Receptor alkylation in intact BMα3β4 cells.

Surface receptors were irreversibly inactivated via alkylation with bromoacetylcholine (brACh) using technique following the previous procedure of Free et al. (109). To reduce its disulfide bonds, nAChRs located on intact BMα3β4 cells were treated with 30 mM dithiothrietol (DTT) in Physiological salt solution (PSS) pH 8.0. Subsequently, they were irreversibly alkylated with 100 μM brACh. Finally, its disulfide bonds were re-oxidized by 3 mM 5,5′-dithio-bis(2-nitrobenzoic acid) (DTNB) in PSS pH 7.3 Controls were processed in parallel with the alkylation groups, without addition of reducing, alkylating or re-oxidizing agents.

Preparation

Prepared the following solutions

1. PSS pH 7.3 (109)

- To ddH_2O at the approximate volume 2/3 of total volume, add the concentrated stock solution. The $CaCl_2$ solution should be added in the last. The final concentration of these ingredients could be 140 mM NaCl, 4.4 mM KCl, 1.2 mM KH_2PO_4, 3.6 mM $NaHCO_3$, 1.2 mM $MgSO_4$ and 2 mM $CaCl_2$. After each addition, mix well by magnetic stirrer.

- Add glucose and HEPES to make final concentration to 10 mM and 5 mM, respectively. Stir well.

- Add BSA to make final concentration to 0.5% and stir until dissolve.
- In graduated cylinder, bring the volume up to final volume with ddH_2O.
- Adjust pH to 7.3 by 1M NaOH solution.

2. 30 mM DTT in PSS pH 8.0 (MW 154)

- Calculate the needed volume and amount of DTT for preparing solution

: 500 µl/well x 10 wells/plate x 2 plates = 10 ml of DTT solution.

From calculation, prepare 15 ml of DTT solution for 2 plates.

: Amount of DTT (mg)/ 4.62 = Volume of added PSS pH 8.0 (ml)

Amount of DTT (mg) = Volume (ml) x 4.62

= 15 ml x 4.62 = 69.3 mg

- Adjust pH of 20 ml PSS pH 7.3 to 8.0 by diluted NaOH. This step should be freshly prepared on the experiment day.
- Dissolve 69.3 mg of DTT in 15 ml of PSS pH 8.0 and stir well by magnetic stirrer.
- Adjust pH to 8.0 with diluted NaOH.
- 30 mM DTT in PSS pH 8.0 is a colorless sulfur-smelt solution.

3. 3 mM DTNB solution in PSS pH 7.3 (MW 396)

- Calculate the needed volume and amount of DTNB for preparing solution

: 500 µl/well x 10 wells/plate x 2 plates = 10 ml of DTNB solution.

From calculation, prepare 15 ml of DTNB solution for 2 plates.

: Amount of DTNB (mg)/ 1.188

= Volume of added PSS pH 7.3 (ml)

Amount of DTNB (mg)

= Volume (ml) x 1.188 = 15 ml x 1.188 = 17.82 mg

- Dissolve 17.82 mg of DTNB in 15 ml of PSS pH 7.3 and stir well by magnetic stirrer.
- 3 mM DTNB in PSS pH 7.3 is a yellow solution.

4. 100 μM brACh in PSS pH 7.3

- In a 50 ml conical tube, add 20 μl of neostigmine (10^{-2} M stock solution) to 20 ml of PSS pH 7.3 to give a final concentration of 10 μM neostigmine.

- Immediately prior to adding this solution to the cells, add 200 μl of brACh (10^{-2} M stock solution) to give a final concentration of 100 μM brACh.

Note Before starting the alkylation procedure, placed PSS pH 7.3, DTT solution and DTNB solution in 37°C water bath.

Procedure

1. Culture BMα3β4 cells at density of $6x10^4$ cells/well in 24 well culture plate until ready to be used. Remove culture plate from 37°C, 5%CO_2 humidify incubator and scan the cells under microscope.

2. At the binding station, aspirate off culture media. Wash cells with 1 ml/well PSS solution (pH 7.3) for 5 minutes and aspirate off PSS.

3. Add DTT solution 500 μl/well in alkylated wells and only add PSS 500 μl/well in non-alkylated wells. Incubate culture plate in 37°C, 5%CO_2 humidify incubator for 15 minutes. It is important to maintain the temperature of DTT solution at 37°C.

4. Remove culture plate from 37°C, 5%CO_2 humidify incubator. Aspirate off DTT solution. To wash cells, add 1 ml/well of PSS and incubate at room temperature for 5 minutes. Then, aspirate off PSS. During incubation time, freshly add brACh to neostigmine- PSS solution

5. Add brACh solution 500 μl/well in alkylated wells and only add PSS 500 μl/well in non-alkylated wells. Incubate culture plate at room temperature for 6 minutes.

6. Aspirate off brACh solution. To wash cells, add 1 ml of PSS and incubate at room temperature for 5 minutes. Then, aspirate off PSS.

7. Add DTNB solution 500 μl/well in alkylated wells and only add PSS 500 μl/well in non-alkylated wells. Incubate culture plate in 37°C, 5%CO_2 humidify incubator for 15 minutes.

8. Remove culture plate from 37°C, 5%CO_2 humidify incubator. Aspirate off DTNB solution. To wash cells, add 1 ml of PSS and incubate at room temperature for 5 minutes. Then, aspirate off PSS.

9. Repeat washing step once.

10. Continue with receptor binding assay or place back in media for recovery experiment.

B. [^{3}H] Epibatidine binding assay to intact BMα3β4 cells.

This assay was done following the protocol described by Free et al. (109)**.**

Preparation

Make up all solution as following, depending on conditions.

1. 1 M NaOH solution, 250 ml (MW = 40)

- In a 250 ml volumetric flask, add 10 g of NaOH into 100 ml of ddH_2O and swirl until completely dissolved.

- Bring volume up to 250 ml with ddH_2O

2. 1x10^{-6} M [^{3}H] Epibatidine (EB) stock solution, 0.25 ml

- For dilution, calculate the amount of [^{3}H] EB by using program GraphPad (191).

Original dilution = 1 mCi/ml

Original activity = 38.40 and 55.5 Ci/mmol

- Dilute [^{3}H] EB with ethanol

- Keep stock solution in -20°C freezer.

3. 2 nM of [^{3}H] EB buffer, 18 ml

- In a 50 ml conical tube, add 36 µl of 1x10^{-6} M [^{3}H] EB stock solution to 18 ml of PSS pH 7.3 and mix well.

4. 1x10^{-1} M Nicotine stock solution, 1 ml (MW = 462.4)

- Dissolve 46.24 mg in 1 ml of ddH_2O

- Keep stock solution in freezer

1x10^{-3} M Nicotine working solution, 8 ml

- Add 80 µl of 1x10^{-1} M Nicotine stock solution to 7,920 µl of 2 nM of [^{3}H] EB buffer

Procedure

1. Culture BMα3β4 cells at density of $6x10^4$ cells/well in 24 well culture plate until ready to be used. Remove culture plate from 37°C, 5%CO_2 humidify incubator and scan the cells under microscope.

2. At binding station, aspirate off culture media. Wash cells with 1 ml/well of PSS (pH 7.3) for 5 minutes and aspirate off PSS. Repeated washing step or go to nAChR alkylation protocol.

3. After receptor alkylation step, aspirate off PSS. Added 300 µl/well of treatments as designed: $1x10^{-3}$ M Nicotine working solution to define nonspecific binding or 2 nM of [^{3}H] EB buffer for total binding. Incubate plate for 60 minutes at room temperature.

4. After incubation, rapidly wash each well individually by inserting aspirator and immediately adding 1 ml PSS from the repeating pipette and then immediately aspirating this wash. Repeat 4 times for a total of less than 10 seconds for all 4 wash. Leave well dry and move on to the next well and continue washing until the entire plate is washed.

5. Add 500 µl of 1 M NaOH to each well. Take the plate to 37°C, 5%CO_2 humidify incubator and incubated for at least 3 hours to overnight.

6. Remove plate to binding station. Place rubber policeman with the flat end, not slope end into a 50 ml of tube containing 1M NaOH. Scrap each well using the policeman by rotating it in the well 5 rotations. After scraping each well, scrap the policeman against the side of the well , and dip the policeman back in the conical tube of NaOH to wash and avoid any carry-over between wells.

7. After scraping, set pipette up to 650 µl. Pipette the entire contents of each well up and down and remove them to scintillation vials.

8. To each vial, add 70 µl of concentrated HCl . Gently shake the vial tray to mix. It would bubble as HCl neutralized NaOH.

9. Add 4.5 ml of Scintiverse E Scintillation cocktail to the vials and count in Liquid Scintillation Spectroscopy.

Data analysis

Total = Total counts

Total - Excess nicotine = Rs + Ri specific counts

After alkylation : Total – Excess nicotine = Ri specific counts

11. [^{3}H] Epibatidine Binding Assay to Membrane Preparation of BMα3β4 Cells.

[^{3}H] Epibatidine binding assay to membrane preparation was performed to determine specific total receptors in BMα3β4 cells. This assay was done following the protocol described by Free et al. (26)**.**

A. Preparing membrane preparation from BMα3β4 cells.

Procedure

1. BMα3β4 cells (split 1:2) are grown in 60 mm culture plate for 3 days.

2. To wash cells, aspirate old media. Then, add 4 ml/plate of PBS and aspirate off.

3. Add 400 μl of MPER reagent to cells. Shake well for 5 minutes then, scrape cells by using rubber policeman with the flat end.

4. Take all solution from culture plate into vial. Centrifuge at 14x1,000 rpm (or 18,000xg) for 15 minutes.

5. Keep supernatant and do protein assay.

6. Pipette 0.1 ml of supernatant and dilute to 1 mg/ml with assay buffer [without [^{3}H] Epibatidine, Phenylmethylsulfonyl fluoride (PMSF)].

7. Freeze in -20°C freezer or do binding assay.

B. [^{3}H] Epibatidine binding assay to membrane preparation

Preparation

Prepare the following solutions

1. Assay/Rinse buffer

- To ddH_2O at the approximate volume 2/3 of total volume, add the concentrated stock solutions, HEPES and iodoacetamide (not PMSF). After each addition, mix well by magnetic stirrer.

- Bring the volume up to final volume with ddH_2O. Pour the solution into a beaker, mix well by magnetic stirrer.

- Adjust the pH to 7.4 by drop-wise addition of HCl solution

- Keep in refrigerator. This buffer (without PMSF) should be used within 1 week.

- Immediately prior to binding experiment, add PMSF to assay buffer. After adding to assay solution, PMSF is rapidly decayed within 15 minutes.

STOCKS	**Final concentration**	**To make 500 ml**
NaCl, 1.2 M 70.13 g/1,000 ml (FW: 58.44)	120 mM	50 ml
KCl, 0.5 M 3.73 g/100 ml (FW: 74.56)	5 mM	5 ml
Na_2HPO_4, 0.08 M 11.36 g/1,000 ml (FW: 142)	8 mM	50 ml
EDTA, 0.2 M 7.44 g/100 ml (FW: 372.2) Added EDTA to H_2O, then pH to 8 to get EDTA in solution	2 mM	5 ml
EGTA, 0.2 M 7.61 g/100 ml (FW: 380.4) Added EGTA to H_2O, then pH to 8 to get EGTA in solution	2 mM	5 ml
HEPES (FW: 238.3)	5 mM	0.6 g
Iodoacetamide (FW: 185)	5 mM	463 mg
PMSF, 0.1 M 17.42 mg/ml isopropanol (FW: 174.2) Added just prior to experiment	0.1 mM	500 µl

2. [^{3}H] Epibatidine buffer

- To 12 ml of assay buffer, add 12 µl of 10^{-6} M [^{3}H] EB stock solution, to make 12 ml of 1 nM of [^{3}H] EB buffer.

- Immediately add 12 µl of 0.1 M PMSF stock solution prior to binding experiment to make final concentration of 0.1 mM PMSF in [^{3}H] EB buffer.

3. $1x10^{-1}$ M Nicotine stock solution, 1 ml (MW = 462.4)

- Dissolve 46.24 mg in 1 ml of ddH_2O
- Keep stock solution in freezer

4. Treatment buffer

Treatment	Total vol. (ml)	10^{-1}M Nicotine (µl)	[^{3}H] EB buffer (µl)	HEK Membrane (µl)
Total	1	-	900	100
Excess nicotine ($3x10^{-4}$ M)	1	3	897	100

5. 5% Polyethyleneimine (PEI)

- To 450 ml of ddH_2O, add 50 ml of 50% PEI stock solution, mix well using magnetic stirrer.

Procedure

1. Pre-soak filter membranes in 5% PEI for at least 5 hours.

2. Make treatment buffers according to experimental design. Total volume for each treatment buffer is 1 ml in one tube. Add nicotine and [^{3}H] EB buffer to all tubes.

3. Add 100 µl of membrane preparation to the tube and start timer. Membrane preparation should be mixed well before adding. After adding membrane preparation, mix treatment buffer well by vortex. Incubate for 60 minutes on the shaker (200 rpm) at room temperature.

4. Split the contents of each tube into a duplicate tube (500 µl/tube, 2 tubes) by using cut end tip pipette.

5. During this incubation, attach rinse buffer bottle to the manifold pump and flush manifold with cold buffer. Shortly before the end of the 60 minutes incubation, take the filter membrane which are pre-soaked in 5% PEI, and lay across the binding manifold. Lock middle clamp first then the outer two clamps at the same time.

6. At the end of the incubation period, aspirate entire volume of the tubes, then do 3 times washes with cold binding buffer. Remove the filter and set it aside. Repeat for second set of treatment if need.

7. Remove filter circles with tweezers and place one in each scintillation vial. Add 4.5 ml of scintillation cocktail into each vial, cap vial, label vial and vigorously shake vials for 20 seconds. Tap membrane circles down to the bottom of the vial. Leave vials overnight.

8. Remove two 20 μl aliquots of the radioactive binding assay buffer, place each into its own vial. Add scintillation cocktail, cap, label and vigorously shake vials as before. This is to estimate the concentration of radioactive used in the experiment. On the next day, place all vials in the Beckman 6800 liquid scintillation counter for analysis.

Statistical Analysis

The results were expressed as mean ± the standard error of mean (SEM). The data of cells were compared at 0, 24, and 48 hours after complete siRNA transfection by using ANOVA (one way analysis of variance). Turkey's Multiple Comparison Test was used to differentiate the difference between groups. The data of puromycin-treated cells were compared to control group by using student's t-test. A p-value of less than 0.05 ($p<0.05$) or 95% confidence limit was considered statistically significant difference.

CHAPTER IV
RESULTS

Presence of APC Protein in Bovine Adrenal Chromaffin Cells and HEK293 Expressing Recombinant Bovine Adrenal α3β4* nAChRs Cells.

To establish the presence of APC protein in two cell types, bovine adrenal chromaffin cells (BAC), and HEK293 expressing recombinant bovine adrenal α3β4* nAChRs Cells (BMα3β4), at densities of $5x10^6$ and $1.4x10^6$ cells/ 60 mm plate, respectively were cultured for 5 and 3 days, respectively. Thirty micrograms protein extracts from both cells were electrophoresed on 5% SDS-PAGE and electroblotted. Using western analyses, the blots were probed with dilutions 1:100, 1:200, or 1:500 of APC (C20) rabbit polyclonal IgG for 1 hour at room temperature. After incubation with a dilution 1:2,000 of anti-rabbit HRP-linked whole antibody (from donkey) for 1 hour at room temperature, these blots were visualized by autoradiography using ECL. Band sizes were determined by comparison with high molecular weight pre-stained protein standards. As shown in Figure 8, Bands of protein isolated from BAC and BMα3β4 cells have the molecular weights of 270±4 and 283±6 kD, respectively. These bands were supposed to be band of APC protein, because the molecular weigh of APC were range between 300-310 kD (163, 192-195). Although, the primary and secondary antibodies used in western blot were high specific to APC protein, we also did PCR technique to confirm the expression of APC RNA in both cells.

To establish the presence of APC RNA in both cells, using PCR technique, cDNA were amplified from RNA which were isolated from both cells. Then, PCR products were separated on 2% agarose gel. The correct size bands were cloned and sequenced. As shown in Figure 9, when compared to human adenomatous polyposis

coli (XM _000038.3), the sequence homologies of cDNAs from BAC and from BMα3β4 cells were 93% and 97%, respectively. Compared to bovine adenomatous polyposis coli (APC) (XM_588239.1), the sequence homologies of cDNAs from BAC and from BMα3β4 cells were 98% and 92%, respectively.

The western blot and PCR data confirmed the presence of APC protein and RNA in both BAC and BMα3β4 cells.

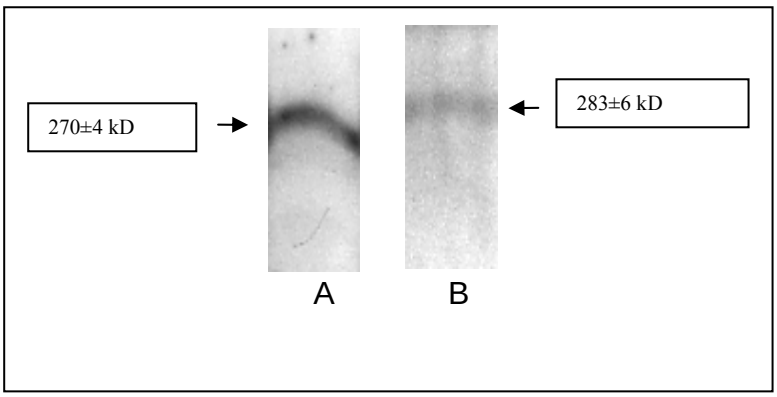

Figure 8. **Presence of proteins in adrenal chromaffin cells (BAC) and HEK 293 cells expressing recombinant bovine adrenal α3β4* nAChRs (BMα3β4 cells)**
A) protein of adrenal chromaffin cells; B) protein of BMα3β4 cells

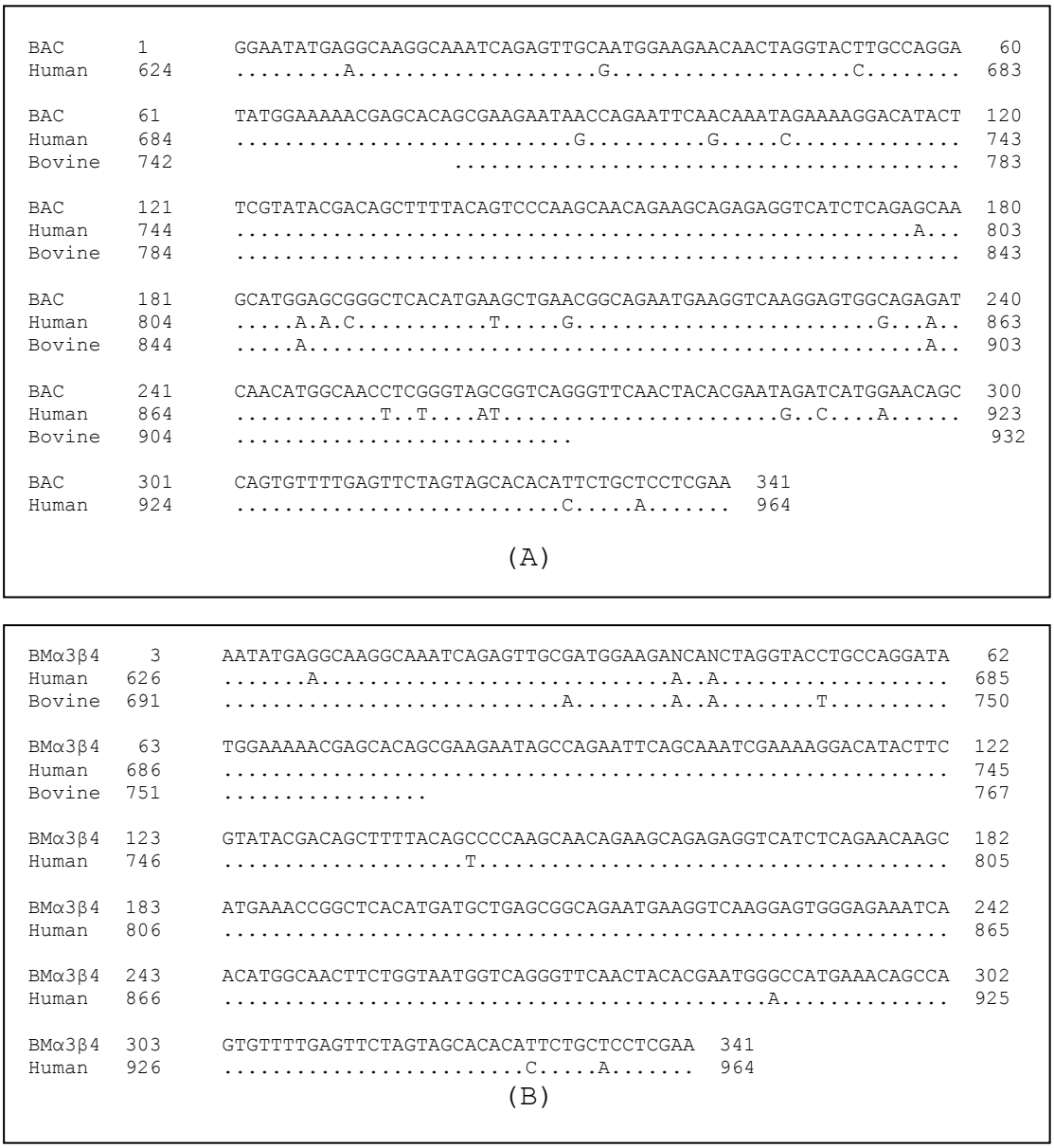

Figure 9. Sequence of PCR products obtained from BAC and BMα3β4 cells

Compared to human adenomatous polyposis coli (APC) (XM_000038.3), the sequence homologies of cDNAs from BAC (A) and from BMα3β4 cells (B) were 93% and 97%, respectively. Compared to bovine APC (XM_588239.1), the sequence homologies of cDNAs from BAC (A) and from BMα3β4 cells (B) were 98% and 92%, respectively.

siRNA Transfection Technique Development.

1. HEK293 cells expressing recombinant bovine adrenal α3β4* nAChRs (BMα3β4 cells) clone 2 or clone 3

BMα3β4 cells clone 2 or clone 3 at a density of $1.5x10^5$ cells/well were grown for 1 day. To determine the amount of nAChR expressed on these cells, [^{3}H] Epibatidine binding coupled receptor alkylation were performed. As shown in Table 3, and Figure 10, there were non-significant differences in the amount of total receptor (Rt), and surface receptor (Rs) expressed on either BMα3β4 cells clone 2 or clone 3. Contrarily, the expression of intracellular receptors (Ri) on clone 2 was significantly less than that on clone 3 (976±37 VS 1241±109 fmol/mg protein, respectively). However when concerning to the proportion of Ri or Rs to total receptor, they were 67±3, 33±3 %, respectively for clone 2 and 74±3, 26±3%, respectively for clone 3. Statistical analysis revealed that there were non-significant differences of both Ri proportion and Rs proportion between clone 2 and clone 3.

On the other hand, BMα3β4 cells clone 2 or clone 3 were grown for 3 days. Membrane preparations were prepared from these cells. To determine the amount of nAChR (total receptor) expressed on these cells, [^{3}H] Epibatidine binding assays were performed on these membrane preparations. As shown in Figure 11, the total receptor (Rt) on clone 2 was significantly more than that on clone 3 (606±45 VS 414±26 fmol/mg protein, respectively).

Based on [^{3}H] Epibatidine binding assay in membrane preparation, BMα3β4 cells clone 2 was chosen for siRNA transfection because this clone expressed more number of total receptor expression than those of clone 3.

Table 3. Comparison of nAChR expression in intact BM α3β4 cells clone 2 and 3

BM $\alpha_3\beta_4$ cells	The amount of nAChR			The proportion of nAChR to total receptor	
	(fmol/mg protein)			(% of total receptor)	
	Rt	Ri	Rs	Ri	Rs
Clone 2	1471±63	976±37	495±56	67±3	33±3
Clone 3	1567±69	1241±108*	442±41	74±2	26±2

All values were expressed as mean+/-SEM, n=6

* : significant differences from clone 2, $p<0.05$

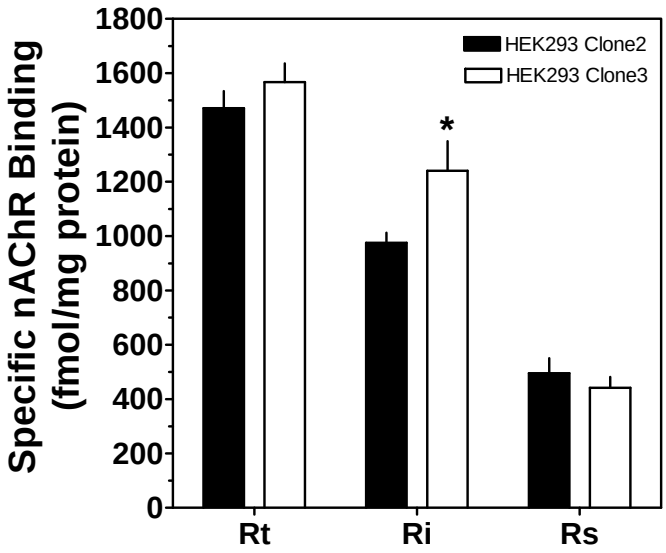

(A)

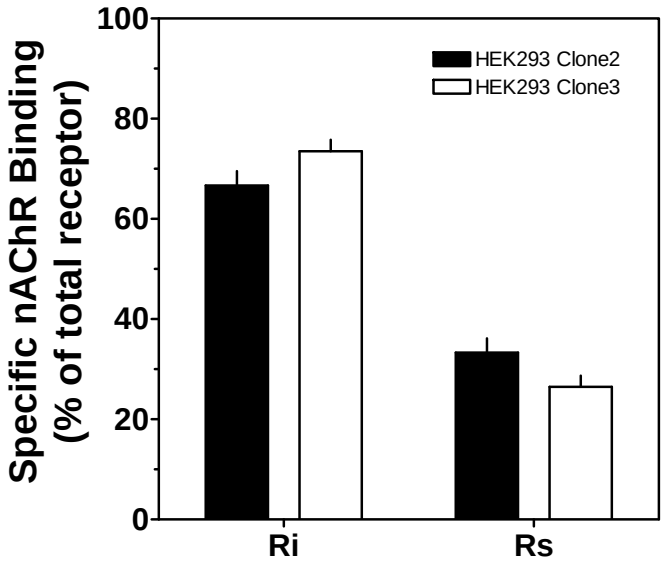

(B)

Figure 10. **Comparison of nAChR expression in intact BM α3β4 cells clone 2 and 3.**

A) The amount of nAChR; B) The proportion of nAChR to total receptor

All values were expressed as mean+/-SEM, n=6

* : significant differences from clone 2, $p<0.05$

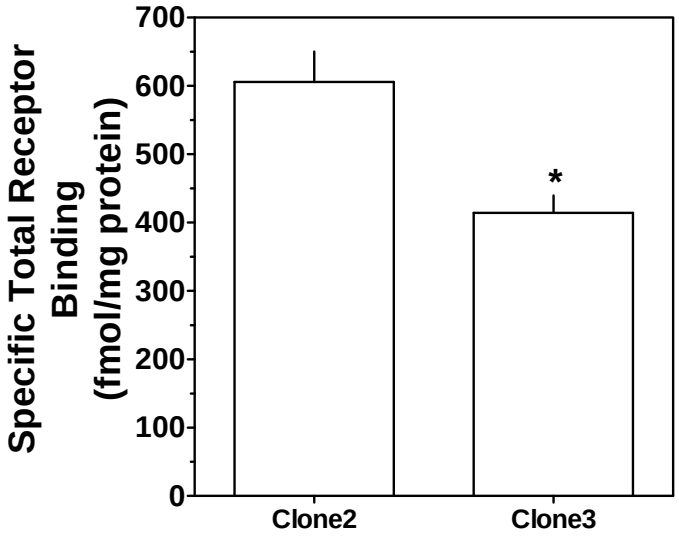

Figure 11. Comparison of nAChR (total receptor) expression in membrane preparation of BM α3β4 cells clone 2 and 3.

All values were expressed as mean+/-SEM, n=10

* : significant differences from clone 2, $p<0.05$

2. Ratio of lipid-based delivery reagent and fluorescence-labeled oligo

BMα3β4 cells at density of $6x10^4$ cells/well were cultured in 24 well plate for 2 days. Then, they were incubated with 400 µl/well mixture of lipid-based delivery reagent and fluorescence-labeled oligo. The amount of lipid-based delivery reagent was fixed at 1.5 µl/well, a maximal level, while the amount of fluorescence-labeled oligo were vary within range of 50-100 pmol/well as recommended by the company. After 24 hours incubation, these transfected cells were determined for transfection efficiency by 2 methods: fluorescence plate reader and fluorescence-labeled cell counting. As shown in Table 4 and Figure 12, the fluorescence-labeled of 1.5 µl delivery reagent plus fluorescence-labeled oligo 50, 75 and 100 pmol were 5520, 6543 and 7509 relative units, respectively. The fluorescence-labeled cell counting were 52, 58 and 67%. Both results consistently showed that the more amount of fluorescence-labeled oligo was used, the higher transfection efficiency could be obtained. For the highest transfection efficiency, the mixture of 1.5 µl lipid-based

delivery reagent plus 100 pmol/well fluorescence-labeled oligo was chosen for further siRNA transfection process.

Table 4. Effect of the ratio of lipid-based delivery reagent and fluorescence-labeled oligo on transfection efficiency in BMα3β4 cells

Transfection efficiency (Fluorescence-labeled cells)	Lipid-based delivery reagent + Fluorescence-labeled oligo (µl + pmol)		
	1.5 + 50	1.5 + 75	1.5 + 100
Fluorescence plate reader (Relative units), n=3	5,520 ± 392	6,543 ± 33	7,509 ± 78
Fluorescence-labeled cell counting (%), n=6	52± 2	58 ± 3	67 ± 2

All values were expressed as mean ± SEM.

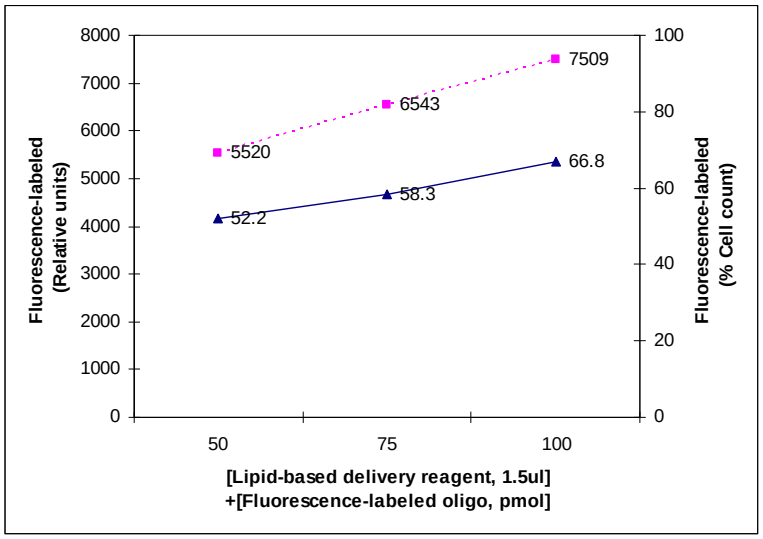

Figure 12. Effect of the ratio of lipid-based delivery reagent and fluorescence-labeled oligo on transfection efficiency in BMα3β4 cells

3. Transfection time

BMα3β4 cells at density of $6x10^4$ cells/well were cultured in 24 well plate for 2 days. Then, they were incubated with 400 µl/well mixture of 1.5 µl/well lipid-based delivery reagent and 50 pmol/well fluorescence-labeled oligo for 0, 2, 4, 6, 8 and 24 hours. These transfected cells were determined for transfection efficiency by 2 methods: fluorescence plate reader and fluorescence-labeled cell counting. As shown in Table 5 and Figure 13, the fluorescence-labeled of transfected cells at different incubation times 0, 2, 4, 6, 8 and 24 hours were 993, 695, 1283, 5843 and 8992 relative units, respectively. The fluorescence-labeled cell counting were 23, 36, 49, 58 and 66%. Both results confirmed that increasing incubation time caused increasing of transfection efficiency. For high transfection efficiency, the 24 hour incubation time was chosen for further siRNA transfection process.

Table 5. Effect of transfection time on transfection efficiency in BMα3β4 cells

Transfection efficiency (Fluorescence-labeled cells)	Transfection time (hours)				
	2	4	6	8	24
Fluorescence plate reader (Relative units), n=3	993±207	695±174	1283±327	5843±243	8992±522
Fluorescence-labeled cell counting (%), n=6	23±4	36±4	49±2	58±2	66±3

All values were expressed as mean ± SEM

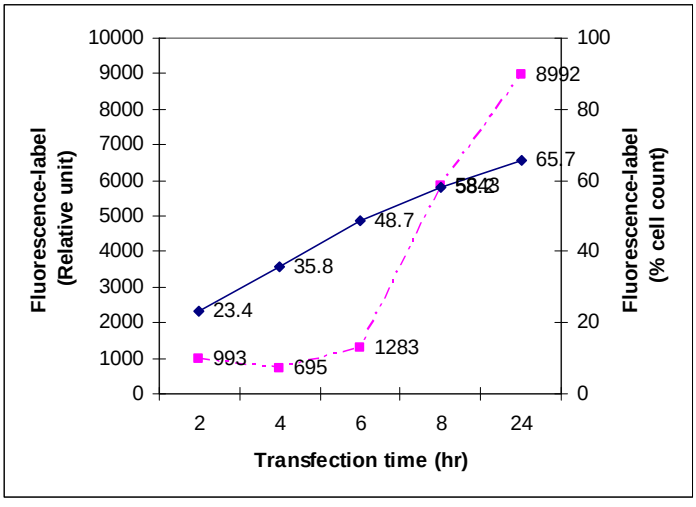

Figure 13. Effect of transfection time on transfection efficiency in BMα3β4 cells

4. Fluorescence lasting time in BMα3β4 cells

After 24 hours incubation of 1.5 µl/well lipid-based delivery reagent with 50 pmol/well fluorescence-labeled oligo, fluorescence plate reader was performed in these cells at day 0, 1, 2, 3 and 4. As shown in Table 6 and Figure 14, the amount of fluorescence-labeled cells were non-significantly different all the period of times ,comparing to day 0 post-incubation. These indicated that fluorescence-label in cells can be long-lasting at least 4 days after 24 hours incubation.

Table 6. **The long-lasting time of fluorescence-label in BMα3β4 cells**

	Post-incubation time (days)				
	0	1	2	3	4
Fluorescence plate reader (Relative units), n=3	8980 ±940	12492 ±1164	10017 ±630	8607 ±1275	6068 ±632

All values were expressed as mean ± SEM.

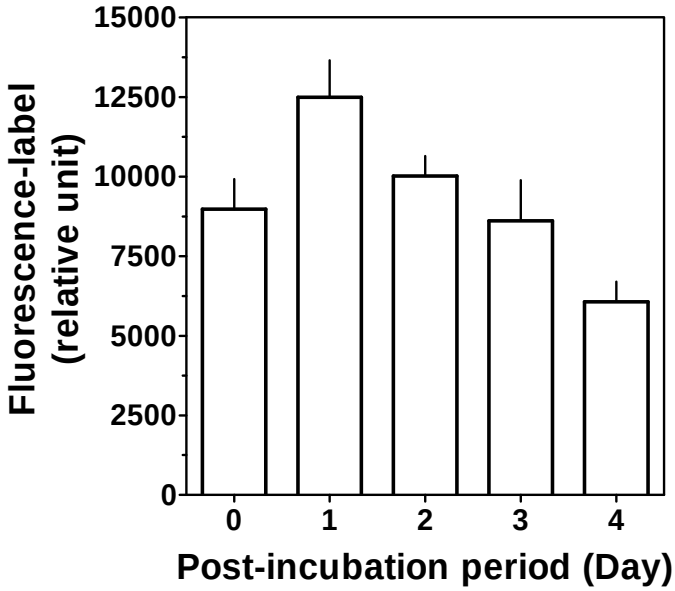

Figure 14. The long-lasting time of fluorescence-label in BMα3β4 cells

All values were expressed as mean ± SEM.

5. Transfection efficiency

$BM\alpha_3\beta_4$ cells were transfected overnight with 150 pmol APC siRNA type C or negative control siRNA, 1.5 μl lipid-based delivery reagent and 100 pmol fluorescence-labeled oligo. Under fluorescent microscope, photomicrographs of these cells were taken. Fluorescence-labeled cells were counted for transfection efficiency, as shown in Figure 15, 16 and Table 7. Comparing under normal light to fluorescent light, photomicrographs showed that almost siRNA and fluorescence-labeled oligo can pass through and accumulate in cells. This was correlated with 72 and 70% fluorescence-labeled cell counting of siRNA type C and negative control siRNA, respectively.

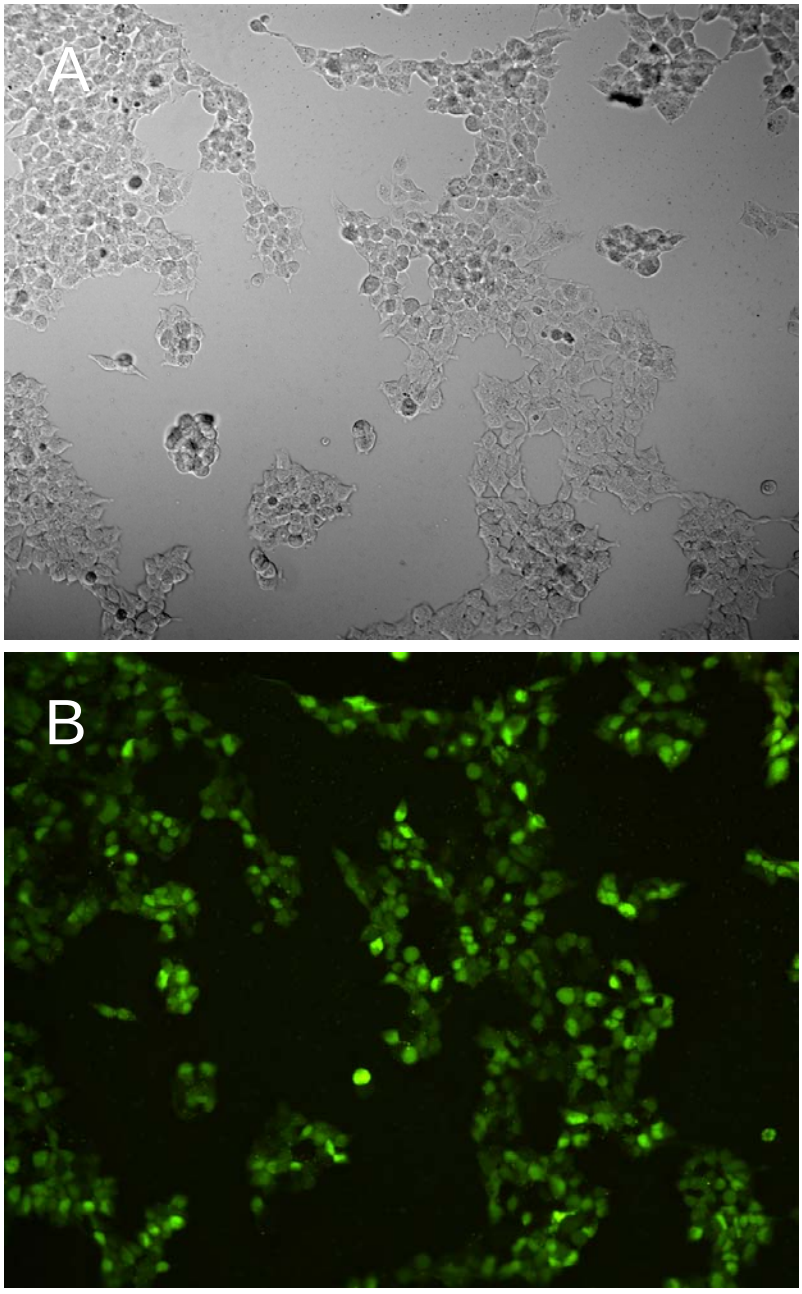

Figure 15. Transfection efficiency of APC siRNA transfection in BMα3β4 cells expressed via photomicrographs.

Photomicrographs were taken under Normal light **(A)**, and Fluorescent light **(B)**

Table 7. Transfection efficiency determined via fluorescence labeled cell count

Treatment	The number of cells (Cells)		Transfection efficiency (% Total cells)
	Total Cells	Fluorescence-labeled cells	
Control	211±6	0	0
APC siRNA	342±7	246±6	72±1
Negative control siRNA	165±4	115±2	70±1

All values were expressed as mean ± SEM, n=4

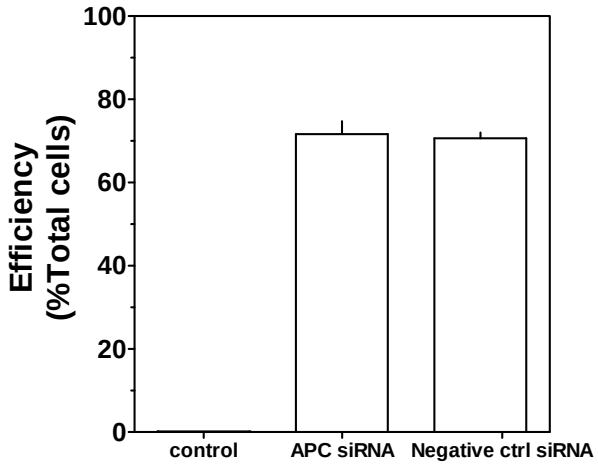

Figure 16. Transfection efficiency determined via fluorescence-labeled cell count. All values were expressed as mean ± SEM, n=4

6. Type of siRNA

BMα3β4 cells were transfected overnight with 150 pmol APC siRNA type A, B or C (Table 8), 1.5 µl lipid-based delivery reagent and 100 pmol fluorescence-labeled oligo. To determine the siRNA effects on these cells, [^{3}H] Epibatidine binding assay coupled with receptor alkylation and western blot assay were performed at 0, 24 and 48 hours after complete transfection.

Effect of three types of siRNA (type A, B and C) on the number of total receptors (Rt) was shown in Table 9 and Figure 17. The number of total receptors were unchanged throughout 48 hrs for siRNA type A, compared to control.

Contrarily, the reduction of total receptors was observed only at 24 hrs for siRNA B, whereas these reductions were observed at 24 and 48 hrs for siRNA type C. As shown in Table 10 and Figure 18, the number of intracellular receptors (Ri) remained constant throughout 48 hrs for siRNA type A, while these reductions were obtained since 24 hrs for siRNA type B and C, compared to control. As shown in Table 11 and Figure 19, the increases in surface receptors (Rs) were found throughout 48 hrs for siRNA type A and B, but this increase was found since 24 hrs for siRNA type C. These results indicated that the changes of the number of Rt, Ri and Rs in siRNA type B and C were more correlated than in siRNA type A treated group. Therefore, siRNA type B and C were chosen for further experiment and Western Blot analysis was used to determine the changes of the amount of APC protein. As shown in Table 12 and Figure 20, the amounts of APC proteins induced by siRNA type B and C at 24 hrs were 51 and 50% of control, respectively and were 62 and 71% of control, respectively at 48 hrs. These suggested that both type B and C transfection caused the reductions of APC protein at 24 and 48 hrs with the indifferent degree.

These receptor binding and Western Blot data supported the similar effects of both siRNA type B and C on BMα3β4 cells. Therefore, APC siRNA type C was used in the next siRNA transfection experiment.

Table 8 The properties of 3 types of APC-siRNA (203)

NM_ 000038.3	Type A	Type B	Type C
Sequence (5′ to 3′)	UAA AGU AUC AGC AUC UGG AAG AAC C	GGU UCU UCC AGA UGC UGA UAC UUU A	AAA GGA UGG AAU CUG AAU CAG ACG A
%GC	40	40	48
Primer length	25	25	25

Table 9. Effect of 3 types APC siRNA on total receptor (Rt) of BMα3β4 cells

Type of siRNA	SpecificTotal Receptor (Rt) (fmol/mg protein)								
	Time after complete transfection (hr)								
	0			24			48		
	control	siRNA	%ctrl	control	siRNA	%ctrl	control	siRNA	%ctrl
A	1678	1603	96±3	1290	1325	103±3	1164	1094	94±1
B	1126	1326	118±3	1182	968	82±2	1080	1017	94±3
C	1258	1218	97±2	1045	791	76±1	1050	720	69±1

Values of %control were expressed as mean ± SEM, n=4

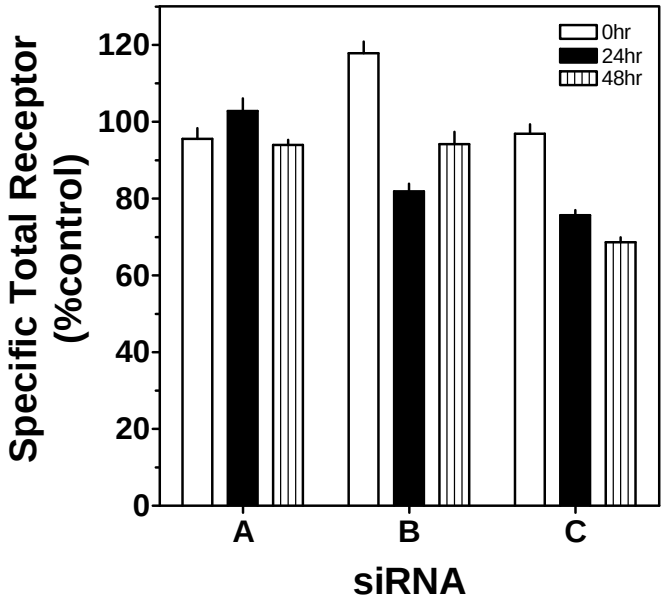

Figure 17. Effect of 3 types APC siRNA on total receptor (Rt) of BMα3β4 cells

Values of %control were expressed as mean ± SEM, n=4

Table10. Effect of 3 types APC siRNA on intracellular receptor (Ri) of BMα3β4 cells

Type of siRNA	Specific Intracellular Receptor (Ri) (fmol/mg protein)								
	Time after complete transfection (hr)								
	0			24			48		
	control	siRNA	%ctrl	control	siRNA	%ctrl	control	siRNA	%ctrl
A	1365	1234	90±2	1179	1127	96±3	1083	985	91±4
B	970	1041	107±1	1092	640	59±3	1012	756	75±3
C	933	948	102±1	957	541	57±3	993	517	52±2

Values of %control were expressed as mean ± SEM, n=4

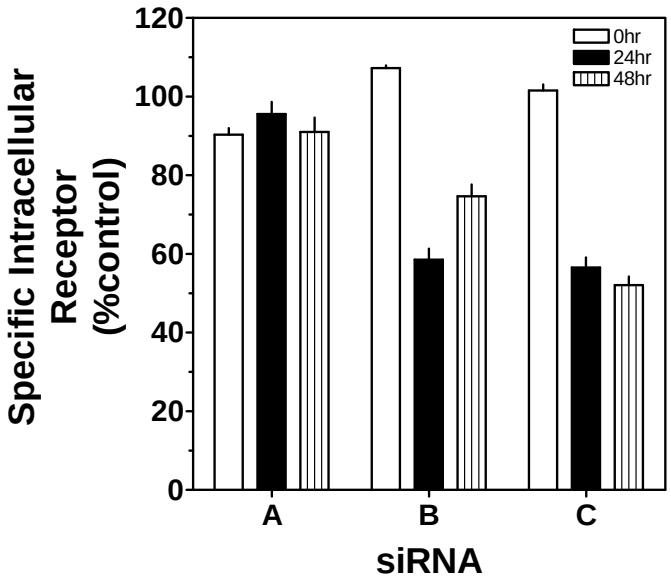

Figure 18. Effect of 3 types APC siRNA on intracellular receptor (Ri) of BMα3β4 cells

Values of %control were expressed as mean ± SEM, n=4

Table 11. Effect of 3 types APC siRNA on surface receptor (Rs) of BMα3β4 cells

Type of siRNA	Specific Surface Receptor (Rs) (fmol/mg protein)								
	Time after complete transfection (hr)								
	0			24			48		
	ctrl	siRNA	%ctrl	ctrl	siRNA	%ctrl	ctrl	siRNA	%ctrl
A	313	370	118±21	110	198	180±15	81	108	133±45
B	155	285	184±23	89	328	367±50	68	261	383±65
C	324	270	83±11	89	249	281±33	57	203	354±21

Values of %control were expressed as mean ± SEM, n=4

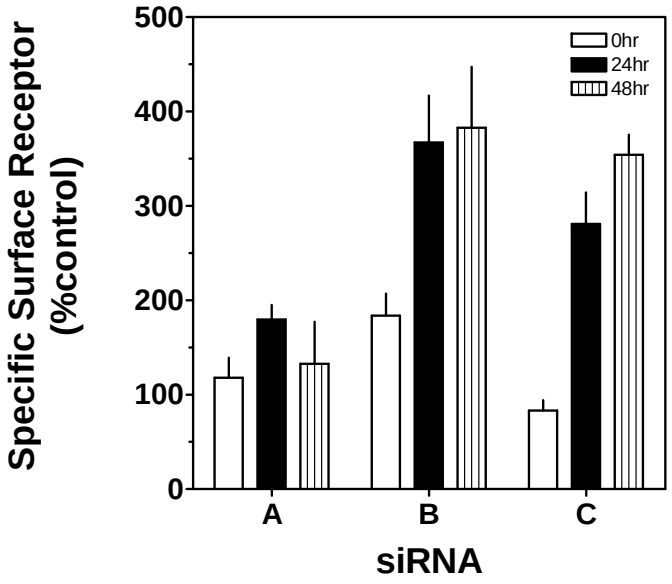

Figure 19. Effect of 3 types APC siRNA on surface receptor (Rs) of BMα3β4 cells

Values of %control were expressed as mean ± SEM, n=4

Table 12. Effect of 2 types APC siRNA on the amount of APC protein in siRNA transfected BMα3β4 cells via Western Blot analysis

Type of siRNA	Amount of APC protein (μg)								
	Time after complete transfection (hr)								
	0			24			48		
	control	siRNA	%ctrl	control	siRNA	%ctrl	control	siRNA	%ctrl
B	3.65	3.64	99.80	5.47	2.79	50.94	5.86	3.63	61.92
C	2.86	2.71	94.61	6.06	2.99	49.49	3.35	2.36	70.51

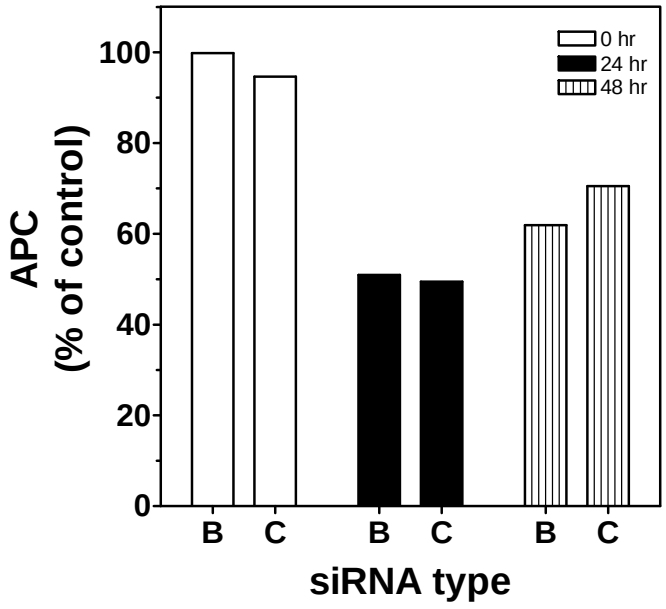

Figure 20. Effect of 2 types siRNA on the amount of APC protein in siRNA transfected BMα3β4 cells determined via Western Blot analysis

Effects of Transfection Technique on BMα3β4 Cells.

BMα3β4 cells were either untransfected (non-treated control) and transfected overnight with 150 pmol APC siRNA type C or negative control siRNA, 1.5 μl lipid-based delivery reagent and 100 pmol fluorescence-labeled oligo. To determine the effects of transfection procedure on BMα3β4 cells, total proteins quantification assay and [^{3}H] Epibatidine binding assay coupled with receptor alkylation were performed

at 0, 24 and 48 hours after complete transfection of APC siRNA, and only at 24 hours for negative control siRNA compared to non-treated control. Microphotographs of these cells were taken under normal light at 0 hr.

1. Effect on cell shape and growth

As shown in Figure 21, slightly difference in cell shape of APC siRNA or Negative control siRNA transfected cells was observed, comparing to control non-treated cells. But, they were still alive, grew and tightly attached to surface of culture wells.

2. Effect on total protein level

The amount of total proteins in either APC siRNA or Negative control siRNA transfected groups was shown in Table 13 and Figure 22. As shown in Table 13(A) and Figure 22(A), in control groups, total proteins significantly increased at 48 hrs, compared to 0 hr (0.31 ± 0.02 VS 0.26 ± 0.01 mg/well). Among APC siRNA transfected groups, there were non-significant differences throughout the period of assay. Comparing to their own controls, the amount of total proteins in APC siRNA transfected groups were non-significant differences. These indicated that APC siRNA transfection have no effect on BMα3β4 cells. As shown in Table 13(B) and Figure 22(B), both siRNA treatment decreased total protein, comparing to control, but no significant differences in total protein were observed between APC siRNA-treated and negative siRNA-treated cells. These indicated that APC siRNA and negative control siRNA have similar effect on BMα3β4 cells.

3. Effect on the number of nAChR

Regarding to the effects of transfection procedure on nicotinic receptor of BMα3β4 cells, the amount of receptors in negative control siRNA treated groups compared to control non-treated groups at 24 hrs after complete transfection were shown in Table 14 and Figure 23. There were non-significant differences in the amount of total receptors (Rt), intracellular receptors (Ri) and surface receptors (Rs) when comparing negative control siRNA to control groups. These indicated that transfection procedure did not affect the number of receptors on these cells.

The consistent result of microphotographs, total amount of proteins and the number of receptors, suggested that transfection procedure did not have effects on cell growth and nicotinic receptors expression on BMα3β4 cells.

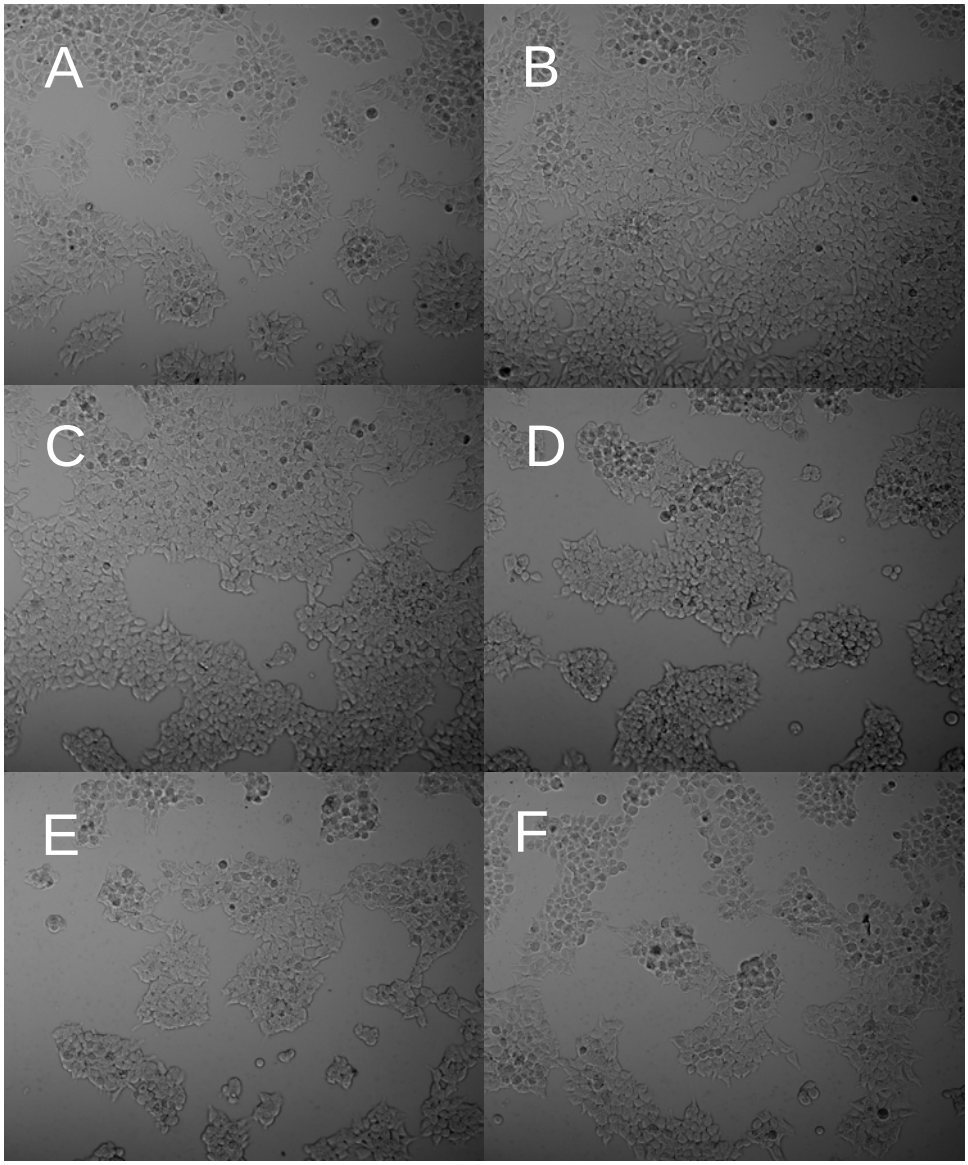

Figure 21. Effects of transfection technique on BMα3β4 cells as determined via photomicrographs

A,B) Control non-treated; C,D) APC siRNA transfection; E,F) Negative control siRNA transfection.

Table 13. Effects of transfection technique on BMα3β4 cells as determined via total protein assay

(A) In APC siRNA transfected cells

Treatment	Amount of Total Protein (mg/well)		
	Time after complete transfection (hr)		
	0	24	48
Control	0.26 ± 0.01	0.29 ± 0.02	0.31 ± 0.02 *
APC siRNA	0.24 ± 0.01	0.24 ± 0.01	0.26 ± 0.01

All values are expressed as mean ± SEM, n=12

* : significant differences from control at 0 hr, $p<0.05$.

(B) In Negative control siRNA transfected cells

Amount of Total Protein at 24 hr after complete transfection (mg/well)			
Control	Positive siRNA	Control	Negative siRNA
0.29±0.03	0.24±0.02	0.30±0.01	0.23±0.02

All values are expressed as mean ± SEM, n=4.

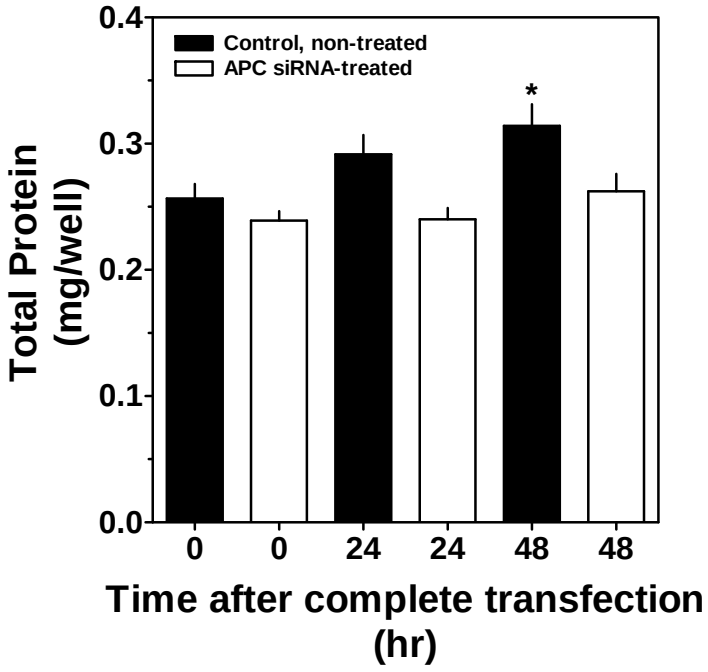

(A)

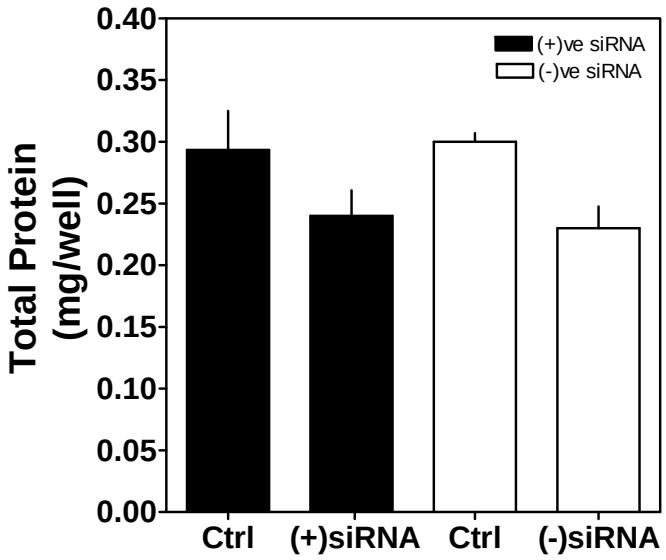

(B)

Figure 22. **Effects of transfection technique on BMα3β4 cells as determined via total protein assay.** A) In APC siRNA transfected cells; B) In Negative control siRNA transfected cells. * : significant differences from control at 0 hr, $p<0.05$.

Table 14. Effects of transfection technique on BMα3β4 cells as determined via Receptor binding assay

Treatment	Amount of Receptor (% control)		
	Total receptor (Rt)	Intracellular receptor (Ri)	Surface receptor (Rs)
Control	100±2	100±1	100±7
Negative control siRNA	92±4	93±3	91±17

All values are expressed as mean ± SEM, n=4.

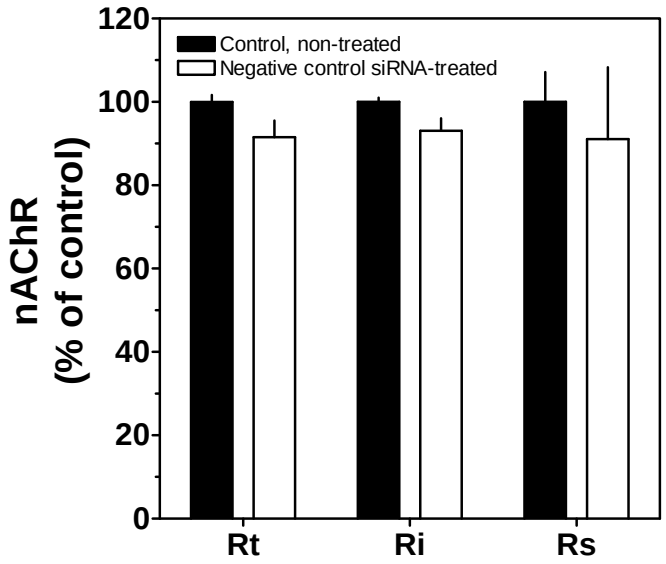

Figure 23. Effects of transfection technique on BMα3β4 cells as determined via Receptor binding assay

Effects of APC siRNA transfection on BMα3β4 Cells.

BMα3β4 cells were either untransfected (non-treated control) or transfected overnight with 150 pmol APC siRNA type C, 1.5 µl lipid-based delivery reagent and 100 pmol fluorescence-labeled oligo. To determine the effects of APC siRNA

transfection on APC protein levels and nicotinic receptor expression on BMα3β4 cells, Western blot analysis, total proteins quantification assay and [^{3}H] Epibatidine binding assay coupled with receptor alkylation were performed at 0, 24 and 48 hours after complete transfection.

1. **Effects on APC protein levels**

As shown in Figure 24, 25 and Table 15, APC siRNA transfection in BMα3β4 cells significantly decreased the amount of APC protein at 24 and 48 hrs after complete transfection. The APC level at 24 and 48 hrs were 52.4±1.6 and 61.9±5.0 % of control, respectively. The results illustrated the reduction of APC level at 48 hrs with slightly less extent than the reduction at 24 hrs.

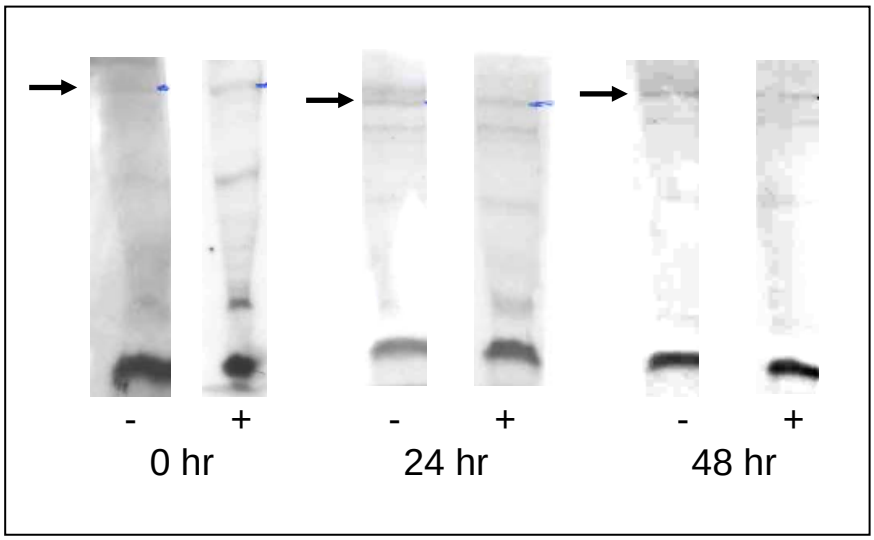

Figure 24. Representative western blot of APC protein in siRNA transfected BMα3β4 cells

Table 15. Effects of APC siRNA Treatment on APC Protein in BMα3β4 Cells

APC Concentration (arbitrary units)								
0 hr			24 hr			48 hr		
Ctrl	siRNA	%Ctrl	Ctrl	siRNA	%Ctrl	Ctrl	siRNA	%Ctrl
10.1±3.6	10.3±3.8	100.2±2.8	9.2±2.6	4.9±1.5	52.4±1.6	10.7±3.8	6.3 ±2.0	61.9±5.0

All values are expressed as means ± SEM (n = 3).

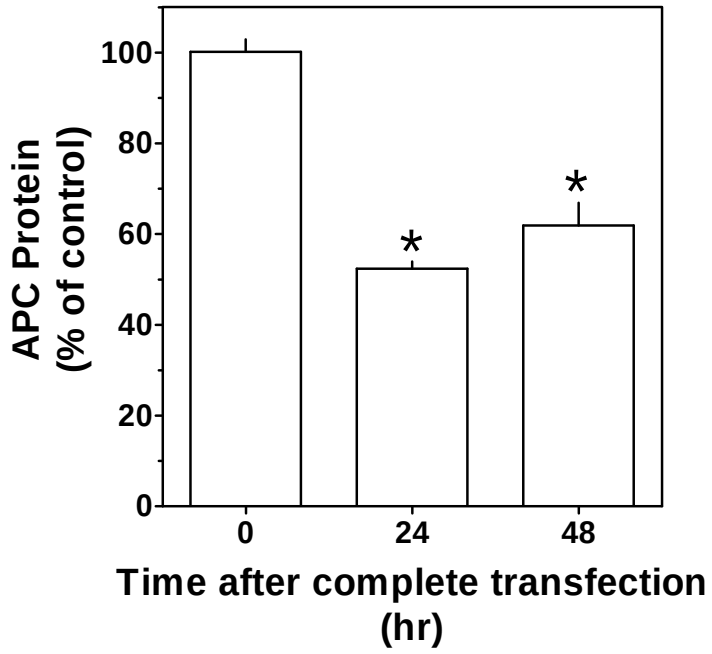

Figure 25. Effects of siRNA on APC protein in BM α3β4 cells

* : significant differences from control group, $p<0.05$.

2. Effects on the number of nAChRs.

The amounts of nAChR on siRNA-treated cells at 0, 24 and 48 hrs after complete transfection were shown in Table 16 and Figure 26. These amounts were expressed as specific nAChR binding in unit of fmol/mg protein. Total receptor (Rt) values were obtained from [^{3}H] Epibatidine binding assay, while intracellular receptor (Ri) values were obtained from receptor alkylation prior to [^{3}H] Epibatidine binding assay. Surface receptor (Rs) values were indirectly calculated by subtraction of intracellular binding values from total specific binding values.

As shown in Figure 27(A), the total population of nAChRs in both control and APC siRNA-treated cells remained constant over 48 hr. Immediately following the 24 hr transfection period (t= 0 hr), the Ri level in control group was 1044±24 fmol/mg protein and slightly nonsignificant increased throughout 48 hr (Figure 27B). At 0 hr posttransfection period, the Ri level in siRNA-treated cells was closed to that in control cells. At 24 and 48 posttransfection period, siRNA-treatment caused significant reduction of Ri levels to 836±91 and 811±93 fmol/mg protein (72±3 and 68±4% of control at each time point), respectively. Regarding to surface receptor, at 0 hr, the population of surface nAChRs in both control and APC siRNA-treated cells were 289±20 and 258±15 fmol/mg protein, respectively (Figure 27C). The significant reductions of Rs were observed at 24 and 48 hr (89±16 and 91±13 fmol/mg protein, respectively) in control group. Contrarily, during these time points the significant increments of Rs were observed as 318±24 and 243±20 fmol/mg protein (357±21 and 299±34 % of control), respectively in siRNA treated cells.

The effects of APC siRNA treatment on the relative distribution of nAChRs were shown in Table 17 and Figure 28. All values were calculated as the percentage of the amount of intracellular or surface receptors to the amount of total receptors. Immediately following the 24 hr transfection period (t= 0 hr), 80% of total receptors were located in intracellular area and 20% of total receptors were located at cell surface in both control and APC-siRNA treated groups. After 24 hr posttransfection, control Ri increased to 93±1 % of Rt and remained at this level until 48 hrs with concomitant reduction in Rs to approximately 10% of Rt. With siRNA treatment, a small but significant decrease in Ri was observed only at 24 hrs, compared to at 0 hr (71±2% vs 79±1% of Rt). Concomitantly, Rs in siRNA treated cells significantly increased at 24 hr after transfection, compared to at 0 hr (29±2% vs 21±1% of Rt). Comparing between siRNA treated groups to control groups, at 24 hrs, the distribution of Ri in siRNA-treated group was reduced (71±2 VS 93±1%, respectively), while the distribution of Rs was increased (29±2 VS 7±1%, respectively). Similar to siRNA-treated group at 24 hrs, the distribution of Ri in siRNA-treated group at 48 hrs, was reduced (76±2 VS 93±1%, respectively), while the distribution of Rs was increased (24±2 VS 7±1%, respectively) compared to

control. The distribution of receptors together with the amount of receptors supported the evidence of a reduction of Ri and the increment of Rs at 24 and 48 hrs after complete siRNA transfection.

Table 16. **[^{3}H] Epibatidine binding assay, coupled with receptor alkylation to intact** BM **α3β4 cells treated with siRNA**

nAChR	Specific nAChR binding (fmol/mg protein)					
	0 hr		24 hr		48 hr	
	Control	siRNA	Control	siRNA	Control	siRNA
Total (Rt)	1326±29	1255±24	1222±92	1154±109	1268±82	1098±109
Intracellular (Ri)	1044±24	997±29	1133±88	836±91	1176±73	811±93
Surface (Rs)	289±20	258±15	89±16	318±24	91±13	243±20

All values were expressed as mean+/-SEM, n=12

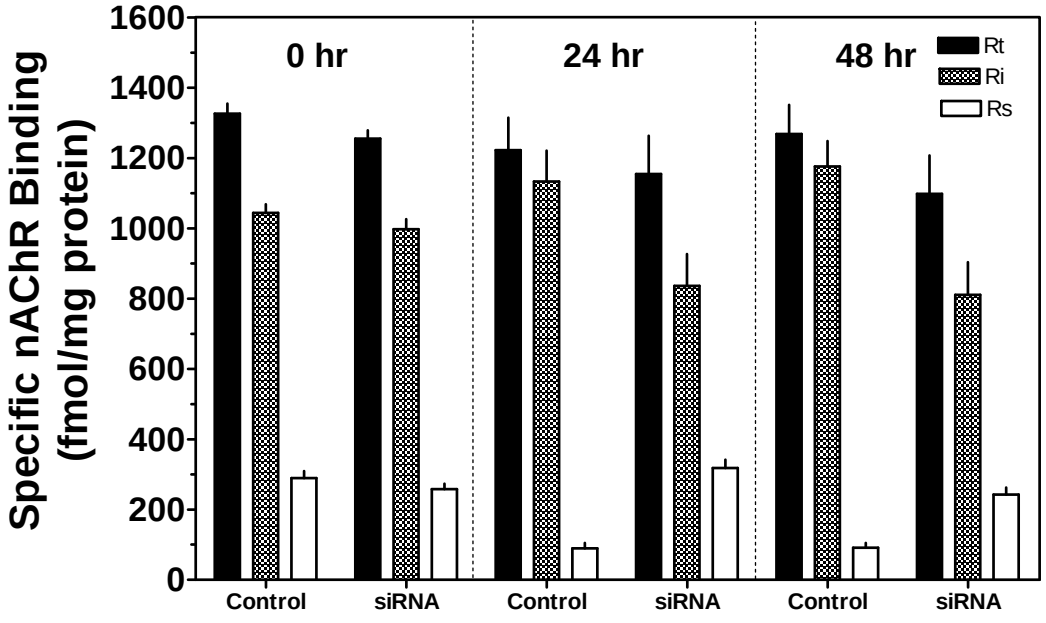

Figure 26. **[^{3}H] Epibatidine binding assay, coupled with receptor alkylation to intact** BM **α3β4 cells treated with siRNA**

All values were expressed as mean+/-SEM, n=12

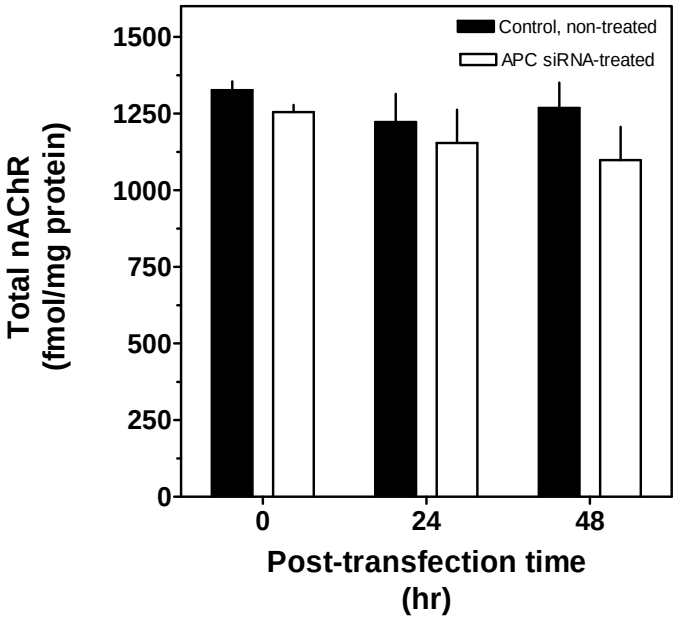
Control, non-treated
APC siRNA-treated
Total nAChR
(fmol/mg protein)
1500
1250
1000
750
500
250
0
0
24
48
Post-transfection time
(hr)

(A)

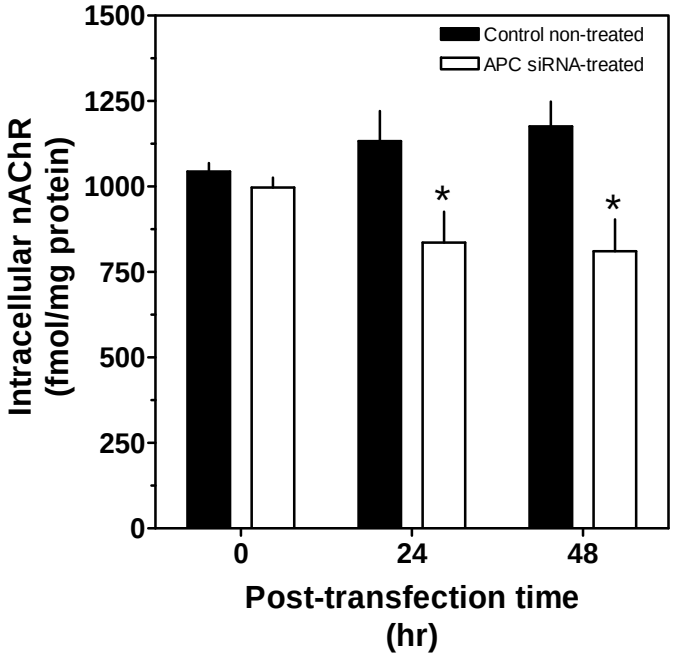
Control non-treated
APC siRNA-treated
Intracellular nAChR
(fmol/mg protein)
1500
1250
1000
750
500
250
0
*
*
0
24
48
Post-transfection time
(hr)

(B)

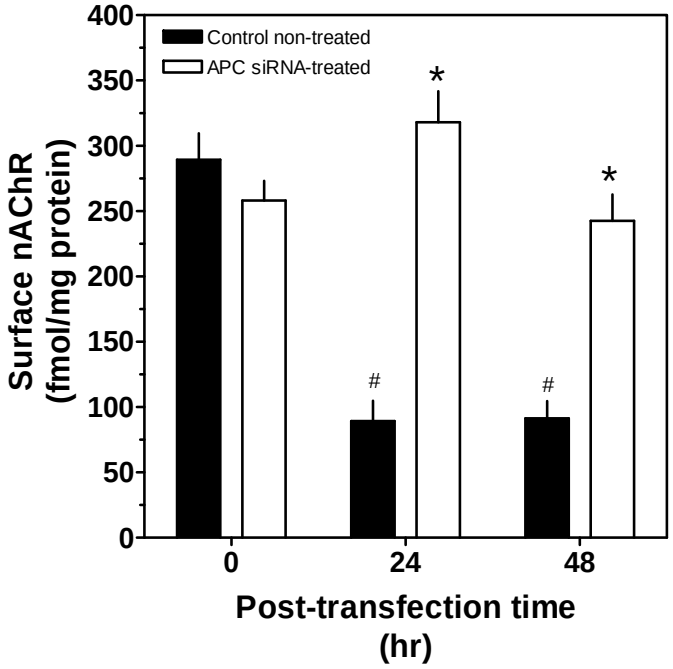

(C)

Figure 27. **Effects of siRNA treatment on the amount of nAChRs in** BM $\alpha_3\beta_4$ **cells.**

A) Total Receptor (Rt); B) Intracellular Receptor (Ri); C) Surface Receptor (Rs)

All values were expressed as mean+/-SEM, n=12

* : significant differences from control at each time point, $p<0.001$

: significant differences from control at 0 hr, $p<0.001$

Table 17. Effects of siRNA treatment on the distribution of Intracellular receptor or Surface receptor in BM **α3β4 cells**

Time after complete transfection	Control		siRNA	
	Ri	Rs	Ri	Rs
	(% of total Rc)	(% of total Rc)	(% of total Rc)	(% of total Rc)
0 hr	78±1	22±1	79±1	21±1
24 hr	93±1 #	7±1 #	71±2 *	29±2 *
48 hr	93±1 #	7±1 #	76±2 *	24±2 *

All values were expressed as mean+/-SEM, n=12

* : significant differences from control at each time point, $p<0.001$

: significant differences from control at 0 hr, $p<0.001$

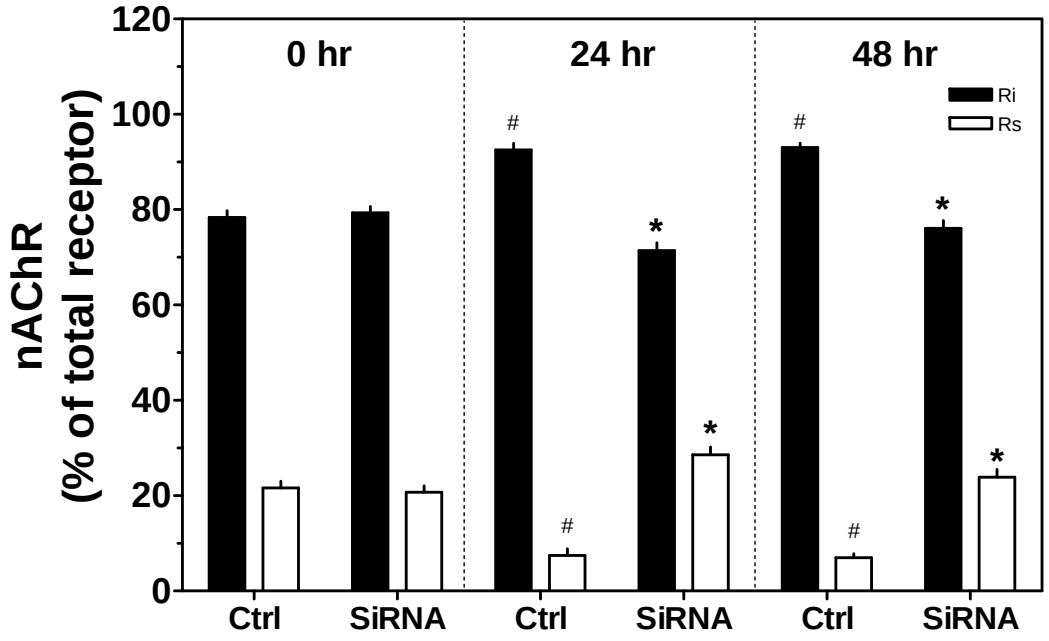

Figure 28. Effects of siRNA treatment on the distribution of Intracellular receptor or Surface receptor in BM **α3β4 cells**

All values were expressed as mean+/-SEM, n=12

* : significant differences from control at each time point, $p<0.001$

: significant differences from control at 0 hr, $p<0.001$

Effects of Puromycin Treatment in BMα3β4 Cells.

BMα3β4 cells at a density of $6x10^4$ cells/well were grown for 2 days. Then, they were incubated with 10 μg/well puromycin for 24 hrs. Subsequently, the protein assay, western blot analysis and [^{3}H] Epibatidine binding assay coupled with receptor alkylation were performed in these cells at 0 hr after complete incubation, to determine the effects of puromycin on total proteins, APC protein and nAChRs of BMα3β4 cells.

1. Effects on total proteins

As shown in Table 18 and Figure 29, the amounts of total proteins were significantly reduced from 0.21±0.01 mg/well in control to 0.17±0.01 mg/well in puromycin-treated group (83.09±2.5% of control)

Table 18. Effects of Puromycin treatment on BMα3β4 cells as determined via total protein assay

The amount of Total Proteins		
Control	Puromycin	
(mg/well)	(mg/well)	(% of control)
0.21±0.01	0.17±0.01*	83.09±2.50*

All values are expressed as means ± SEM (n =5) * : significant differences from control , $p<0.05$

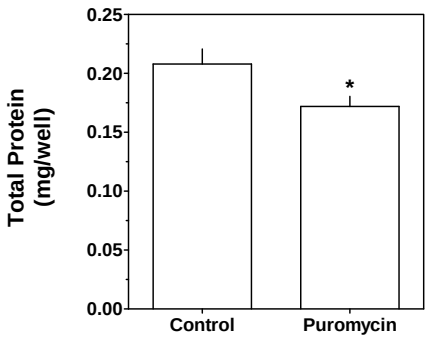

Figure 29. Effects of Puromycin treatment on BMα3β4 cells as determined via total protein assay

All values are expressed as means ± SEM (n =5) * : significant differences from control , $p<0.05$

2. Effects on APC protein

Puromycin treatment significantly reduced APC protein level to 44.76±8.03 % of control, as shown in Table 19 and Figure 30.

Table 19. Effects of puromycin treatment on APC protein in BMα3β4 Cells

APC Concentration (arbitrary units)		% Control
Control	Puromycin	
8.30±2.24	4.06±1.57	44.76±8.03*

All values are expressed as means ± SEM (n =3).

* : significant differences from control, $p<0.05$

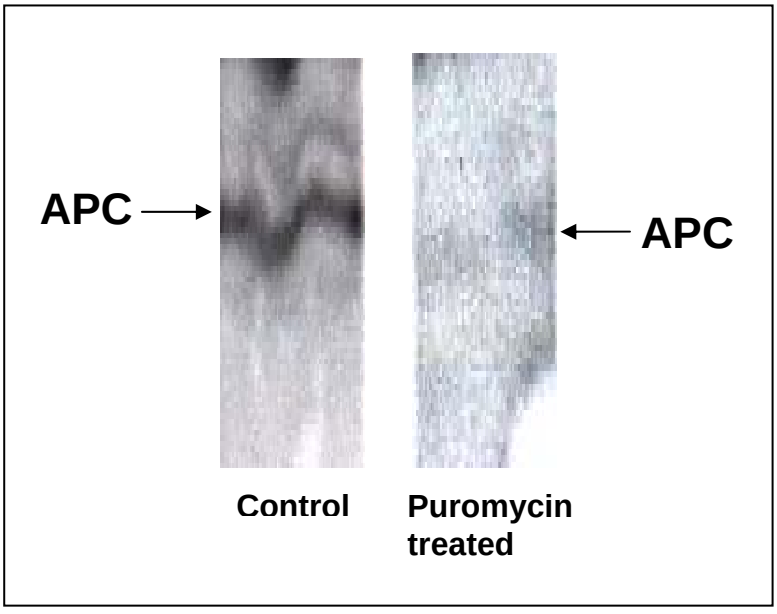

Figure 30. Representative Western Blot of APC protein in puromycin-treated BMα3β4 cells

All values are expressed as means ± SEM (n =3).

3. Effects on the number of nAChRs

The amounts of nAChRs on puromycin-treated BMα3β4 cells in unit of fmol/mg protein were shown in Table 20 and Figure 31. Comparing to control, puromycin treatment caused significant reduction in nAChR levels. The amount of Rt, Ri and Rs were 23, 16 and 40% of control, respectively.

The distribution of Ri or Rs in puromycin-treated group and control were shown in Table 21 and Figure 32. In control group, 80% of total receptors were located intracellular, whereas 20% located on cell surface. Contrarily, in puromycin-treated group, the distribution of receptor was changed, 60% were intracellular and 40% on cell surface.

Table 20. [^{3}H] Epibatidine binding assay, coupled with receptor alkylation to intact BM **α3β4 cells treated with puromycin**

nAChR	Specific nAChR binding (fmol/mg protein)		% of control
	Control	Puromycin	
Total ,(Rt)	1231±61	277±36*	23±3*
Intracellular ,(Ri)	970±65	157±17*	16±2*
Surface ,(Rs)	261±58	99±19*	40±13*

All values were expressed as mean+/-SEM, n=5

* : significant differences from control, p=0.0001

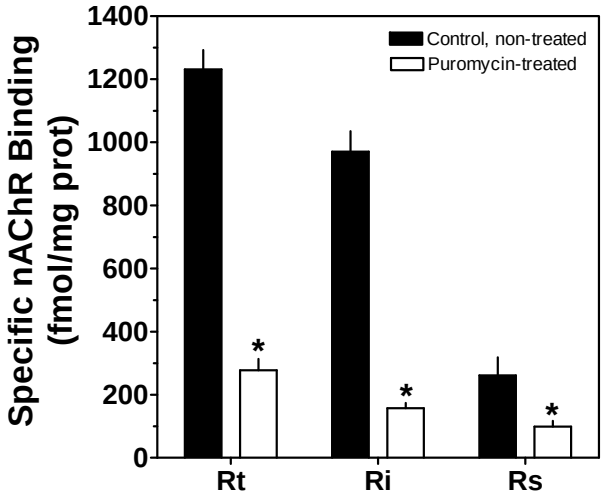

Figure 31. **[^{3}H] Epibatidine binding assay, coupled with receptor alkylation to intact** BM **α3β4 cells treated with puromycin**

All values were expressed as mean+/-SEM, n=5

* : significant differences from control, p=0.0001

Table 21. **Effects of puromycin treatment on the distribution of Intracellular receptor or Surface receptor in** BM **α3β4 cells**

The distribution of Intracellular or surface receptor (% of total receptors)			
Control		siRNA	
Ri	Rs	Ri	Rs
79±5	21±5	58±5 *	42±5 *

All values were expressed as mean+/-SEM, n=5

* : significantly differences from control, p<0.01

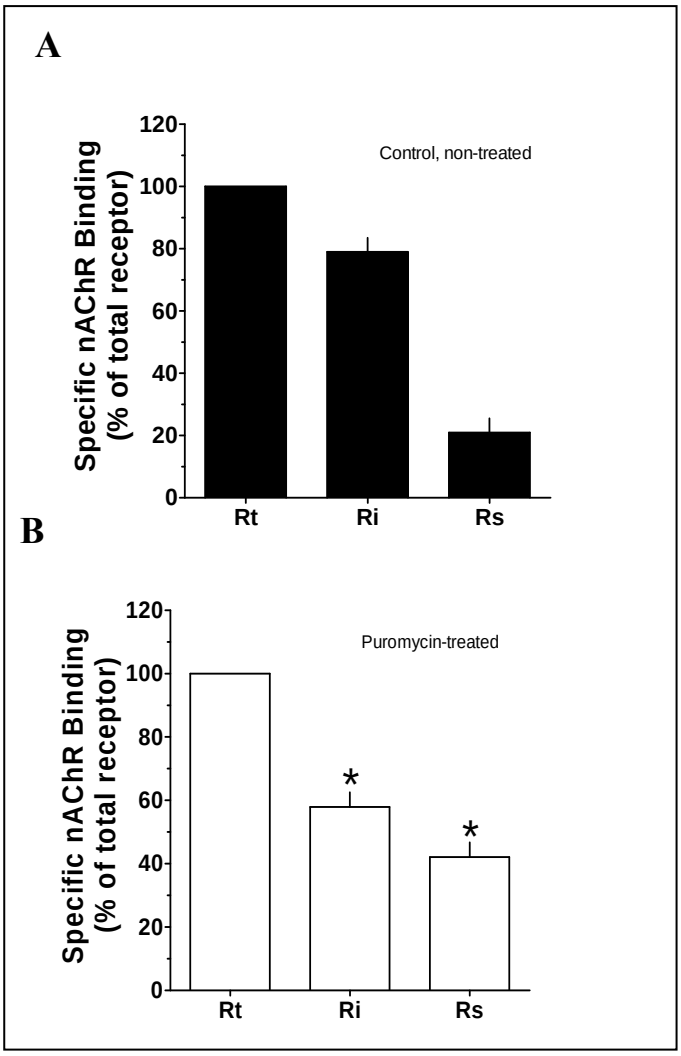

Figure 32. **Effects of puromycin treatment on the distribution of Intracellular receptor or Surface receptor in** BM **α3β4 cells**

All values were expressed as mean+/-SEM, n=5

* : significantly differences from control, $p<0.01$

CHAPTER V
DISCUSSION

In these studies we have established the expression of APC protein in cultured BAC cells, which express native nAChRs, and a recombinant cell line, which expresses recombinant nAChRs (BM$\alpha_3\beta_4$ cells) using Western Blot and PCR techniques. The presence of APC protein and RNA in both cells were found. Consistent with other researchers, APC protein is ubiquitously localized in various types of tissues, including CNS, NMJ, colon, lung, aorta, and spleen (17). The high level of APC in brain and during development state indicated its important role in nervous system (160, 163-166). Concerning its subcellular location, APC is primarily located in cytoplasm, but this protein can shuttle in and out of nucleus (160, 167, 196). APC is found in relatively large amount adjacent to neuronal plasma membranes (160). The neuronal localization and the subcellular movement of APC protein supports its role as a subcellular shuttle within neurons, in addition to its more classical function as a negative regulator of Wnt pathway (14, 16).

BAC cells are an excellent neuronal model to study native nAChRs. These cells express multiple nAChR subunits including α_3, α_5, α_7, and β_4 subunits. Two principal nAChR subtypes that are expressed include α-bungarotoxin sensitive nAChRs and mAb35-nAChRs (23, 156). Expression of multiple nAChR subtypes likely mimics the truly complicated responses in neurons; however, it presents many difficults when studying the expression on individual nAChR subtypes. *Xenopus laevis* oocytes expressing specific nAChRs subtypes have been used as a model for studying pharmacology of nAChR with regars to function and binding (197, 198). Similarly, the pharmacological properties of specific nAChR subtypes have been studied using mouse fibroblast cell lines, human embryonic kidney (HEK293) cells lines (199, 200) and human epithelial (SH-EP1) cell lines (201, 202). In our studies, HEK293 cells stably expressing of bovine α3β4 nAChRs, developed in the McKay laboratory (26)

were used. These cells are easily cultured, have good adhesion to plastic or glass surfaces and have a high transfection efficiency (86). Moreover, since several HEK293cell lines exist that express specific nAChRs, it is easy to compare data between different nAChR subtypes in this same cell line. Free et al. (26) constructed HEK293 cells expressing only bovine α_3 and β_4 subunits, named BM$\alpha_3\beta_4$ cells, and confirmed that this cell line had similar pharmacological characteristics to native bovine $\alpha_3\beta_4^*$ cells nAChR. They also reported that the number of nAChRs expressed on these cells appeared more than 100 fold higher than that on native BAC cells (26, 27). Initially, BAC cells were considered for our proposed studies investigating the role of APC on nAChR expression; however, the relatively small expression levels of nAChRs in BAC cells, as well as the expression of multiple nAChR subtypes in BAC cells would make these types of studies difficult to perform and more complicated to interpret using BAC cells. Both the expression of a single nAChR subtype and the large numbers of nAChRs support the use of BM$\alpha_3\beta_4$ cells in these studies.

A few studies are found in the literatures that implicate the involvement of APC with nAChR expression in both skeletal muscle and neuronal systems. Temburni et al. (21) showed that an APC dominant-negative, which blocked the interaction of APC with its binding partners, led to dramatic reduction of α_3-nAChR surface clusters in chick ciliary ganglion (CG) neurons. In our studies, we investigate the role of APC protein in the expression of $\alpha_3\beta_4$ nAChR using BM$\alpha_3\beta_4$ cells. APC siRNA transfection was performed in BM$\alpha_3\beta_4$ cells in order to down regulate the expression of APC protein in these cells. Our first series of experiments investigated the effects of the transfection procedure of cell number. Using total protein levels as an index of cell number, the effects of the transfection procedure on our cells were determined. The results indicate a slight reduction in total protein content in negative control and positive APC siRNA treatment groups compared to non treated, control groups. This slight reduction in total protein content supports a slight reduction in cell growth and/or cell viability. It is possible that some components used in the transfection procedures had effects on cells; for example, the high concentration of Lipofectamine might affect cell viability. However, the concentration of Lipofectamine used in these studies is within normal ranges recommended by the manufacturer (203). With

titration, this concentration gave the best response, with the least effect on cell viability. In addition to this reagent, the technique might also affect cell viability. During aspiration or addition of solution into each well, loss of cells could occur. However, when comparing positive and negative siRNA treatment, there was not significant difference in total protein content; these results indicated that APC siRNA, itself, has no effect on BM$\alpha_3\beta_4$ cells.

siRNA transfection is used to specifically down-regulate the targeted RNA, thus reducing expression of the protein of interest. Transfection experiments using Lipofectamine 2000 typically produce the high transfection efficiency (70-99%) depending on cell types (203). Our transfection efficiencies with BM$\alpha_3\beta_4$ cells using both negative control siRNA and APC siRNA were ~70%. Using our transfection procedure, APC siRNA treatment reduced APC protein content to ~50% of control at 24 hr and 48 hr post-transfection. It should be pointed out, however that, based on our transfection efficiency of ~70%, it is likely that the actual reduction of APC protein levels are an underestimation of the actual reduction in APC content. In addition, effects of siRNA transfection have been reported to be transient, lasting only 24-72 hrs, depending on the secondary readout (172, 185).

Recently, [^{3}H]epibatidine has been used to characterize neuronal nAChRs. This radiolabeled nAChR agonist has relatively high affinity for many subtypes of neuronal nAChRs including $\alpha3\beta4$, $\alpha4\beta2$, and $\alpha7$ nAChRs. Although [^{3}H]epibatidine has a somewhat lower affinity for $\alpha3\beta4$ nAChRs when compared to $\alpha4\beta2$ nAChRs (204), evidence exists that show [^{3}H]epibatidine is an excellent radioligand for recombinant $\alpha3\beta4$ nAChRs expressed in cell lines (205, 206). Free et al. (26) used [^{3}H]epibatidine binding approaches to characterize nAChRs in bovine adrenal medulla. Their results support the characterization of BAC nAChRs as $\alpha3\beta4$* nAChRs. Using standard nAChR binding assays, these investigators developed new approaches for investigating intracellular nAChRs (207). By alkylating nAChRs expressed on the cell surface, intracellular nAChR populations can be quantified. To accomplish this, BM$\alpha_3\beta_4$ cells were treated with dithiothreitol (DTT) to reduce nAChR disulfide bonds. This step was required for the alkylating agent,

bromoacetylcholine (brACh), to irreversible bind the agonist binding site. Finally, these cells were treated with 5,5′-dithio-bis(2-nitrobenzoic acid) (DTNB) to reoxidize any disulfide bonds that were reduced during the initial DTT treatment (109). Wenger et al. (207) demonstrated that brACh alkylation of BAC cells caused a complete loss of nAChR-stimulated neurosecretion which supports alkylation of all surface nAChRs (109). By coupling [^{3}H]epibatidine binding assays with nAChR alkylation, $\alpha_3\beta_4$ nAChRs in culture BM$\alpha_3\beta_4$ can be quantify. This approach directly estimates the number of intracellular nAChRs (Ri). The number of surface receptors (Rs) was indirectly obtained by subtraction Ri value from total receptor (Rt) value. Based on a Kd of 0.66±0.09 nM for [^{3}H]epibatidine, approximate 75% of nAChRs were located in the intracellular compartment and 25% are located on the surface in control cells..

Using this approach, the effects of APC siRNA treatment on the cellular distribution of nAChRs was investigated. We found that the total populations of nAChRs in APC siRNA-treated cells remained constant over the 48 hr post-transfection period and were not statistically different from control cells. However we found that APC siRNA treatment produced changes in the relative distribution of nAChRs and that these effects were time-dependent. Immediately following the 24 hr transfection period (t = 0 hr), no significant differences between control and APC siRNA–treated cells were seen in populations of intracellular or surface nAChRs. However, 24 and 48 hr after the transfection period, significant reductions of intracellular nAChRs were observed and significant increases in surface nAChRs were observed. It is important to note that these changes in distribution of nAChR populations parallel the observed changes in APC protein levels, supporting the involvement of APC in maintaining normal distributions of nAChRs in cells. These results are consistent with the results obtained by others (21, 22), who showed that changes of APC expression lead to changes in nAChRs expression.

Immediately following the 24 hr APC siRNA tranfection period, 80% and 20% of total receptors were located in intracellular area and at cell surface, respectively. At 24 hr after complete transfection, control Ri was increased to approximate 90% and

remained at this level over 48 hrs. Concomitantly, reductions in control Rs to approximate 10% of total receptors were found at 24 and 48 hr after complete transfection. Because of constant Rt level over 48 hr, this changes in relative distribution might be involved with the turnover or trafficking of α3β4 nAChRs between intracellular reservoir and cell surface. These changes in relative distribution of Ri and Rs might be resulted from the differences of cell age. In preliminary experiments, the distribution of Ri and Rs located on 3 days old α3β4 nAChRs (clone 2) were 70% and 30% of Rt, respectively. In this siRNA experiment, the distribution of Ri and Rs using 4 day old (or at 0 hr after complete transfection) cells were 80% and 20%, respectively. The distribution of Ri and Rs using 5 and 6 days old cells (or at 24 and 48 hrs after complete transfection) were 90% and 10%, respectively. These results suggest that as cells are cultured, the relative distribution of nAChRs may change, resulting in a decrease in surface nAChRs. Whether or not this decrease in surface expression also produces a reduction in functional responses is not known. Because of the observed time-dependent changes in α3β4 nAChR distribution, our data are expressed as a percentage of total receptors at each time point.

Temburni et al. (21) used anti-APC antibodies, which recognize distinct N-terminal and C-terminal epitopes, to establish the presence of APC protein in CG neurons. Their reported molecular weight of APC is similar to our reported APC molecular weight. These similarities support our identification of APC in both BAC cells and our BM$\alpha_3\beta_4$ cell line. Temburni et al. (21) subsequently showed that a dominant-negative peptide (APC-dn) blocked the binding of APC with its binding partners. Using mAb35 saturation binding assays these investigators observed a dramatic reduction of surface α3-nAChRs, but no significant changes in both intracellular α3-nAChRs and α3 nAChR subunit mRNA levels. In contrast, we found using siRNA transfection that deprived-APC protein resulted in a reduction of Ri and an increase of Rs in BMα3β4 cells. The discrepancy may be explained be due to their use of CG neurons during synapse formation. Their model contains many types of receptors and more than one subtype of nAChR. Innervation of these neurons is also very complex. In our studies, a HEK293 cell line expressing bovine α3β4 nAChRs

was used as a model. Moreover, Temburni et al.(21) used mAb35 which specifically recognizes α3 subunits (and possibly α5 subunits). Therefore, the signal produced by this antibody may be mis-identified as a fully assembled nAChR. Our radiolabeled binding assays will only identify high affinity binding sites which are only seen on the fully assembled nAChRs. Therefore, the changes in α3-nAChRs reported by Temburni et al.(21) might represent changes in α3 subunit protein rather than those of the assembled α3-pentameric nAChR. Finally, APC protein has different influences on various subtypes of nAChRs and species-differences might also contribute to the differences in both observations.

A model for surface expression of adrenal α3β4* nAChRs has been previously proposed (13). Several steps may be involved with the expression of nAChRs. It was also found that two-third of total receptors were intracellular receptors. A large pool of Ri might be responsible for the maintenance of the surface receptor expression. Concomitantly, the results from this study showed that the reduction of APC protein caused the increment of surface receptors in BMα3β4 cells. The overall data suggested that the increasing of surface receptors may be resulted from increasing movement of intracellular pool Ri to surface or decreasing movement of surface receptor into intracellular for endocytosis and degradation or slowing the surface receptor maturation. However, total receptors remained constant. Thus, it is possible that APC protein is not involved with the step of endocytosis and degradation. Therefore, the experiment was focused on the involvement of APC protein on the surface receptor insertion step. The proposed explanation was that APC protein can be either reversible bind or unbind with intracellular receptors (Ri) (Figure Equation). Only free formed Ri can move to the cell surface, APC-bound form Ri still remain within cells. In this study, the decreasing of control Rs at 24 and 48 hr after complete transfection comparing to those of at 0 hr was observed. In control cell, normal level of APC may bind with Ri and keep Ri within cells, leading to reduction of movement of Ri to cell surface and reduction of Rs expression. In contrast, the increasing of Rs at 24 and 48 hr after complete siRNA transfection comparing to control at each time point were found in this experiment. It is possible that APC siRNA transfection

caused a dramatic reduction of intracellular APC protein level which led to the shift of backward reaction (figure equation) and resulted in less number of APC-Ri complex and more number of free form Ri. The more number of free form Ri can insert to cell surface as seen by the increase of surface receptor (Rs). Thus, the result led to a conclusion that the deprived APC protein might enhance the trafficking of newly synthesized nAChRs to cell surface in order to maintain or stabilize the normal Rs expression.

Figure Equation

$$\text{APC} + \text{Ri} \leftrightarrow \text{APC-Ri}$$
$$\downarrow$$
$$\text{Cell surface (Rs)}$$

Canonical Wnt signaling has been documented as essential pathway for neuronal development (208). Activation of Wnt signaling was involved with the dissociation of β-catenin from a destructive complex, containing APC protein, glycogen synthase kinase-3β (GSK-3β) and axin. The stabilized β-catenin is then translocated into nucleus where it binds with Tcf/LEF transcription factors to activate the expression of Wnt target gene. In the absence of Wnt activation, a destructive complex binds and phosphorylates β-catenin, leading to the degradation of β-catenin and thus its function was inhibition (209, 210). Farias et al. (22) reported that the stimulation of canonical Wnt pathway by Wnt 7a induced dissociation of APC protein from the β-catenin destructive complex, leading to β-catenin stabilization. Then, APC protein quickly associated with membrane compartment. It also increased coclustering of APC protein and α7 nAChRs at presynaptic terminal in hippocampal neuron. They indicated that APC protein may serve as an intermediate in the α7 nAChR relocalization and expression on presynaptic terminal of hippocampal neuron. The results obtained in this study showed that APC-siRNA induced the reduction of APC protein level, leading to maintenance the surface nAChR expression in BM$\alpha_3\beta_4$ cells.

Similar to the activation of Wnt pathway, the reduction of APC protein might result in stabilization and accumulation of cytoplasmic β-catenin which was translocated into nucleus to activate transcription of several Wnt target gene. In addition, it could move to cell-cell adhesion. Therefore, the experiment was designed to focus on the involvement of β-catenin, APC and nAChR expression.

The distribution and functions of β-catenin in neuronal system have been investigated previously (211-218). The cellular distribution of β-catenin in nucleus and cytoplasm was related to cell differentiation and its function via Wnt/β-catenin pathway was important for neuronal differentiation in medulloblastoma (211). Inactivation of β-catenin resulted in dramatic brain malformation and failure of craniofacial development (212). Zaghetto et al. reported that activation of Wnt-β-catenin is essential for the establishment of olfactory axon connection (213). β-catenin overexpression has been associated with the mood stabilizer-like effect in lithium-sensitive mouse brain (214). Wnt/Axin1/β-catenin pathway regulated asymmetric nodal pathway gene expression and in the elaboration of brain asymmetries (215). Melker et al. (216) found the primarily β-catenin function in cell adhesion events in migrating neuronal crest cells. Schuller et al. stated that β-catenin function is required for cerebellar morphogenesis (217). Cadherin inhibition of β-catenin was also shown to be capable in regulating the proliferation and differentiation of neural precursor-cells (218).

In addition, there were studies supported the role of β-catenin and APC protein on nAChR expression. Wang et al. reported that neural agrin, required APC protein to induce nAChR clustering on muscle cells via promoting anchoring of the receptor protein to postsynaptic cytoskeleton (20). Zhang et al. (219) also confirmed that inhibitions of β-catenin expression or β-catenin and α-catenin binding reduced agrin-induced AChR clustering in NMJ of muscle cells. They proposed that β-catenin may serve as a linker between AChR and α-catenin associated cytoskeleton. In addition, Shao-Jun (220) indicated that Wnt signal stabilized β-catenin, subsequently activated transcription of Wnt target genes and promoted synaptic plasticity. Thus, it could be

explained that the reduction of APC protein may lead to less destabilization of β-catenin resulting in the increment of functional/active β-catenin.

Recently, Rosenberg et al. (221) documented that APC organized a multi-molecular complex which was essential for targeting α3* nAChRs to synapse. A dominant negative (dn) APC C-terminal fragment consisting of the EB1 binding domain were transfected into chick ciliary ganglion (CG) neurons during synapse formation to block APC binding with EB1. And, mAb35 immunoblotted on an extracellular epitope on α3* nAChR was used to detect the receptor expression under confocal microscope. The blockade of APC and EB1 interactions, in vivo, led to the reduction of α3* surface receptor expression relative to control. This blockade activity was specific only to α3* nAChRs, not to α7 nAChRs or glycine receptors expressed on this CG neuron. A quantitative correlation between the extent of α3* surface receptors reductions and APC:EB1-dn expression level were found in this experiment. The reductions of α3* nAChRs were the consequences of the reduction of α3* nAChRs insertion into the surface membrane and the increasing in endocytosis of surface α3* nAChRs. The results suggested that APC organized a complex of key cytoskeletal regulating proteins at neuronal nicotinic synapse in vivo. EB1 tagged the plus-ends of a subset of microtubules. APC interacted with EB1-tagged microtubule plus-ends and thereby, positioned a microtubule-based transport pathway for delivery of α3*nAChRs to a precise synapse. APC and EB1 interacted with proteins IQGAP1 and MACF at nicotinic postsynaptic sites. IQGAP1 and MACF stabilized the EB1-tagged microtubule and submembranous F-actin cytoskeleton network. They also linked APC-containing postsynaptic complex to the cytoskeleton (221). In addition, 14-3-3 adapter protein was indentified as a linker of α3 subunit to APC at postsynaptic site. This adapter protein was proposed to bind with the α3 long cytoplasmic loop then masked endocytosis motif in the α3*nAChRs. Normally, endocytosis was regulated by phosphorylation so 14-3-3 protein might bind to a specific phosphorylated motif in its target protein and protected the site from phosphatase. In conclusion, these APC and other proteins interactions promoted the stable binding of α3* nAChRs to local cytoskeleton and at postsynaptic site. In

contrast to our results, Rosenberg et al. (221) defined APC protein as an in vivo coordinator of nicotinic postsynaptic assembly in CG neuron. One explanation of the differences in both observations might be the complicated responses of native CG neuron contained multiple receptors including α7 nAChRs, α3*nAChRs and glycine receptor in APC-EB1 dominant negative (dn) experiment. But in siRNA experiment, only α3β4 nAChR was expressed on BMα3β4 cells. Moreover, the methods for determination of nAChRs were different. Using mAb35 labeled, both assembly and disassembly α3 subunits could be detected in CG neuron, whereas [^{3}H] Epibatidine binding assay could only detect the whole pentameric assemble α3β4 nAChRs. In addition, the difference of studied model, native CG neuron and in cell culture and species-differences might also contribute to the inconsistent observations.

Free et al. (13) previously reported that puromycin, protein synthesis inhibitor caused the reduction of Rt, Ri and Rs level without any changes on receptor distribution in BAC cells. Protein synthesis was therefore necessary for the maintenance of both of Rs and Ri. However, the role of protein synthesis inhibitor has not yet been clarified in BMα3β4 cells elsewhere. So, this study has focused on the effect of puromycin on APC protein level which led to changes of receptor expression on BMα3β4 cells. In the experiment, the effects of puromycin on APC protein level and nAChRs expression were investigated. Puromycin caused the dramatic reduction of APC protein level with similar to those of siRNA transfection. This indicated that the procedures used in this study were able to reduce APC protein level with a similar degree as others. Actually, based on mechanism of action, siRNA treatment should be more specific to APC protein than puromycin treatment. For this reason, puromycin caused the reduction of not only APC protein but also other nonspecific proteins which may also involved with nAChRs expression. In addition to the effect of puromycin on APC protein content, it was also found that the control Rt of puromycin treatment was similar to those of siRNA transfection. Approximate 80% of Rt were located in intracellular while the rest were located on cell surface. The same amount of receptors and its distribution confirmed the consistency of the receptor binding technique used in this study. After 24 hr transfection, puromycin caused the dramatic

reduction of Rt, Ri and Rs to 23, 16 and 40% of control. Although all receptors were reduced, Rs were reduced in a lesser degree than Rt or Ri. It suggested that cells tried to maintain Rs level as much as they can to maintain normal cellular function. Besides the changes of number, the distribution of Ri and Rs were also changed. In puromycin treated cells, approximate 60% of Rt were located in intracellular area, while the other 40% of Rt were located on cell surface.

In contrast to the above results, Free et al. (13) reported that puromycin caused the reduction of receptor level with a constant receptor distribution in BAC cells. Since bovine adrenal chromaffin cells contained multiple populations of neuronal nAChRs including α7, mAb35 and α3β4* nAChRs (24, 156). The differences of results from both experiments might be due to the characteristics of [^{3}H] Epibatidine that could bind with many nAChRs subtypes. Thus, the results obtained from [^{3}H] Epibatidine assay in BAC cells could be an overestimated binding data. Although, 1μM of α-bungarotoxin was added in this binding experiment to eliminate binding to α-bungarotoxin binding or α7 binding sites. Moreover, there might be an unknown compensatory mechanism among many nAChRs subtypes in BAC cells to overcome the précised changes of only α3β4* subtype. In addition, when the changes of cellular protein were occurred, at the beginning, cells tried to response to by compensatory adaptation in order to maintain normal cellular function. If these changes interfered cells was in a low extent, cells should be able to maintain their normal expression of receptors with a constant receptor distribution. But, if these changes interfered cells was in a higher degree, cells could not maintain normal receptors expression and resulted in changes of receptor distribution. However, functional surface receptors were the most important to be preserve at the normal level. To maintain normal Rs level, Ri might firstly be trafficked to cell surface. This explanation was supported by the result obtained from this experiment that the changes of Rs were occurred in a lesser extent than those of Ri. In conclusion, overall data confirmed the importance of constitutive de novo protein synthesis in maintenance of normal nAChRs expression.

In addition, both APC siRNA and puromycin treatment caused the changes of nAChRs expression which were not resulted from a loss of cells. For siRNA

transfection, non-differences of cell survival and total protein content between treated and non-treated cells were obtained. In puromycin treatment, the reduction of total protein content which should occur according to the action of puromycin as protein synthesis inhibitor was found. In concord with the observation of this experiment, after removing of puromycin from BAC cells, cells grew well. Consistent with other experiment, Free et al. (13) observed that the effect of puromycin on the reduction of nAChRs function and expression returned to pretreated levels.

So, from the data of this study, the role of APC protein on the changes of number of $\alpha_3\beta_4$ nAChR expressing on BMα3β4 cells was established. Normally, the number of receptors, especially Rs has been correlated with their function. We proposed the idea that the increment of functional α3β4 nAChR surface receptors should increase its function such as calcium release function.

CHAPTER VI
CONCLUSION

Results obtained in our studies indicated that with 72% transfection efficiency, APC-siRNA caused a reduction of APC protein production leading to a reduction of Ri and an increasing of Rs at 24 and 48 hr after complete transfection time in BMα3β4 cells. Total receptors remained constant over 48 hr. These changes of receptors expression were correlated to the changes in relative distribution of Ri and Rs. In addition, puromycin treatment caused a reduction of APC protein level with similar degree to a reduction obtained from APC-siRNA transfection . Puromycin also caused a reduction of α3β4 nAChRs as Rt, Ri and Rs concomitant with the changes in relative distribution of receptors. However, the changes of Rs were occurred in lesser extent than the changes of Ri. In conclusion, our results suggested that the deprived APC within BMα3β4 cells led to movement of Ri to cell surface for maintenance of normal Rs expression. This finding confirmed the role of APC on intracellular trafficking of α3β4 nAChRs in BMα3β4 cells.

REFERENCES

1. Gotti C, Clementi F. Neuronal nicotinic receptors: from structure to pathology. Prog Neurobiol. 2004 Dec;74(6):363-96.
2. Lindstrom J. Nicotinic acetylcholine receptors in health and disease.Mol Neurobiol. 1997 Oct;15(2):193-222.
3. Golan DE, Tashjian AH, Armstrong EJ,Galanter JM, Armstrong AW, Arnaout RA, Rose HS. Cholinergic pharmacology. In: Golan D E, Tashjian AH, Armstrong EJ, Galanter JM, Armstrong AW, Arnaout RA, Rose HS, editor. Principles of Pharmacology The pathophysiologic basis of drug therapy. 1st ed. Baltimore: Lippincott William & Wilkins; 2005. p. 89-106.
4. Gahring LC, Rogers SW. Neuronal nicotinic acetylcholine receptor expression and function on nonneuronal cells. Aaps J. 2005;7(4):E885-94.
5. Jensen AA, Frolund B, Liljefors T, Krogsgaard-Larsen P. Neuronal nicotinic acetylcholine receptors: structural revelations, target identifications, and therapeutic inspirations. J Med Chem. 2005 Jul 28;48(15):4705-45.
6. Lloyd GK WM. Neuronal nicotinic acetylcholine receptors as novel drug targets. J Pharmacol Exp Ther. 2000;292(2):461-7.
7. Xu W, Gelber S,Orr-Urtreger A,Armstrong D, Lewis RA, Ou CN, et al.Megacystis, mydriasis, and ion channel defect in mice lacking the alpha3 neuronal nicotinic acetylcholine receptor. Proc Natl Acad Sci U S A. 1999 May11; 96(10):5746-51.
8. Richardson CE, Morgan JM, Jasani B, Green JT, Rhodes J, Williams GT, et al. Megacystis-microcolon-intestinal hypoperistalsis syndrome and the absence of the alpha3 nicotinic acetylcholine receptor subunit. Gastroenterology.2001 Aug ;121(2):350-7.
9. Vernino S, Low PA, Lennon VA.Experimental autoimmune autonomic neuropathy. J Neurophysiol. 2003 Sep;90(3):2053-9.
10. Vernino S, Low PA, Fealey RD, Stewart JD, Farrugia G, Lennon VA.

Autoantibodies to ganglionic acetylcholine receptors in autoimmune autonomic neuropathies. N Engl J Med. 2000 Sep 21;343(12):847-55.

11. Darsow T, Booker TK, Pina-Crespo JC, Heinemann SF. Exocytic trafficking is required for nicotine-induced up-regulation of alpha 4 beta 2 nicotinic acetylcholine receptors. J Biol Chem. 2005 May 6;280(18):18311-20.
12. Pons S, Sallette J, Bourgeois JP, Taly A, Changeux JP, Devillers-Thiery A. Critical role of the C-terminal segment in the maturation and export to the cell surface of the homopentameric alpha 7-5HT3A receptor. Eur J Neurosci. 2004 Oct;20(8):2022-30.
13. Free RB, McKay SB, Gottlieb PD, Boyd RT, McKay DB. Expression of native alpha3beta4* neuronal nicotinic receptors: binding and functional studies investigating turnover of surface and intracellular receptor populations. Mol Pharmacol. 2005 Jun;67(6):2040-8.
14. Fearnhead NS, Britton MP, Bodmer WF. The ABC of APC. Hum Mol Genet. 2001 Apr;10(7):721-33.
15. Hanson CA, Miller JR. Non-traditional roles for the Adenomatous Polyposis Coli (APC) tumor suppressor protein. Gene. 2005 Nov 21;361:1-12.
16. Bienz M, Hamada F. Adenomatous polyposis coli proteins and cell adhesion. Curr Opin Cell Biol. 2004 Oct;16(5):528-35.
17. Bhat R, Baraban JM, Johnson RC,Eipper BA, Mains RE.High levels of expression of the tumor suppressor gene APC during development of the rat central nervous system. J Neurosci. 1994 May;14(5 Pt 2):3059-71.
18. Dobashi Y, Bhattacharjee RN,Toyoshima K, Akiyama T.Upregulation of the APC gene product during neuronal differentiation of rat pheochromocytomaPC12 cells. Biochem Biophys Res Commun. 1996 Jul 16;224(2):479-83.
19. Leroy K, Duyckaerts C, Bovekamp L, Muller O, Anderton BH, Brion JP. Increase of adenomatous polyposis coli immunoreactivity is a marker of reactive astrocytes in Alzheimer's disease and in other pathological conditions.Acta Neuropathol (Berl). 2001 Jul;102(1):1-10.
20. Wang J, Jing Z, Zhang L, Zhou G, Braun J, Yao Y, et al. Regulation of acetylcholine receptor clustering by the tumor suppressor APC. Nat Neurosci. 2003 Oct; 6(10):1017-8.

21. Temburni MK, Rosenberg MM, Pathak N, McConnell R, Jacob MH. Neuronal nicotinic synapse assembly requires the adenomatous polyposis coli tumor suppressor protein. J Neurosci. 2004 Jul 28;24(30):6776-84.
22. Farias GG, Valles AS, Colombres M, Godoy JA, Toledo EM, Lukas RJ, et al. Wnt-7a induces presynaptic colocalization of alpha7-nicotinic acetylcholine receptors and adenomatous polyposis coli in hippocampal neurons. J Neurosci. 2007 May 16; 27 (20):5313-25.
23. Gu H, Wenger BW, Lopez I, McKay SB, Boyd RT, McKay DB. Characterization and localization of adrenal nicotinic acetylcholine receptors: evidence that mAb35-nicotinic receptors are the principal receptors mediating adrenal catecholamine secretion. J Neurochem. 1996 Apr;66(4):1454-61.
24. Garcia-Guzman M, Sala F, Sala S, Campos-Caro A, Stuhmer W, Gutierrez LM, et al. alpha-Bungarotoxin-sensitive nicotinic receptors on bovine chromaffin cells: molecular cloning, functional expression and alternative splicing of the alpha 7 subunit. Eur J Neurosci. 1995 Apr 1;7(4):647-55.
25. Tachikawa E, Mizuma K, Kudo K, Kashimoto T, Yamato S, Ohta S. Characterization of the functional subunit combination of nicotinic acetylcholine receptors in bovine adrenal chromaffin cells. Neurosci Lett. 2001 Oct 26;312(3):161-4.
26. Free RB, von Fischer ND, Boyd RT, McKay DB.Pharmacological characterization of recombinant bovine alpha3beta4 neuronal nicotinic receptors stably expressed in HEK 293 cells. Neurosci Lett. 2003 Jun 12; 343(3):180-4.
27. Free RB, Bryant DL, McKay SB, Kaser DJ, McKay DB. [3H]Epibatidine binding to bovine adrenal medulla: evidence for alpha3beta4* nicotinic receptors. Neurosci Lett. 2002 Jan 25;318(2):98-102.
28. Kittler JT, Moss SJ.Neurotransmitter receptor trafficking and the regulation of synaptic strength. Traffic. 2001 Jul;2(7):437-48.
29. Wang H, Sun X. Desensitized nicotinic receptors in brain. Brain Res Brain Res Rev. 2005 Jun;48(3):420-37.
30. Marszalec W, Yeh JZ, Narahashi T. Desensitization of nicotine acetylcholine receptors: modulation by kinase activation and phosphatase inhibition. Eur J

Pharmacol. 2005 May 9;514(2-3):83-90.

31. Vann RE, James JR, Rosecrans JA, Robinson SE. Nicotinic receptor inactivation after acute and repeated in vivo nicotine exposures in rats. Brain Res. 2006 May1;1086 (1):98-103.
32. Kenny PJ, Markou A. Nicotine self-administration acutely activates brain reward systems and induces a long-lasting increase in reward sensitivity. Neuropsychopharmacology. 2006 Jun;31(6):1203-11.
33. Besson M, Granon S, Mameli-Engvall M, Cloez-Tayarani I, Maubourguet N,Cormier A, et al. Long-term effects of chronic nicotine exposure on brain nicotinic receptors. Proc Natl Acad Sci U S A. 2007 May 8;104(19):8155-60.
34. Robinson SE, Vann RE, Britton AF, O'Connell MM, James JR, Rosecrans JA. Cellular nicotinic receptor desensitization correlates with nicotine-induced acute behavioral tolerance in rats. Psychopharmacology (Berl). 2007 May;192(1):71-8.
35. Mugnaini M, Garzotti M, Sartori I, Pilla M, Repeto P, Heidbreder CA, et al. Selective down-regulation of [(125)I]Y0-alpha-conotoxin MII binding in rat mesostriatal dopamine pathway following continuous infusion of nicotine. Neuroscience. 2006;137(2):565-72.
36. Sokolova E, Matteoni C, Nistri A. Desensitization of neuronal nicotinic receptors of human neuroblastoma SH-SY5Y cells during short or long exposure to nicotine. Br J Pharmacol. 2005 Dec;146(8):1087-95.
37. Sallette J, Pons S, Devillers-Thiery A, Soudant M, Prado de Carvalho L,Changeux JP, et al. Nicotine upregulates its own receptors through enhanced intracellular maturation. Neuron. 2005 May 19;46(4):595-607.
38. Mitra M, Wanamaker CP, Green WN. Rearrangement of nicotinic receptor alpha subunits during formation of the ligand binding sites. J Neurosci. 2001 May 1; 21 (9):3000-8.
39. Keller SH, Lindstrom J, Ellisman M, Taylor P. Adjacent basic amino acid residues recognized by the COP I complex and ubiquitination govern endoplasmic reticulum to cell surface trafficking of the nicotinic acetylcholine receptor alpha-Subunit. J Biol Chem. 2001 May 25;276(21):18384-91.
40. Peng X, Gerzanich V, Anand R, Whiting PJ, Lindstrom J. Nicotine-induced

increase in neuronal nicotinic receptors results from a decrease in the rate of receptor turnover. Mol Pharmacol. 1994 Sep;46(3):523-30.

41. Peng X, Gerzanich V, Anand R, Wang F, Lindstrom J. Chronic nicotine treatment up-regulates alpha3 and alpha7 acetylcholine receptor subtypes expressed by the human neuroblastoma cell line SH-SY5Y. Mol Pharmacol. 1997 May;51(5):776-84.
42. Marchand S, Devillers-Thiery A, Pons S, Changeux JP, Cartaud J. Rapsyn escorts the nicotinic acetylcholine receptor along the exocytic pathway via association with lipid rafts. J Neurosci. 2002 Oct 15;22(20):8891-901.
43. Bruneau E, Sutter D, Hume RI, Akaaboune M.Identification of nicotinic acetylcholine receptor recycling and its role in maintaining receptor density at the neuromuscular junction in vivo. J Neurosci. 2005 Oct 26;25(43):9949-59.
44. Johnson AE, van Waes MA. The translocon: a dynamic gateway at the ER membrane. Annu Rev Cell Dev Biol. 1999;15:799-842.
45. Alder NN, Johnson AE. Cotranslational membrane protein biogenesis at the endoplasmic reticulum. J Biol Chem. 2004 May 28;279(22):22787-90.
46. Ren XQ, Cheng SB, Treuil MW, Mukherjee J, Rao J, Braunewell KH, et al. Structural determinants of alpha4beta2 nicotinic acetylcholine receptor trafficking. J Neurosci. 2005 Jul 13;25(28):6676-86.
47. Green WN, Millar NS. Ion-channel assembly. Trends Neurosci. 1995Jun; 18(6):280-7.
48. Smith MM, Lindstrom J, Merlie JP. Formation of the alpha-bungarotoxin binding site and assembly of the nicotinic acetylcholine receptor subunits occur in the endoplasmic reticulum. J Biol Chem. 1987 Mar 25;262(9):4367-76.
49. Merlie JP, Sebbane R, Tzartos S, Lindstrom J. Inhibition of glycosylation with tunicamycin blocks assembly of newly synthesized acetylcholine receptor subunits in muscle cells. J Biol Chem. 1982 Mar 10;257(5):2694-701.
50. Blount P, Merlie JP. Native folding of an acetylcholine receptor alpha subunit expressed in the absence of other receptor subunits. J Biol Chem. 1988 Jan 15;263 (2):1072-80.
51. Blount P, Smith MM, Merlie JP. Assembly intermediates of the mouse muscle

nicotinic acetylcholine receptor in stably transfected fibroblasts. J Cell Biol. 1990 Dec;111(6 Pt 1):2601-11.

52. Blount P, Merlie JP. Mutational analysis of muscle nicotinic acetylcholine receptor subunit assembly. J Cell Biol. 1990 Dec;111(6 Pt 1):2613-22.
53. Blount P, Merlie JP. BIP associates with newly synthesized subunits of the mouse muscle nicotinic receptor. J Cell Biol. 1991 Jun;113(5):1125-32.
54. Forsayeth JR, Gu Y, Hall ZW.BiP forms stable complexes with unassembled subunits of the acetylcholine receptor in transfected COS cells and in C2 muscle cells. J Cell Biol. 1992 May;117(4):841-7.
55. Gelman MS, Chang W, Thomas DY, Bergeron JJ, Prives JM. Role of the endoplasmic reticulum chaperone calnexin in subunit folding and assembly of nicotinic acetylcholine receptors. J Biol Chem.1995 Jun 23;270(25):15085-92.
56. Keller SH, Lindstrom J, Taylor P. Involvement of the chaperone protein calnexin and the acetylcholine receptor beta-subunit in the assembly and cell surface expression of the receptor. J Biol Chem. 1996 Sep 13;271(37):22871-7.
57. Keller SH, Lindstrom J, Taylor P. Inhibition of glucose trimming with castanospermine reduces calnexin association and promotes proteasome degradation of the alpha-subunit of the nicotinic acetylcholine receptor. J Biol Chem. 1998 Jul 3;273(27):17064-72.
58. Wanamaker CP, Christianson JC, Green WN. Regulation of nicotinic acetylcholine receptor assembly. Ann N Y Acad Sci. 2003 Sep;998:66-80.
59. Wang JM, Zhang L, Yao Y, Viroonchatapan N, Rothe E,Wang ZZ. A transmembrane motif governs the surface trafficking of nicotinic acetylcholine receptors. Nat Neurosci. 2002 Oct;5(10):963-70.
60. Pediconi MF, Gallegos CE, De Los Santos EB, Barrantes FJ.Metabolic cholesterol depletion hinders cell-surface trafficking of the nicotinic acetylcholine receptor. Neuroscience. 2004;128(2):239-49.
61. Borroni V, Baier CJ, Lang T, Bonini I, White MM, Garbus I, et al. Cholesterol depletion activates rapid internalization of submicron-sized acetylcholine receptor domains at the cell membrane. Mol Membr Biol. 2007 Jan-Feb; 24(1):1-15.
62. Kellner RR, Baier CJ, Willig KI, Hell SW, Barrantes FJ. Nanoscale organization

of nicotinic acetylcholine receptors revealed by stimulated emission depletion microscopy. Neuroscience. 2007 Jan 5;144(1):135-43.

63. Roccamo AM, Barrantes FJ. Charged amino acid motifs flanking each extreme of the alphaM4 transmembrane domain are involved in assembly and cell-surface targeting of the muscle nicotinic acetylcholine receptor. J Neurosci Res. 2007 Feb 1;85(2):285-93.
64. Baier CJ, Barrantes FJ. Sphingolipids are necessary for nicotinic acetylcholine receptor export in the early secretory pathway. J Neurochem. 2007 May;101(4):1072-84.
65. Madhavan R, Zhao XT, Ruegg MA, Peng HB. Tyrosine phosphatase regulation of MuSK-dependent acetylcholine receptor clustering. Mol Cell Neurosci. 2005 Mar;28(3):403-16.
66. Aridor M, Traub LM. Cargo selection in vesicular transport: the making and breaking of a coat. Traffic. 2002 Aug;3(8):537-46.
67. Christianson JC, Green WN. Regulation of nicotinic receptor expression by the ubiquitin-proteasome system. Embo J. 2004 Oct 27;23(21):4156-65.
68. Corringer PJ, Sallette J, Changeux JP. Nicotine enhances intracellular nicotinic receptor maturation: a novel mechanism of neural plasticity? J Physiol Paris. 2006 Mar-May;99(2-3):162-71.
69. Gaimarri A, Moretti M, Riganti L, Zanardi A, Clementi F, Gotti C. Regulation of neuronal nicotinic receptor traffic and expression.Brain Res Rev. 2007 Feb 24.
70. Buisson B, Bertrand D. Chronic exposure to nicotine upregulates the human (alpha)4 (beta)2 nicotinic acetylcholine receptor function. J Neurosci. 2001 Mar 15;21(6):1819-29.
71. Nguyen HN, Rasmussen BA, Perry DC. Binding and functional activity of nicotinic cholinergic receptors in selected rat brain regions are increased following long-term but not short-term nicotine treatment. J Neurochem. 2004 Jul;90(1):40-9.
72. Nuutinen S, Ahtee L, Tuominen RK. Time and brain region specific up-regulation of low affinity neuronal nicotinic receptors during chronic nicotine administration in mice. Eur J Pharmacol. 2005 May 16;515(1-3):83-9.
73. Harkness PC, Millar NS. Changes in conformation and subcellular distribution of

alpha4beta2 nicotinic acetylcholine receptors revealed by chronic nicotine treatment and expression of subunit chimeras. J Neurosci. 2002 Dec 1; 22 (23) :10172-81.

74. Vallejo YF, Buisson B, Bertrand D, Green WN. Chronic nicotine exposure upregulates nicotinic receptors by a novel mechanism. J Neurosci. 2005 Jun 8;25(23):5563-72.
75. Ficklin MB, Zhao S, Feng G. Ubiquilin-1 regulates nicotine-induced up-regulation of neuronal nicotinic acetylcholine receptors. J Biol Chem. 2005 Oct7;280 (40):34088-95.
76. Lansdell SJ, Gee VJ, Harkness PC, Doward AI, Baker ER, Gibb AJ, et al. RIC-3 enhances functional expression of multiple nicotinic acetylcholine receptor subtypes in mammalian cells. Mol Pharmacol. 2005 Nov;68(5):1431-8.
77. Castillo M, Mulet J, Gutierrez LM, Ortiz JA, Castelan F, Gerber S, et al. Dual role of the RIC-3 protein in trafficking of serotonin and nicotinic acetylcholine receptors. J Biol Chem. 2005 Jul 22;280(29):27062-8.
78. Liu Z, Tearle AW, Nai Q, Berg DK. Rapid activity-driven SNARE-dependent trafficking of nicotinic receptors on somatic spines. J Neurosci. 2005 Feb 2;25 (5):1159-68.
79. Briggs CA, Gubbins EJ, Marks MJ, Putman CB, Thimmapaya R,Meyer MD, et al. Untranslated region-dependent exclusive expression of high-sensitivity subforms of alpha4beta2 and alpha3beta2 nicotinic acetylcholine receptors. Mol Pharmacol. 2006 Jul;70(1):227-40.
80. Grailhe R, de Carvalho LP, Paas Y, Le Poupon C, Soudant M, Bregestovski P, etal. Distinct subcellular targeting of fluorescent nicotinic alpha 3 beta 4 and serotoninergic 5-HT3A receptors in hippocampal neurons. Eur J Neurosci. 2004 Feb;19(4):855-62.
81. Cooper J R, Bloom FE, Roth RH. Acetylcholine. In: Cooper J R, Bloom FE, RothRH, editor. The biochemical basis of neuropharmacology. 8th ed. New York: Oxford university press; 2003. p. 151-81.
82. Levitan I B, Kaczmarek LK. Receptors and transduction mechanism I: receptor coupled directly to ion channel. In: Levitan I B,Kaczmarek LK, editor.The neuron

cell and molecular biology. 3rd ed. New York: Oxford university press; 2002. p. 253-84.

83. Yeh JJ, Yasuda RP, Davila-Garcia MI, Xiao Y, Ebert S, Gupta T, et al. Neuronal nicotinic acetylcholine receptor alpha3 subunit protein in rat brain and sympathetic ganglion measured using a subunit-specific antibody: regional and ontogenic expression. J Neurochem. 2001 Apr;77(1):336-46.
84. Lukas RJ,Changeux JP, Le Novere N,Albuquerque EX, Balfour DJ,Berg DK,et al. International Union of Pharmacology. XX. Current status of the nomenclature for nicotinic acetylcholine receptors and their subunits. Pharmacol Rev. 1999Jun; 51(2):397-401.
85. Kimura R, Ushiyama N, Fujii T, Kawashima K. Nicotine-induced Ca2+ signaling and down-regulation of nicotinic acetylcholine receptor subunit expression in theCEM human leukemic T-cell line. Life Sci.2003 Mar 28;72(18-19):2155-8.
86. Xiao Y, Kellar KJ. The comparative pharmacology and up-regulation of rat neuronal nicotinic receptor subtype binding sites stably expressed in transfected mammalian cells. J Pharmacol Exp Ther. 2004 Jul;310(1):98-107.
87. Meyer EL, Xiao Y, Kellar KJ. Agonist regulation of rat alpha 3 beta 4 nicotinic acetylcholine receptors stably expressed in human embryonic kidney 293 cells. Mol Pharmacol. 2001 Sep;60(3):568-76.
88. Wong ET, Holstad SG, Mennerick SJ, Hong SE, Zorumski CF, Isenberg KE. Pharmacological and physiological properties of a putative ganglionic nicotinic receptor, alpha 3 beta 4, expressed in transfected eucaryotic cells. Brain Res Mol Brain Res. 1995 Jan;28(1):101-9.
89. Conroy WG, Berg DK. Neurons can maintain multiple classes of nicotinic acetylcholine receptors distinguished by different subunit compositions. J Biol Chem. 1995 Mar 3;270(9):4424-31.
90. Mao D, Yasuda RP, Fan H, Wolfe BB, Kellar KJ. Heterogeneity of nicotinic cholinergic receptors in rat superior cervical and nodose Ganglia. Mol Pharmacol. 2006 Nov;70(5):1693-9.
91. Poth K, Nutter TJ, Cuevas J, Parker MJ, Adams DJ, Luetje CW. Heterogeneity of

nicotinic receptor class and subunit mRNA expression among individual parasympathetic neurons from rat intracardiac ganglia. J Neurosci. 1997 Jan 15;17 (2):586-96.

92. Taraschenko OD, Panchal V, Maisonneuve IM, Glick SD. Is antagonism of alpha3beta4 nicotinic receptors a strategy to reduce morphine dependence? Eur J Pharmacol. 2005 Apr 25;513(3):207-18.
93. Flores CM, DeCamp RM, Kilo S, Rogers SW, Hargreaves KM. Neuronal nicotinic receptor expression in sensory neurons of the rat trigeminal ganglion: demonstration of alpha3beta4, a novel subtype in the mammalian nervous system. J Neurosci. 1996 Dec 15;16(24):7892-901.
94. Campos-Caro A, Smillie FI, Dominguez del Toro E, Rovira JC, Vicente-Agullo F, Chapuli J, et al. Neuronal nicotinic acetylcholine receptors on bovine chromaffin cells: cloning, expression, and genomic organization of receptor subunits. J Neurochem. 1997 Feb;68(2):488-97.
95. Hernandez SC, Vicini S, Xiao Y, Davila-Garcia MI, Yasuda RP, Wolfe BB, et al. The nicotinic receptor in the rat pineal gland is an alpha3beta4 subtype. Mol Pharmacol. 2004 Oct;66(4):978-87.
96. Whiteaker P, Peterson CG, Xu W, McIntosh JM, Paylor R, Beaudet AL, et al. Involvement of the alpha3 subunit in central nicotinic binding populations. J Neurosci. 2002 Apr 1;22(7):2522-9.
97. Turner JR, Kellar KJ. Nicotinic cholinergic receptors in the rat cerebellum: multiple heteromeric subtypes. J Neurosci. 2005 Oct 5;25(40):9258-65.
98. Perry DC, Xiao Y, Nguyen HN, Musachio JL, Davila-Garcia MI, Kellar KJ. Measuring nicotinic receptors with characteristics of alpha4beta2, alpha3beta2 and alpha3beta4 subtypes in rat tissues by autoradiography. J Neurochem. 2002 Aug;82(3):468-81.
99. Alkondon M, Albuquerque EX. A non-alpha7 nicotinic acetylcholine receptor modulates excitatory input to hippocampal CA1 interneurons. J Neurophysiol. 2002 Mar;87(3):1651-4.
100. Mulle C, Vidal C, Benoit P, Changeux JP. Existence of different subtypes of nicotinic acetylcholine receptors in the rat habenulo-interpeduncular system. J Neurosci. 1991 Aug;11(8):2588-97.

101. Zoli M, Lena C, Picciotto MR, Changeux JP. Identification of four classes of brain nicotinic receptors using beta2 mutant mice. J Neurosci. 1998 Jun15;18(12):4461-72.

102. Quick MW, Ceballos RM, Kasten M, McIntosh JM, Lester RA. Alpha3beta4 subunit-containing nicotinic receptors dominate function in rat medial habenula neurons. Neuropharmacology. 1999 Jun;38(6):769-83.

103. Marritt AM, Cox BC, Yasuda RP, McIntosh JM, Xiao Y, Wolfe BB, et al. Nicotinic cholinergic receptors in the rat retina: simple and mixed heteromeric subtypes. Mol Pharmacol. 2005 Dec;68(6):1656-68.

104. Winzer-Serhan UH, Leslie FM. Codistribution of nicotinic acetylcholine receptor subunit alpha3 and beta4 mRNAs during rat brain development. J Comp Neurol. 1997 Oct 6;386(4):540-54.

105. Gotti C, Zoli M, Clementi F. Brain nicotinic acetylcholine receptors: native subtypes and their relevance. Trends Pharmacol Sci. 2006 Sep;27(9):482-91.

106. Woo RS, Park EY, Shin MS, Jeong MS, Zhao RJ, Shin BS, et al. Mechanism of nicotine-evoked release of 3H-noradrenaline in human cerebral cortex slices. Br J Pharmacol. 2002 Dec;137(7):1063-70.

107. Di Angelantonio S, Giniatullin R, Costa V, Sokolova E, Nistri A. Modulation of neuronal nicotinic receptor function by the neuropeptides CGRP and substance P on autonomic nerve cells.Br J Pharmacol.2003Jul;139(6):1061-73.

108. Dani JA, Bertrand D. Nicotinic acetylcholine receptors and nicotinic cholinergic mechanisms of the central nervous system. Annu Rev Pharmacol Toxicol. 2007; 47:699-729.

109. Free RB, McKay DB. Surface and intracellular nicotinic receptors expressed in intact adrenal chromaffin cells: direct measurements using [3H]epibatidine. Brain Res. 2003 Jun 6;974(1-2):60-9.

110. Slotkin TA, Seidler FJ.Cholinergic receptor subtypes in the olfactory bulbectomy model of depression. Brain Res Bull. 2006 Jan 30;68(5):341-5.

111. Dube GR, Kohlhaas KL, Rueter LE, Surowy CS, Meyer MD, Briggs CA. Loss of functional neuronal nicotinic receptors in dorsal root ganglion neurons in a rat model of neuropathic pain. Neurosci Lett. 2005 Mar 7;376(1):29-34.

112. Araki H, Suemaru K, Gomita Y. Neuronal nicotinic receptor and psychiatric

disorders: functional and behavioral effects of nicotine. Jpn J Pharmacol. 2002 Feb;88(2):133-8.

113. Picciotto MR, Brunzell DH, Caldarone BJ. Effect of nicotine and nicotinic receptors on anxiety and depression. Neuroreport. 2002 Jul 2;13(9):1097-106.
114. Picciotto MR, Zoli M. Nicotinic receptors in aging and dementia. J Neurobiol. 2002 Dec;53(4):641-55.
115. Pavlov VA, Wang H, Czura CJ, Friedman SG, Tracey KJ. The cholinergic anti-inflammatory pathway: a missing link in neuroimmunomodulation. Mol Med. 2003 May-Aug;9(5-8):125-34.
116. Wang H, Yu M, Ochani M, Amella CA, Tanovic M, Susarla S, et al. Nicotinic acetylcholine receptor alpha7 subunit is an essential regulator of inflammation. Nature. 2003 Jan 23;421(6921):384-8.
117. Chernyavsky AI, Arredondo J, Marubio LM, Grando SA. Differential regulation of keratinocyte chemokinesis and chemotaxis through distinct nicotinic receptor subtypes. J Cell Sci. 2004 Nov 1;117(Pt 23):5665-79.
118. Arredondo J, Nguyen VT, Chernyavsky AI, Bercovich D, Orr-Urtreger A, Kummer W, et al.Central role of alpha7 nicotinic receptor in differentiation of the stratified squamous epithelium. J Cell Biol. 2002 Oct 28;159(2):325-36.
119. Ilcol YO, Gurun MS, Taga Y, Ulus IH. Intraperitoneal administration of choline increases serum glucose in rat:involvement of the sympathoadrenal system. Horm Metab Res. 2002 Jun;34(6):341-7.
120. Pestana IA, Vazquez-Padron RI, Aitouche A, Pham SM. Nicotinic and PDGF receptor function are essential for nicotine-stimulated mitogenesis in human vascular smooth muscle cells. J Cell Biochem. 2005 Dec 1;96(5):986-95.
121. Sershen H, Balla A, Lajtha A, Vizi ES. Characterization of nicotinic receptors involved in the release of noradrenaline from the hippocampus. Neuroscience. 1997 Mar;77(1):121-30.
122. Luo S, Kulak JM, Cartier GE, Jacobsen RB, Yoshikami D, Olivera BM, et al. alpha-conotoxin AuIB selectively blocks alpha3 beta4 nicotinic acetylcholine receptors and nicotine-evoked norepinephrine release. J Neurosci. 1998 Nov 1; 18(21):8571-9.
123. Azam L, McIntosh JM. Characterization of nicotinic acetylcholine receptors that

modulate nicotine-evoked [3H]norepinephrine release from mouse hippocampal synaptosomes. Mol Pharmacol. 2006 Sep;70(3):967-76.

124. Kulak JM, Nguyen TA, Olivera BM, McIntosh JM. Alpha-conotoxin MII blocks nicotine-stimulated dopamine release in rat striatal synaptosomes. J Neurosci. 1997 Jul 15;17(14):5263-70.

125. Cao YJ, Surowy CS, Puttfarcken PS. Nicotinic acetylcholine receptor-mediated [3H]dopamine release from hippocampus. J Pharmacol Exp Ther. 2005Mar; 312(3):1298-304.

126. Champtiaux N, Gotti C, Cordero-Erausquin M, David DJ, Przybylski C, Lena C, et al. Subunit composition of functional nicotinic receptors in dopaminergic neurons investigated with knock-out mice. J Neurosci. 2003 Aug; 23(21) :7820-9.

127. Salminen O, Murphy KL, McIntosh JM, Drago J, Marks MJ, Collins AC, et al. Subunit composition and pharmacology of two classes of striatal presynaptic nicotinic acetylcholine receptors mediating dopamine release in mice. Mol Pharmacol. 2004 Jun;65(6):1526-35.

128. Marubio LM, del Mar Arroyo-Jimenez M, Cordero-Erausquin M, Lena C, LeNovere N, de Kerchove d'Exaerde A, et al. Reduced antinociception in mice lacking neuronal nicotinic receptor subunits. Nature.1999Apr29; 398(6730) :805-10.

129. Kawa K. Inhibitory synaptic transmission in area postrema neurons of the rat showing robust presynaptic facilitation mediated by nicotinic ACh receptors. Brain Res. 2007 Jan 26;1130(1):83-94.

130. Zhu PJ, Stewart RR, McIntosh JM, Weight FF. Activation of nicotinic acetylcholine receptors increases the frequency of spontaneous GABAergic IPSCs in rat basolateral amygdala neurons. J Neurophysiol. 2005 Nov; 94(5):3081-91.

131. Salas R, Cook KD, Bassetto L, De Biasi M. The alpha3 and beta4 nicotinic acetylcholine receptor subunits are necessary for nicotine-induced seizures and hypolocomotion in mice. Neuropharmacology. 2004 Sep;47(3):401-7.

132. De Biasi M. Nicotinic mechanisms in the autonomic control of organ systems. J Neurobiol. 2002 Dec;53(4):568-79.

133. Skok VI. Nicotinic acetylcholine receptors in autonomic ganglia. Auton Neurosci. 2002 Apr 18;97(1):1-11.

134. Bibevski S, Zhou Y, McIntosh JM, Zigmond RE, Dunlap ME. Functional nicotinic acetylcholine receptors that mediate ganglionic transmission in cardiac parasympathetic neurons. J Neurosci. 2000 Jul 1;20(13):5076-82.

135. Zhou Y, Deneris E, Zigmond RE. Differential regulation of levels of nicotinic receptor subunit transcripts in adult sympathetic neurons after axotomy. J Neurobiol. 1998 Feb 5;34(2):164-78.

136. Yeh J, Ferreira M, Ebert S, Yasuda RP, Kellar KJ, Wolfe BB. Axotomy and nerve growth factor regulate levels of neuronal nicotinic acetylcholine receptor alpha3 subunit protein in the rat superior cervical ganglion. J Neurochem. 2001 Oct;79 (2):258-65.

137. Xu W, Orr-Urtreger A, Nigro F, Gelber S, Sutcliffe CB, Armstrong D, et al. Multiorgan autonomic dysfunction in mice lacking the beta2 and the beta4 subunits of neuronal nicotinic acetylcholine receptors. J Neurosci. 1999 Nov 1;19 (21):9298-305.

138. Park KS, Cha SK, Kim MJ, Kim DR, Jeong SW, Lee JW, et al. An alpha3beta4 subunit combination acts as a major functional nicotinic acetylcholine receptor in male rat pelvic ganglion neurons. Pflugers Arch. 2006 Sep;452(6):775-83.

139. Zhou X, Ren J, Brown E, Schneider D, Caraballo-Lopez Y, Galligan JJ. Pharmacological properties of nicotinic acetylcholine receptors expressed by guinea pig small intestinal myenteric neurons. J Pharmacol Exp Ther. 2002 Sep; 302(3):889-97.

140. Picciotto MR, Caldarone BJ, Brunzell DH, Zachariou V, Stevens TR, King SL. Neuronal nicotinic acetylcholine receptor subunit knockout mice: physiological and behavioral phenotypes and possible clinical implications. Pharmacol Ther. 2001 Nov-Dec;92(2-3):89-108.

141. Wang N, Orr-Urtreger A, Korczyn AD. The role of neuronal nicotinic acetylcholine receptor subunits in autonomic ganglia: lessons from knockout mice. Prog Neurobiol. 2002 Dec;68(5):341-60.

142. De Biasi M. Nicotinic receptor mutant mice in the study of autonomic function. Curr Drug Targets CNS Neurol Disord. 2002 Aug;1(4):331-6.

143. Klein CM, Vernino S, Lennon VA, Sandroni P, Fealey RD, Benrud-Larson L, et al. The spectrum of autoimmune autonomic neuropathies. Ann Neurol. 2003 Jun;53 (6):752-8.

144. Lennon VA, Ermilov LG, Szurszewski JH, Vernino S. Immunization with neuronal nicotinic acetylcholine receptor induces neurological autoimmune disease. J Clin Invest. 2003 Mar;111(6):907-13.

145. Vernino S, Ermilov LG, Sha L, Szurszewski JH, Low PA, Lennon VA. Passive transfer of autoimmune autonomic neuropathy to mice. J Neurosci. 2004 Aug 11;24(32):7037-42.

146. Wang N, Orr-Urtreger A, Chapman J, Ergun Y, Rabinowitz R, Korczyn AD. Hidden function of neuronal nicotinic acetylcholine receptor beta2 subunits in ganglionic transmission: comparison to alpha5 and beta4 subunits. J Neurol Sci. 2005 Feb 15;228(2):167-77.

147. Arredondo J, Chernyavsky AI, Marubio LM, Beaudet AL, Jolkovsky DL, Pinkerton KE, et al. Receptor-mediated tobacco toxicity: regulation of gene expression through alpha3beta2 nicotinic receptor in oral epithelial cells. Am J Pathol. 2005 Feb;166(2):597-613.

148. Ho YS, Chen CH, Wang YJ, Pestell RG, Albanese C, Chen RJ, et al. Tobacco-specific carcinogen 4-(methylnitrosamino)-1-(3-pyridyl)-1-butanone (NNK) induces cell proliferation in normal human bronchial epithelial cells through NFkappaB activation and cyclin D1 up-regulation. Toxicol Appl Pharmacol. 2005 Jun 1;205(2):133-48.

149. Tsurutani J, Castillo SS, Brognard J, Granville CA, Zhang C, Gills JJ, et al. Tobacco components stimulate Akt-dependent proliferation and NFkappaB-dependent survival in lung cancer cells. Carcinogenesis. 2005 Jul; 26(7):1182-95.

150. Terzano S, Court JA, Fornasari D, Griffiths M,Spurden DP, Lloyd S, et al. Expression of the alpha3 nicotinic receptor subunit mRNA in aging and Alzheimer's disease. Brain Res Mol Brain Res. 1998 Dec 10;63(1):72-8.

151. Peng JH, Fryer JD, Hurst RS, Schroeder KM, George AA, Morrissy S, et al.

High-affinity epibatidine binding of functional, human alpha7-nicotinic acetylcholine receptors stably and heterologously expressed de novo in human SH-EP1 cells. J Pharmacol Exp Ther. 2005 Apr;313(1):24-35.

152. Boulter J, O'Shea-Greenfield A, Duvoisin RM, Connolly JG, Wada E, Jensen A, et al. Alpha 3, alpha 5, and beta 4: three members of the rat neuronal nicotinic acetylcholine receptor-related gene family form a gene cluster. J Biol Chem. 1990 Mar 15;265(8):4472-82.
153. Rogers SW, Mandelzys A, Deneris ES, Cooper E, Heinemann S. The expression of nicotinic acetylcholine receptors by PC12 cells treated with NGF. J Neurosci. 1992 Dec;12(12):4611-23.
154. Criado M, Alamo L, Navarro A. Primary structure of an agonist binding subunit of the nicotinic acetylcholine receptor from bovine adrenal chromaffin cells. Neurochem Res. 1992 Mar;17(3):281-7.
155. Mousavi M, Hellstrom-Lindahl E, Guan ZZ, Bednar I, Nordberg A. Expression of nicotinic acetylcholine receptors in human and rat adrenal medulla. Life Sci. 2001 Dec 21;70(5):577-90.
156. Wilson SP, Kirshner N. The acetylcholine receptor of the adrenal medulla. J Neurochem. 1977 Apr;28(4):687-95.
157. Halvorsen SW, Berg DK. Subunit composition of nicotinic acetylcholine receptors from chick ciliary ganglia. J Neurosci. 1990 Jun;10(6):1711-8.
158. Vernallis AB, Conroy WG, Berg DK. Neurons assemble acetylcholine receptors with as many as three kinds of subunits while maintaining subunit segregation among receptor subtypes. Neuron. 1993 Mar;10(3):451-64.
159.Burgoyne RD, Morgan A, Robinson I, Pender N, Cheek TR. Exocytosis in adrenal chromaffin cells. J Anat. 1993 Oct;183 (Pt 2):309-14.
160. Bienz M. The subcellular destinations of APC proteins. Nat Rev Mol Cell Biol. 2002 May;3(5):328-38.
161. Reilein A, Nelson WJ. APC is a component of an organizing template for cortical microtubule networks. Nat Cell Biol. 2005 May;7(5):463-73.
162. Langford KJ, Askham JM, Lee T, Adams M, Morrison EE. Examination of actin and microtubule dependent APC localisations in living mammalian cells. BMC Cell Biol. 2006;7:3.

163. Brakeman JS, Gu SH, Wang XB, Dolin G, Baraban JM. Neuronal localization of the Adenomatous polyposis coli tumor suppressor protein. Neuroscience.1999; 91(2):661-72.

164. Shimomura A, Kohu K, Akiyama T, Senda T. Subcellular localization of the tumor suppressor protein APC in developing cultured neurons. Neurosci Lett. 2005 Feb 28;375(2):81-6.

165. Bhat RV, Axt KJ, Fosnaugh JS, Smith KJ, Johnson KA, Hill DE, et al. Expression of the APC tumor suppressor protein in oligodendroglia. Glia. 1996 Jun;17 (2) :169-74.

166. Senda T, Iino S, Matsushita K, Matsumine A, Kobayashi S, Akiyama T. Localization of the adenomatous polyposis coli tumour suppressor protein in the mouse central nervous system. Neuroscience. 1998 Apr;83(3):857-66.

167. Brocardo M, Nathke IS, Henderson BR. Redefining the subcellular location and transport of APC: new insights using a panel of antibodies. EMBO Rep. 2005 Feb;6(2):184-90.

168. Matsumine A, Ogai A, Senda T, Okumura N, Satoh K, Baeg GH, et al. Binding of APC to the human homolog of the Drosophila discs large tumor suppressor protein. Science. 1996 May 17;272(5264):1020-3.

169. Fujita A, Kurachi Y. SAP family proteins. Biochem Biophys Res Commun. 2000 Mar 5;269(1):1-6.

170. Parker MJ, Zhao S, Bredt DS, Sanes JR, Feng G. PSD93 regulates synaptic stabilityat neuronal cholinergic synapses.J Neurosci.2004 Jan14;24(2):378-88.

171. Scherer LJ, Rossi JJ. Approaches for the sequence-specific knockdown of mRNA. Nat Biotechnol. 2003 Dec;21(12):1457-65.

172. Achenbach TV, Brunner B, Heermeier K. Oligonucleotide-based knockdown technologies: antisense versus RNA interference. Chembiochem. 2003 Oct 6;4(10):928-35.

173. Phillips M I. Antisense therapeutics. In: Phillips M I, editor. Methods in molecular medicine^{TM}, Antisense therapeutics. 2nd ed. Totowa: Humana Press; 2005. p. 3-10.

174. Zhang Y, C, Taylor MM, Samson WK, Phillips MI. Antisense inhibitions. In:

Phillips M I, editor. Methods in molecular medicine™, Antisense therapeutics. 2nd ed. Totowa: Humana Press; 2005. p. 11-34.

175. Agrawal N, Dasaradhi PV, Mohmmed A, Malhotra P, Bhatnagar RK,Mukherjee SK. RNA interference: biology, mechanism, and applications. Microbiol Mol Biol Rev. 2003 Dec;67(4):657-85.

176. Genc S, Koroglu TF, Genc K. RNA interference in neuroscience. Brain Res Mol Brain Res. 2004 Dec 20;132(2):260-70.

177. Meister G, Tuschl T. Mechanisms of gene silencing by double-stranded RNA. Nature. 2004 Sep 16;431(7006):343-9.

178. Huppi K, Martin SE, Caplen NJ. Defining and assaying RNAi in mammalian cells. Mol Cell. 2005 Jan 7;17(1):1-10.

179. Pei Y, Tuschl T. On the art of identifying effective and specific siRNAs. Nat Methods. 2006 Sep;3(9):670-6.

180. Matzke MA, Birchler JA. RNAi-mediated pathways in the nucleus. Nat Rev Genet. 2005 Jan;6(1):24-35.

181. Sen CK, Roy S. miRNA: licensed to kill the messenger. DNA Cell Biol. 2007 Apr; 26(4):193-4.

182. Clayton J. RNA interference: the silent treatment. Nature. 2004 Sep 30;431 (7008):599-605.

183. Kretschmer-Kazemi Far R, Sczakiel G. The activity of siRNA in mammalian cells is related to structural target accessibility: a comparison with antisense oligonucleotides. Nucleic Acids Res. 2003 Aug 1;31(15):4417-24.

184. Bertrand JR, Pottier M, Vekris A, Opolon P, Maksimenko A, Malvy C. Comparison of antisense oligonucleotides and siRNAs in cell culture and in vivo. Biochem Biophys Res Commun. 2002 Aug 30;296(4):1000-4.

185. Vickers TA, Koo S, Bennett CF, Crooke ST, Dean NM, Baker BF. Efficient reduction of target RNAs by small interfering RNA and RNase H-dependent antisense agents. A comparative analysis. J Biol Chem. 2003 Feb 28;278(9):7108-18.

186. Senn C, Hangartner C, Moes S, Guerini D, Hofbauer KG. Central administration of small interfering RNAs in rats: a comparison with antisense oligonucleotides. Eur J Pharmacol. 2005 Oct 17;522(1-3):30-7.

187. Chalk AM, Warfinge RE, Georgii-Hemming P, Sonnhammer EL. siRNAdb: a database of siRNA sequences. Nucleic Acids Res. 2005 Jan 1;33(Database issue):D131-4.

188. Maurer JA, McKay DB. Staurosporine-induced reduction of secretory function in cultured bovine adrenal chromaffin cells. Eur J Pharmacol. 1994 Feb 21;253(1-2):115-24.

189. Kilpatrick DL LF, Carson KA, Kirshner AG, Slepetis R, Kirshner N. Stability of bovine adrenal medulla cells in culture. J Neurochem. 1980 Sep;35(3):679-92.

190. Chomczynski P, Sacchi N. Single-step method of RNA isolation by acid guanidinium thiocyanate-phenol-chloroform extraction. Analytical Biochemistry. 1987;162(1):156-9.

191. (http://www.graphpad.com/quickcalcs/radcalcform.cfm).

192. Smith KJ, Johnson KA, Bryan TM, Hill DE, Markowitz S, Willson JK, et al. The APC gene product in normal and tumor cells. Proc Natl Acad Sci U S A. 1993 Apr 1;90(7):2846-50.

193. Groden J, Thliveris A, Samowitz W, Carlson M, Gelbert L, Albertsen H, et al. Identification and characterization of the familial adenomatous polyposis coli gene. Cell. 1991 Aug 9;66(3):589-600.

194. Kinzler KW, Nilbert MC, Su LK, Vogelstein B, Bryan TM, Levy DB, et al. Identification of FAP locus genes from chromosome 5q21. Science. 1991 Aug 9;253(5020):661-5.

195. Su LK, Kinzler KW, Vogelstein B, Preisinger AC, Moser AR, Luongo C, et al. Multiple intestinal neoplasia caused by a mutation in the murine homolog of the APC gene. Science. 1992 May 1;256(5057):668-70.

196. Paola S, Massimo S, Sebastiano M, Lorena L, Luca R, Laura M, et al. Subcellular localization of Î²-catenin and APC proteins in colorectal preneoplastic and neoplastic lesions. Cancer letters. 2006;241(2):203-12.

197. Zhou Y, Nelson ME, Kuryatov A, Choi C, Cooper J, Lindstrom J. Human{alpha}4 {beta}2 Acetylcholine Receptors Formed from Linked Subunits. J Neurosci. 2003 October 8, 2003;23(27):9004-15.

198. Gerzanich V, Wang F, Kuryatov A, Lindstrom J. alpha 5 Subunit Alters

Desensitization, Pharmacology, Ca++ Permeability and Ca++ Modulation of Human Neuronal alpha 3 Nicotinic Receptors. J Pharmacol Exp Ther. 1998 July 1, 1998;286(1):311-20.

199. Chavez-Noriega LE, Gillespie A, Stauderman KA, Crona JH, O'Neil Claeps B, Elliott KJ, et al. Characterization of the recombinant human neuronal nicotinic acetylcholine receptors [alpha]3[beta]2 and [alpha]4[beta]2 stably expressed in HEK293 cells. Neuropharmacology. 2000;39(13):2543-60.

200. Karadsheh MS SM, Tang X, Macdonald RL, Stitzel JA. Functional characterization of mouse alpha4beta2 nicotinic acetylcholine receptors stably expressed in HEK293T cells. J Neurochem. 2004;91(5):1138-50.

201. Eaton JB, Peng J-H, Schroeder KM, George AA, Fryer JD, Krishnan C, et al. Characterization of Human {alpha}4{beta}2-Nicotinic Acetylcholine Receptors Stably and Heterologously Expressed in Native Nicotinic Receptor-Null SH-EP1 Human Epithelial Cells. Mol Pharmacol. 2003 December 1, 2003;64(6):1283-94.

202. Fitch RW, Xiao Y, Kellar KJ, Daly JW. Membrane potential fluorescence: A rapid and highly sensitive assay for nicotinic receptor channel function. Proceedings of the National Academy of Sciences. 2003 April 15, 2003;100(8):4909-14.

203. www.invitrogen.com.

204. Parker MJ, Beck A, Luetje CW. Neuronal Nicotinic Receptor beta 2 and beta 4 Subunits Confer Large Differences in Agonist Binding Affinity. Mol Pharmacol. 1998 December 1, 1998;54(6):1132-9.

205. Stauderman KA, Mahaffy LS, Akong M, Velicelebi G, Chavez-Noriega LE, Crona JH, et al. Characterization of Human Recombinant Neuronal Nicotinic Acetylcholine Receptor Subunit Combinations alpha 2beta 4, alpha 3beta 4 and alpha 4beta 4 Stably Expressed in HEK293 Cells. J Pharmacol Exp Ther. 1998 February 1, 1998;284(2):777-89.

206. Michelmore S, Croskery K, Nozulak J, Hoyer D, Longato R, Weber A, et al. Study of the calcium dynamics of the human a4ß2, a3ß4 and a1ß1?d nicotinic acetylcholine receptors. Naunyn-Schmiedeberg's Archives of Pharmacology. 2002;366(3):235-45.

207. Wenger BW, Bryant DL, Boyd RT, McKay DB. Evidence for spare nicotinic acetylcholine receptors and a beta 4 subunit in bovine adrenal chromaffin cells: studies using bromoacetylcholine, epibatidine, cytisine and mAb35. J Pharmacol Exp Ther. 1997 May;281(2):905-13.

208. Patapoutian A, Reichardt LF. Roles of Wnt proteins in neural development and maintenance. Current Opinion in Neurobiology. 2000;10(3):392-9.

209. Speese SD, Budnik V.Wnts: up-and-coming at the synapse.Trends in Neurosciences. 2007;30(6):268-75.

210. Aoki K, Taketo MM. Adenomatous polyposis coli (APC): a multi-functional tumor suppressor gene. J Cell Sci. 2007 October 1, 2007;120(19):3327-35.

211.Salaroli R, Russo A, Ceccarelli C, Mina GD, Arcella A, Martinelli GN, et al. Intracellular Distribution of beta-Catenin in Human Medulloblastoma Cell Lines with Different Degree of Neuronal Differentiation. Ultrastructural Pathology. 2007;31(1):33 - 44.

212. Brault V, Moore R, Kutsch S, Ishibashi M, Rowitch DH, McMahon AP, et al. Inactivation of the (&bgr;)-catenin gene by Wnt1-Cre-mediated deletion results in dramatic brain malformation and failure of craniofacial development.
Development. 2001 April 15, 2001;128(8):1253-64.

213. Zaghetto AA, Paina S, Mantero S, Platonova N, Peretto P, Bovetti S, et al. Activation of the Wnt {beta}Catenin Pathway in a Cell Population on the Surface of the Forebrain Is Essential for the Establishment of Olfactory Axon Connections. J Neurosci. 2007 September 5, 2007;27(36):9757-68.

214. Gould TD, Einat H, O'Donnell KC, Picchini AM, Schloesser RJ, Manji HK. [beta]-Catenin Overexpression in the Mouse Brain Phenocopies Lithium-Sensitive Behaviors. Neuropsychopharmacology. 2007;32(10):2173-83.

215. Carl M, Bianco IH, Bajoghli B, Aghaallaei N, Czerny T, Wilson SW.Wnt/Axin1/ [beta]-Catenin Signaling Regulates Asymmetric Nodal Activation,Elaboration, and Concordance of CNS Asymmetries. Neuron. 2007;55(3):393-405.

216. Annemieke A. de Melker NDJ-LD. Cellular localization and signaling activity of beta-catenin in migrating neural crest cells. Dev Dyn. 2004;230:708-26.

217. Schüller U, Rowitch DH. [beta]-catenin function is required for cerebellar

morphogenesis. Brain Research. 2007;1140:161-9.

218. Noles SR, Chenn A. Cadherin inhibition of [beta]-catenin signaling regulates the proliferation and differentiation of neural precursor cells. Molecular and Cellular Neuroscience. 2007;35(4):549-58.

219. Zhang B, Luo S, Dong X-P, Zhang X, Liu C, Luo Z, et al. {beta}-Catenin Regulates Acetylcholine Receptor Clustering in Muscle Cells through Interaction with Rapsyn. J Neurosci. 2007 April 11, 2007;27(15):3968-73.

220. Shao-Jun T. The synaptic Wnt signaling hypothesis. Synapse.2007;61(10):866-8.

221. Rosenberg MM, Yang F, Giovanni M, Mohn JL, Temburni MK, Jacob MH. Adenomatous polyposis coli plays a key role, in vivo, in coordinating assembly of theneuronal nicotinic postsynaptic complex.Molecular and Cellular Neuroscience. In Press, Corrected Proof.

BIOGRAPHY

NAME Miss Tulaya Potaros

DATE OF BIRTH 15 October, 1972.

PLACE OF BIRTH Bangkok, Thailand

INSTITUTIONS ATTEND Prince of Songkhla University, 1994
Bachelor of Science in Pharmacy
Mahidol University, 1999
Master of Science in Pharmacy(Pharmacology)
Mahidol University, 2008
Doctor of Philosophy in Biopharmaceutical Sciences

POSITION & OFFICE 1994-1997
Division of Biological Products, Department of Medical Science, Ministry of Public Health, Nonthaburi, Thailand
Position: Medical Scientist
1997-Present
Faculty of Pharmacy, Srinakharinwirot University, Nakorn Nayok, Thailand
Position: Instructor
Tel.: 037-395094-6
Email: Tulayapotaros@yahoo.com

HOME ADDRESS 912 Ngamwongwarn 27 soi 8, Ngamwongwarn Rd., Muang, Nonthaburi, Thailand
Tel.: 02-5882152